

2030 roadmap on two-dimensional materials for energy storage and conversion

Lan Ding , Kezhen Qi , Zimo Huang , Ying Yu , Ze Yang ,
Sepehr Tabibi , Alireza Khataee , Lei Hao , Qitao Zhang ,
Vadim Popkov , Maria Kaneva , Artem Lobinsky , Zhipeng Yu ,
Jun Li , Amir Sultan , Kun Zheng , Gan Qu , Dandan Ma ,
Jian-Wen Shi , Ahmed Ismail

PII: S1001-8417(25)01419-6
DOI: <https://doi.org/10.1016/j.ccllet.2025.112242>
Reference: CCLET 112242

To appear in: *Chinese Chemical Letters*

Received date: 29 September 2025
Revised date: 7 December 2025
Accepted date: 8 December 2025

Please cite this article as: Lan Ding , Kezhen Qi , Zimo Huang , Ying Yu , Ze Yang , Sepehr Tabibi , Alireza Khataee , Lei Hao , Qitao Zhang , Vadim Popkov , Maria Kaneva , Artem Lobinsky , Zhipeng Yu , Jun Li , Amir Sultan , Kun Zheng , Gan Qu , Dandan Ma , Jian-Wen Shi , Ahmed Ismail , 2030 roadmap on two-dimensional materials for energy storage and conversion, *Chinese Chemical Letters* (2025), doi: <https://doi.org/10.1016/j.ccllet.2025.112242>



This is a PDF of an article that has undergone enhancements after acceptance, such as the addition of a cover page and metadata, and formatting for readability. This version will undergo additional copyediting, typesetting and review before it is published in its final form. As such, this version is no longer the Accepted Manuscript, but it is not yet the definitive Version of Record; we are providing this early version to give early visibility of the article. Please note that Elsevier's sharing policy for the Published Journal Article applies to this version, see: <https://www.elsevier.com/about/policies-and-standards/sharing#4-published-journal-article>. Please also note that, during the production process, errors may be discovered which could affect the content, and all legal disclaimers that apply to the journal pertain.

© 2025 Published by Elsevier B.V. on behalf of Chinese Chemical Society and Institute of Materia Medica, Chinese Academy of Medical Sciences.

2030 roadmap on two-dimensional materials for energy storage and conversion

Lan Ding,^a Kezhen Qi,^{a,b,*} Zimo Huang,^{c,*} Ying Yu,^d Ze Yang,^{d,*} Sepehr Tabibi,^e Alireza Khataee,^{e,f,*} Lei Hao,^g Qitao Zhang,^{g,*} Vadim Popkov,^h Maria Kaneva,^h Artem Lobinsky,^{h,*} Zhipeng Yu,^{i,*} Jun Li,^{j,*} Amir Sultan,^k Kun Zheng,^{l,*} Gan Qu,^{m,*} Dandan Ma,ⁿ Jian-Wen Shi,^{n,*}, Ahmed Ismail^{o,*}

^aCollege of Pharmacy, Dali University, Dali 671000, China

^bSchool of Chemistry and Chemical Engineering, Yili Normal University, Yining 835000, China

^cSchool of Metallurgy and Environment, Central South University, Changsha 410083, China

^dInstitute of Nanoscience and Nanotechnology, School of Physical Science and Technology, Central China Normal University, Wuhan 430079, China

^eDepartment of Applied Chemistry, Faculty of Chemistry, University of Tabriz, Tabriz 51666–16471, Iran

^fDepartment of Chemical Engineering, Istanbul Technical University, 34469 Istanbul, Türkiye

^gInternational Collaborative Laboratory of 2D Materials for Optoelectronics Science and Technology of Ministry of Education, Institute of Microscale Optoelectronics, Shenzhen University, Shenzhen 518000, China

^hHydrogen Energy Laboratory, Ioffe institute, Saint Petersburg 194021, Russia

ⁱInternational Iberian Nanotechnology Laboratory (INL), Braga 4715-330, Portugal

^jSchool of Chemical Engineering, Henan Institute of Advanced Technology, Zhengzhou University, Zhengzhou 450001, China

^kJerzy Haber Institute of Catalysis and Surface Chemistry, Polish Academy of Sciences, Niezapominajek 8, 30-239 Krakow, Poland

^lFaculty of Energy and Fuels, AGH University of Krakow, al. A. Mickiewicza 30, 30-059 Krakow, Poland

^mSchool of Materials Science and Engineering, Zhengzhou University, Zhengzhou 450001, China

ⁿState Key Laboratory of Electrical Insulation and Power Equipment, School of Electrical Engineering, Xi'an Jiaotong University, Xi'an 710049, China

^oSchool of Physics, University of Electronic Science and Technology of China, Chengdu 610054, China

ARTICLE INFO

ABSTRACT

Article history:

Received

Received in revised form

Accepted

Available online

Two-dimensional (2D) materials have rapidly emerged as transformative platforms for energy storage and conversion, owing to their atomic-scale thickness, tunable electronic structures, and versatile chemical functionalities. Over the past five years, remarkable advances in material synthesis, interface engineering, and device integration have unlocked new opportunities, yet challenges in stability, scalability, and performance optimization remain. In this roadmap, we

* Corresponding authors.

E-mail addresses: qkzh2003@aliyun.com (K. Qi), zimo.huang@csu.edu.cn (Z. Huang), yz@ccnu.edu.cn (Z. Yang), a_khataee@tabrizu.ac.ir (A. Khataee), qitao-zhang@szu.edu.cn (Q. Zhang), lobinsky.a@mail.ioffe.ru (A. Lobinsky), Zhipeng.yu@inl.int (Z. Yu), junli2019@zzu.edu.cn (J. Li), zheng@agh.edu.pl (K. Zheng), gqu@zzu.edu.cn (G. Qu), jianwen.shi@mail.xjtu.edu.cn (J. Shi), ahmed.ics13@gmail.com (A. Ismail).

Keywords:

Two-dimensional materials
 Energy storage and conversion
 Electrochemical devices
 Photocatalysis
 Electrocatalysis
 Graphene and derivatives
 MXenes
 Covalent and metal-organic frameworks

provide an updated perspective toward 2030, systematically reviewing eleven representative 2D material classes, which can be broadly grouped into carbon-based materials, inorganic semiconductors, framework materials, and layered nanosheet systems. Their opportunities and challenges in electrochemical energy storage, photocatalysis, and electrocatalysis are highlighted. We believe this roadmap can enrich the development of 2D materials for sustainable energy technologies, and provide useful guidance for both fundamental studies and practical applications in the coming decade.

1. Graphene and graphene-composites for energy storage applications

Zimo Huang*

1.1 Status

Graphene is a single-atom-thick honeycomb lattice of sp^2 -hybridized carbon atoms. Its ultrahigh carrier mobility and outstanding mechanical strength have made it a focal material for next-generation energy-storage systems, spanning lithium-ion, sodium-ion, lithium-sulfur, zinc-ion batteries, and supercapacitors [1,2]. In practical electrodes, however, graphene sheets readily restack, which reduces the accessible surface area and thus weakens electrical double-layer (EDL) charge storage. For instance, the practical specific capacitance of graphene in supercapacitors (~80 F/g) is far below its theoretical value (~550 F/g) [3]. To mitigate restacking and accelerate ion transport, Liu *et al.* introduced in-plane pores (“holey graphene”) that disrupt basal-plane continuity and enhance through-plane ion migration [4]. Such perforations not only expedite electrolyte-ion diffusion perpendicular to the sheets but also expose abundant edge-active sites, thereby improving specific capacitance and rate capability. Among porosity-engineering strategies, chemical activation is particularly effective for increasing surface area and the density of ion-storage sites. Wu *et al.* [5] employed low-temperature KOH activation to create nanoscale pores within graphene, providing additional adsorption sites and elevating the specific capacitance to 265 F/g.

Beyond single-component graphene, its intrinsic limitations have spurred composite designs that integrate graphene with functional phases such as metal oxides and polymers. Through judicious component matching and multiscale structural design, these hybrids realize complementary properties and synergistic enhancements. Representative electrochemical properties of graphene-based hybrid composites are shown in Fig. 1 [6]. As highlighted therein, combining active materials with graphene commonly yields high electrical conductivity, hierarchical porosity, and excellent structural stability.

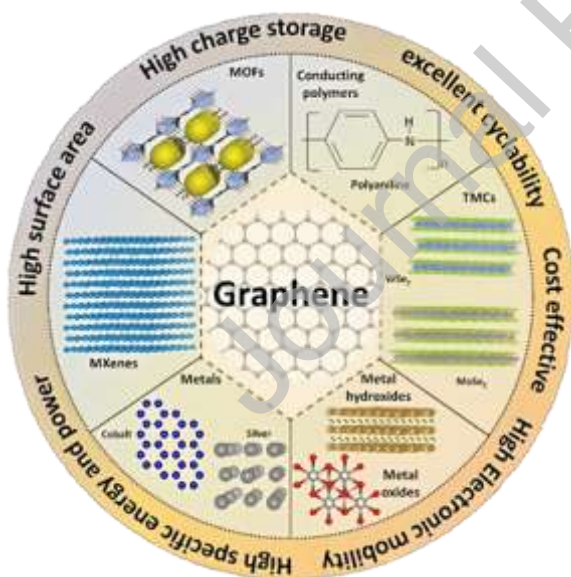


Fig. 1. Various materials are composited with graphene, showcasing their unique properties [6].

1.2 Current and future challenges

There is broad consensus that, despite graphene’s exceptional intrinsic properties, aggregation and limited practical capacity necessitate composite strategies to achieve step-change performance in energy storage [7]. Fig. 2 schematically summarizes composite approaches involving graphene and functional materials—covering application scenarios, material selections, synthetic methods, and

characterization metrics [8]. Notwithstanding significant laboratory-scale progress, translation to industrial applications still faces two overarching challenges-materials processing and performance optimization-issues that likewise confront the broader class of 2D nanomaterials.

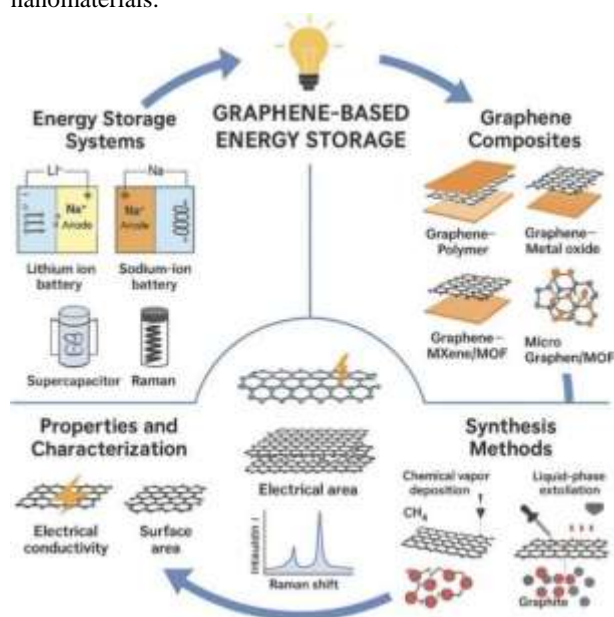


Fig. 2. Overview of graphene-based energy storage systems [8].

Materials processing: Oxygen-containing functional groups (e.g., $-\text{COOH}$, $-\text{OH}$) introduced during oxidation facilitate subsequent functionalization but disrupt graphene's conjugated network and degrade its conductivity [9]. Moreover, the performance of graphene-based composites depends sensitively on interfacial coupling between the active phase and graphene. Common routes (e.g., solution mixing, *in-situ* growth) can lead to aggregation or nonuniform dispersion of the active component, impeding electron and ion transport [10]. Interfacial control in 2D nanocomposites remains a widely recognized bottleneck. Developing greener, sustainable, and scalable fabrication processes is a prerequisite for industrial deployment.

Performance optimization: Electrochemical devices impose multidimensional requirements-high specific capacity, excellent rate capability, long cycle life, and safety, yet it remains difficult to optimize all metrics simultaneously in graphene and its composites [11]. For example, increasing capacity typically requires higher active-material loading, which can lengthen electron pathways and compromise rate performance. Although graphene can buffer volume changes, interfacial delamination may emerge after prolonged cycling. Furthermore, low-temperature performance is underexplored: at $-20\text{ }^{\circ}\text{C}$, ion-transport pathways in graphene-based electrodes can become effectively "frozen", causing severe losses in capacity and rate capability [12].

1.3 Advances in science and technology to meet challenges

To address sheet restacking and sluggish ion transport, researchers have advanced pore-architecture control and heteroatom doping to enlarge accessible surface area and accelerate mass/electron transport. For a direct view of graphene's potential in energy storage, Zhao *et al.* [13] tuned the pore size of monolayer graphene and markedly enhanced overall ion mobility, underscoring the promise of pore-size engineering for customizable 2D materials. In parallel, heteroatom doping can simultaneously modulate pore structure and defect chemistry. Using chemical vapor deposition, Subhabrata Das *et al.* [14] synthesized Co,N-codoped graphene with high hydrophilicity and surface charge density; optimized charge-transfer kinetics from heteroatom doping yielded an ~ 108 -fold improvement in storage performance relative to undoped graphene.

As the field has clarified the advantages and trade-offs of graphene composites, Yin *et al.* [15] reported an area-specific capacitance of $64\text{ }\mu\text{F}/\text{cm}^2$ for monolayer graphene versus $145\text{ }\mu\text{F}/\text{cm}^2$ for six-layer graphene; they further showed that charge storage proceeds predominantly *via* co-ion desorption in monolayers, while counter-ion adsorption dominates in few-layer structures. To realize strong complementarity and synergy, Lu *et al.* [16] "welded" carbon-fiber arrays to a graphene network to form a dense filler framework for thermally conductive polymers: graphene serves as an interconnect that links the vertical heat-conduction pathways of aligned fibers into a more integrated thermal network-an important attribute for heat management in energy-storage devices. Building on conductive-network design and electronic-structure tuning, Wang *et al.* [17] innovatively combined $\text{Ni}(\text{OH})\text{Cl}$ with interstitial carbon atoms and graphene; interstitial-carbon-induced lattice strain together with graphene's percolating conductivity optimized the electronic configuration and redox kinetics, improving long-cycle stability by nearly 20%. Integrating low-conductivity metal oxides such as SnO_2 [13], MnO_2 [18] and Co_3O_4 [19] with graphene effectively mitigates their electronic-transport limitations. Graphene provides a conductive framework for rapid electron percolation across the electrode, lowers charge-transfer resistance, and enhances

rate performance. Its high surface area and 2D morphology also promote uniform nanoparticle dispersion, suppress aggregation, and improve electrolyte contact. Overall, coupling graphene with intrinsically low-conductivity phases yields multifunctional electrodes that combine high energy density with robust cycling stability—key attributes for next-generation, high-performance energy-storage devices.

Beyond electrochemical electrodes, graphene-based constructs mechanistically underpin adjacent components across the device stack. In ultralight aerogels [20], three-dimensional (3D) interconnected graphene frameworks provide continuous electron-percolation pathways and hierarchical meso/macro-porosity that lower tortuosity and shorten ion diffusion lengths; capillary-reinforced architectures also dissipate mechanical stress, stabilizing the electrode/electrolyte interface under high-rate cycling. In metal-ion batteries [21], heteroatom-doped graphene regulates solvation/desolvation and homogenizes local electric fields, thereby lowering nucleation overpotentials, suppressing dendrites, and accommodating volume change through elastic load transfer, surface polarity further anchors intermediates (e.g., polysulfides), accelerating redox conversion. Within solid-state electrolytes [22] graphene-oxide-derived lamellae create ion-selective, angstrom-scale nanochannels and mechanically stiff interlayers that reduce interfacial impedance yet maintain electronic insulation at low loadings. As catalyst supports [17] defect-rich or single-atom-decorated graphene tunes local electronic structure (e.g., charge density and d-band center), lowers activation barriers for surface redox, and mitigates active-site sintering.

In addition to their exceptional electrical conductivity and mechanical robustness, the defect structure of graphene plays a decisive role in dictating its electrochemical behavior in energy storage systems. Unprecedented control over graphene structural order and chemical uniformity has been achieved through shock-wave-assisted exfoliation, as elegantly demonstrated by Liu *et al.* [23] Depending on the orientation of the shock wave relative to the graphite lamellae, two distinct materials were obtained: nearly defect-free “aerodynamically exfoliated graphene” (AES-G) and highly defective “in-plane shock graphene” (IPS-G). AES-G exhibited an I_G/I_D ratio of 14.3 and an oxygen content of 1.3 %, whereas IPS-G showed an I_G/I_D ratio of 1.6 and an oxygen content of 6.2 at %. When employed as current collectors for sodium metal anodes, AES-G delivered outstanding cycling stability in a standard carbonate electrolyte (1 mol/L NaClO₄ in EC/DEC 1:1 with 5 % FEC) at 2 mA/cm², achieving a Coulombic efficiency of ~100 % and an areal capacity of 1 mAh/cm². In sharp contrast, IPS-G performed similarly to bare Cu, exhibiting poor Coulombic efficiency, severe dendrite formation, and periodic short-circuiting. Mechanistic investigations revealed that structural defects and oxygen-containing functional groups destabilize the solid-electrolyte interphase (SEI). Defective regions on IPS-G promote heterogeneous SEI formation and generate fluorine-rich “hot spots” from locally accelerated FEC decomposition, leading to uneven sodium deposition and dendritic growth. Conversely, the smooth and chemically uniform AES-G surface facilitates robust and homogeneous SEI formation, thereby suppressing dendrite growth and enabling highly reversible Na plating/stripping. These findings underscore that structural order and chemical uniformity in graphene are pivotal to ensuring stable electrochemical interfaces and long-term cycling performance. Beyond intrinsic defect regulation, a deeper understanding of how graphene interfaces interact with active materials has become equally essential.

Interfacial coupling lies at the heart of performance optimization in graphene-based composites, as it governs charge transfer, ion diffusion, and structural stability across heterogeneous junctions. However, conventional fabrication routes such as solution mixing or simple *in situ* growth often produce poorly defined contact and irregular bonding, hindering precise control and mechanistic understanding of interfacial behavior. Recent progress in *in situ* and operando characterization has opened new avenues to probe interfacial dynamics with atomic precision under realistic electrochemical environments. Synchrotron-based X-ray absorption spectroscopy (XAS) and X-ray photoelectron spectroscopy (XPS) enable real-time monitoring of charge redistribution and electronic structure modulation at graphene–active phase junctions [24]. Meanwhile, operando X-ray diffraction (XRD) and cryo-transmission electron microscopy (cryo-TEM) visualize interlayer evolution and defect migration during cycling, providing direct insight into strain accommodation and ion transport pathways [25]. On the theoretical front, multiscale modeling integrating density functional theory (DFT) and molecular dynamics (MD) simulations has enabled atomistic elucidation of interfacial polarization, solvation, and defect-induced charge localization. These simulations clarify how dopants, vacancies, and interfacial functional groups tailor energy-level alignment and electronic coupling strength [26]. Furthermore, data-driven interface engineering, supported by high-throughput computation and machine-learning algorithms, is emerging as a transformative paradigm for predictive interface design.

1.4 Concluding remarks and prospects

Graphene and graphene-based composites hold substantial promise for energy storage. While notable challenges remain, continued advances in materials science and processing are poised to establish these systems as core components of future energy technologies. To accelerate widespread application, precision structural design should leverage AI-guided discovery and advanced computational modeling to control atomic-level structures and multiscale morphologies, enabling graphene-based materials with directional ion-transport channels and highly efficient electron-conduction networks. For operation under extreme conditions, pairing tailored electrodes with next-generation electrolytes to construct stable, low-impedance electrode–electrolyte interfaces will be critical to enhancing cycle life and safety. Finally, deep interdisciplinarity-bridging materials science, chemistry, physics, and energy engineering will remain a driving force for innovation in graphene-based composites.

2. Black phosphorus for energy storage

Ze Yang*, Ying Yu

2.1 Status

Black phosphorus (BP), particularly in its few-layer form known as phosphorene, has emerged as a highly promising 2D material for energy storage applications, including alkali-metal ion batteries (Li/Na/K ion batteries), Li-S batteries, and supercapacitors [27,28]. It exhibits a set of unique fundamental properties that distinguish it from other 2D materials such as graphene and transition metal dichalcogenides (TMDs). Notably, BP possesses a layer-dependent direct bandgap, tunable from approximately 0.3 eV in the bulk form to 2.0 eV in a monolayer, effectively bridging the electronic gap between zero-bandgap graphene and large-bandgap TMDs [29]. This is complemented by exceptionally high charge carrier mobility (up to $1000 \text{ cm}^2 \text{ V}^{-1} \text{ s}^{-1}$) and a high theoretical specific capacity for alkali-metal ion batteries (e.g., 2596 mAh/g) [30]. These properties are intrinsically linked to its anisotropic, puckered crystal structure. Among the three crystalline allotropes of phosphorus (orthorhombic, rhombohedral, and cubic), the orthorhombic phase is more thermodynamically stable under ambient conditions and is the primary focus of research. In the orthorhombic structure (space group: *Cmca*), phosphorus atoms are covalently bonded within each layer, forming a puckered honeycomb architecture with strong in-plane anisotropy [29]. The layers are held together by weak van der Waals interactions, facilitating exfoliation down to monolayer phosphorene. The combination of tunable interlayer spacing, high surface-to-volume ratio, and structurally adaptive channels makes BP an ideal platform for enhancing electrochemical performance through efficient ion intercalation, abundant redox-active sites, and versatile charge storage mechanisms (Fig. 3).

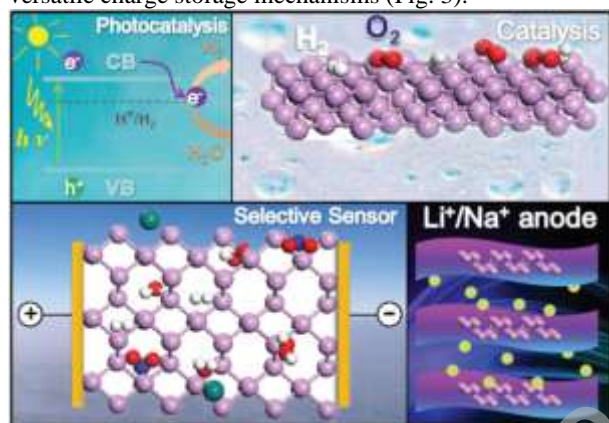


Fig. 3. Scheme showing various applications of black phosphorus.

2.2 Current and future challenges

Despite its promising characteristics, the integration of BP into energy storage systems faces several universal and application-specific challenges. A major issue common to all applications is its inherent susceptibility to ambient degradation, arising from the high reactivity of lone-pair electrons on phosphorus atoms with oxygen and moisture, which necessitates advanced protection strategies [29]. Additionally, scalable and high-quality synthesis remains difficult due to strong interlayer van der Waals forces and anisotropic crystal growth behavior [29]. These fundamental challenges are further compounded by application-specific limitations: in alkali-metal ion batteries, significant volume expansion during cycling causes mechanical degradation and loss of electrical contact, leading to rapid capacity fading [31]; in supercapacitors, the moderate intrinsic electrical conductivity limits rate performance [32]. Addressing these issues requires tailored material designs and multidisciplinary approaches to improve stability, optimize synthesis, and enhance electrochemical performance for each target application.

2.3 Advances in science and technology to meet challenges

Conventional strategies to improve BP stability include covalent functionalization, noncovalent interactions, and van der Waals encapsulation [33]. However, these strategies often rely on trial-and-error approaches and lack systematic design principles. Recently, Yu *et al.* [33] introduced an AI-driven methodology combining large language models (LLMs) and machine learning (ML) to enable rational molecular engineering. Their framework used GPT-4o to extract knowledge from scientific literature and recommend under-explored functional head groups (e.g., $-\text{SiR}_3$, $-\text{PR}_2$, and $-\text{SH}$) with high binding affinity to BP. A graph neural network (GNN)-based high-throughput screening workflow was then applied to evaluate over 117 million molecules from PubChem, identifying 662 candidates with optimal interaction energies (e.g., strong BP adsorption and weak H_2O interaction). The superior stabilization effect of Si-, P-, and S-based head groups can be mechanistically attributed to robust orbital hybridization and interfacial charge transfer between the functional moieties and surface P atoms. This strong electronic coupling effectively passivates dangling bonds, suppresses the formation of surface P_xO_y species, and preserves the structural integrity of BP under ambient and electrochemical conditions. Beyond simple environmental exposure, such chemical anchoring has been shown to significantly enhance long-term electrochemical durability by mitigating interfacial degradation, maintaining high carrier mobility, and reducing the loss of active sites during extended

cycling. These mechanistic insights establish a clear structure–property relationship between molecular anchoring chemistry and device-level stability.

Importantly, the integration of AI-assisted molecular discovery with interfacial engineering not only accelerates identification of stabilizing functional groups, but also enables predictive optimization of multi-objective performance, including capacity, rate capability, and cycle life. AI/ML-driven modeling can further forecast long-term degradation mechanisms under various electrochemical and environmental conditions, guiding rational design of BP-based electrodes and heterostructures for high-energy and durable devices. This approach provides a comprehensive, scalable strategy that bridges molecular-level design and device-level performance, aligning with broader AI/ML-enabled roadmaps for 2D material development.

Although centimeter-scale ultrathin BP films have been successfully fabricated using pulsed laser deposition (PLD) [34], achieving large quantities of BP remains essential for practical energy storage applications. In this regard, high-energy ball milling has emerged as a scalable alternative capable of converting red phosphorus to BP under ambient temperature and pressure conditions. During the milling process, the localized temperature in the grinding jar can reach approximately 200 °C, while the pressure may exceed 6 GPa, creating a favorable environment for phase transformation [35]. This mechanochemical approach not only enables high-yield production but also ensures satisfactory crystallinity and phase purity.

Although BP faces distinct challenges in different energy storage applications, such as significant volume expansion in alkali-metal ion batteries and intrinsically low electrical conductivity in supercapacitors, a common and effective mitigation strategy involves compositing it with highly conductive materials. Conductive matrices, such as graphene and MXene, are widely employed not only to enhance overall electrical conductivity but also to serve as buffering layers that accommodate mechanical strain and volume changes during cycling. For instance, Cui *et al.* [36] designed a phosphorene–graphene hybrid architecture in which phosphorene layers are sandwiched between graphene sheets. This hybrid material delivered a high specific capacity of 2,440 mAh/g along with remarkable cycling stability. Similarly, Tang *et al.* [31] constructed a hierarchical porous composite incorporating BP and $\text{Ti}_3\text{C}_2\text{T}_x$, which provided stable interfacial interactions and additional hydrogen ion adsorption sites. This design significantly improved both ion and electron transport capabilities while maintaining robust structural integrity. Unlike its role as an anode in alkali-metal ion batteries, phosphorus can serve as an effective adsorbent in Li–S batteries to suppress sulfur shuttling and thus improves the cyclic stability [37]. These examples underscore the versatility and effectiveness of composite engineering in overcoming the inherent limitations of BP across diverse energy storage platforms.

2.4 Concluding remarks and prospects

BP has established itself as a highly promising material for next-generation energy storage technologies due to its unique structural and electronic properties, including tunable bandgap, high carrier mobility, and exceptional theoretical capacity. However, BP need to address its ambient instability, limited scalability, moderate conductivity, and volume expansion in batteries. Significant progress has been made in mitigating these challenges through advanced material strategies including composite formation, chemical functionalization, and heterostructure engineering. Among its potential applications, BP shows the greatest commercial promise as an anode material for lithium-ion batteries, where its high lithium storage capacity can significantly enhance energy density. Nevertheless, before widespread commercialization can be realized, further research is imperative to overcome the existing limitations in scalability, stability, and integration into battery systems.

3. MXene materials for electrochemical energy storage

Sepehr Tabibi, Alireza Khataee*

3.1 Status

2D materials, particularly MXenes, have rapidly expanded since graphene’s discovery [38–40]. MXenes are derived from MAX phases $\text{M}_{n+1}\text{AX}_n$ ($n = 1–4$), where A belongs to groups 13–16, M is a transition metal, and X is C or N (Fig. 4a). By selectively etching the A-layer (*e.g.*, Ga, Al, Si), MXenes such as Ti_2CT_x , V_2CO_2 , or $\text{Nb}_4\text{C}_3\text{Cl}_2$ are obtained, often with surface terminations (T_x) [41]. Structural variations include solid solutions ($(\text{M}', \text{M}'')_{n+1}\text{X}_n\text{T}_x$), i-MXenes (in-plane ordering, with formula $\text{M}'_{4/3}\text{M}''_{2/3}\text{XT}_x$, stabilized at a 2:1 $\text{M}':\text{M}''$ ratio with $\geq 0.2 \text{ \AA}$ size difference), O-MXenes (out-of-plane ordering, with formulas $(\text{M}'_2\text{M}'')\text{X}_2\text{T}_x$ and $(\text{M}'_2\text{M}''_2)\text{X}_3\text{T}_x$) [42]. MXenes can be synthesized as delaminated single-layers (d-MXene) or multilayers (ml-MXene), structurally similar to MAX phases with a hexagonal close-packed lattice ($P6_3/mmc$) [43]. Since the first MXene ($\text{Ti}_3\text{C}_2\text{T}_x$) was synthesized, research has mainly focused on their electrochemical properties for ion storage, highlighting their potential in energy storage applications (Fig. 4b) [44].

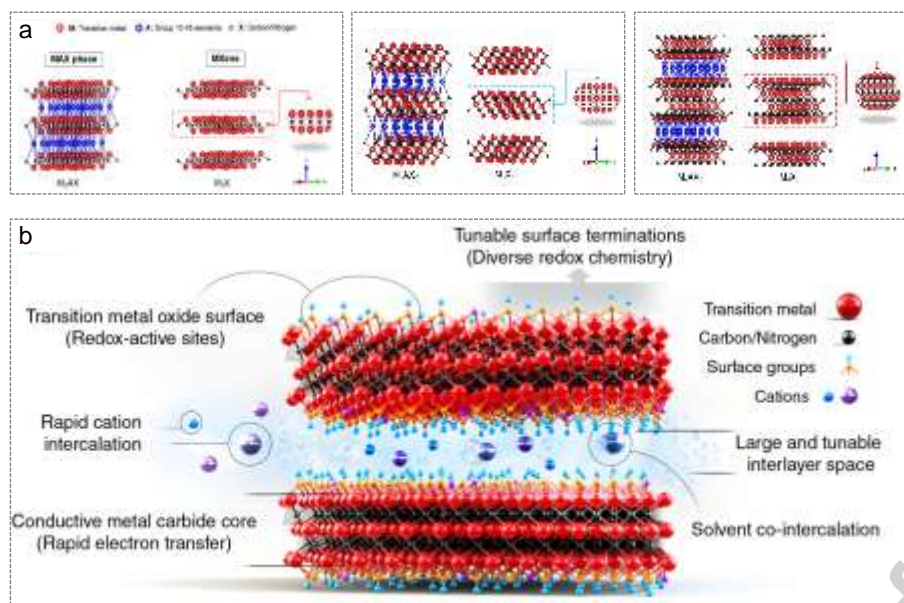


Fig. 4. Schematic illustration of (a) MAX phases and MXene single transition metal structure. (b) MXenes electrochemical properties for ion storage applications. Reproduced with permission [44]. Copyright 2021, AAAS.

MXenes are typically obtained by removing the A-layer of MAX phases using hydrofluoric acid (HF) or *in-situ* HF from fluoride salts. Safer fluoride-free methods with alkaline solutions or molten salts reduce hazardous chemicals, yielding MXenes with higher conductivity and fewer defects [45,46]. Bottom-up approaches such as chemical vapor deposition (CVD) can directly grow nanosheets with tunable thickness, composition, and surface terminations, while electrochemical etching offers precise control [46]. To prevent oxidation, MAX phases are usually synthesized through high-temperature solid-state processes using elemental powders or pre-alloyed precursors in controlled environments. Common methods include spark plasma sintering (SPS) with pressure and pulsed currents for rapid densification, self-propagating high-temperature synthesis (SHS) based on exothermic reactions, and powder metallurgy by compacting and sintering powders [45]. Other routes such as molten salt synthesis and CVD produce highly crystalline MAX phases or thin films with precise stoichiometry. These techniques transform layered MAX phases into versatile 2D MXenes with adjustable properties for electronics, energy storage, and catalysis [44].

3.2 Current and future challenges

MXenes, as promising 2D materials for advanced energy storage systems such as batteries and supercapacitors, offer high electrical conductivity, large surface area, tunable surface chemistry, hydrophilicity, and mechanical robustness, enabling enhanced charge storage, ion transport, and electrode stability. However, their practical deployment faces several challenges [47]. One of the most fundamental issues is chemical instability, particularly surface and edge oxidation in air or aqueous electrolytes, which leads to a significant loss of capacitance, shortened cycle life, and deteriorated long-term performance. Recent studies have revealed that different MXene compositions exhibit distinct oxidation kinetics and pathways. For instance, $Ti_3C_2T_x$ tends to undergo rapid hydrolysis and surface oxide formation, whereas Mo_2CT_x shows relatively slower oxidation rates and different intermediate species. These variations originate from intrinsic material properties, including metal-carbon bond strength, work function, Fermi level position, electronic structure, and surface termination energy. Moreover, the surface functional groups (*e.g.*, $-O$, $-F$, $-OH$) and interlayer spacing play a critical role in controlling oxygen adsorption, water intercalation, and electron transfer, ultimately dictating the oxidation resistance of each MXene type [48-50]. In electrochemical environments, these differences translate into varied stability windows, redox reversibility, and interfacial compatibility with electrolytes. Addressing these issues requires the development of composition- and environment-specific stabilization strategies, such as alloying, heterostructure construction, termination engineering, or protective coating design. A comparative understanding of oxidation kinetics across MXene families is thus essential for rational material selection and device optimization in practical electrochemical systems.

Restacking or aggregation of nanosheets during electrode fabrication decreases accessible surface area and impedes ion diffusion, limiting power density and overall energy efficiency. Additionally, MXenes often exhibit limited performance in non-aqueous electrolytes, while controlling surface terminations ($-OH$, $-F$, $-O$, $-Cl$), which are essential for ion intercalation and electrochemical stability, remains difficult [44]. High irreversible capacity during the first charge-discharge cycle can further reduce practical efficiency, and traditional synthesis methods relying on hazardous fluoride-based acids may produce defect-rich or non-uniform nanosheets. Long-term environmental stability and limited experimental validation of newly predicted MXene compositions further constrain their practical application [51].

To overcome these limitations, current research focuses on functionalization and hybridization with other materials, defect engineering to improve capacitance and rate capability, advanced synthesis techniques to control size, morphology, and surface chemistry, and strategies to enhance environmental stability. Incorporating polymers with polar functional groups, combining MXenes with other 2D or high-entropy MXenes, and exploring related materials such as MAB phases and MBene offer additional routes to improve energy and power density while stabilizing charge-discharge cycles [52]. Future directions may include integrating MXenes with electrode-active materials like lithium iron phosphate (LFP) or lithium nickel manganese cobalt oxide (Li-NMC) to further enhance cycling stability and overall performance in energy storage devices.

3.3 Advances in science and technology to meet challenges

“MXetronics” refers to fully MXene-based devices with versatile electrical, chemical, and mechanical properties. They are widely applied in supercapacitors, providing high capacitance through electric double-layer formation and rapid surface redox reactions [53,54]. In lithium-, sodium-, and potassium-ion batteries, MXenes serve as anode and cathode materials with tunable interlayer spacing, enabling efficient ion intercalation, high-rate capability, and enhanced cycle stability [55-57]. MXenes also act as conductive hosts in metal-sulfur and metal-air batteries, improving electrochemical performance, catalytic activity, and polysulfide adsorption while suppressing dendrite growth [58]. Their flexibility and ability to form composites with carbon or polymers make them suitable for wearable and hybrid energy storage devices. When combined with other 2D materials or high-capacity electrodes, MXenes enhance charge/ion transport, buffer volume changes, and provide smooth charge-discharge profiles, unlike conventional systems that exhibit sharp voltage drops [58,59]. Furthermore, their redox-active surfaces enable efficient energy storage in batteries and supercapacitors, and their high conductivity makes them suitable for current collectors and conductive inks [60]. Acting as conductive binders, MXenes improve charge/ion transport and accommodate the large volume changes of high-capacity materials. Ongoing research addresses challenges such as oxidation, restacking, and long-term stability through surface modification and structural engineering.

In order to solve the problem of layer stacking in 2D MXenes, Zhao *et al.* [61] used a template-assisted approach to produce hollow MXene spheres and 3D macroporous MXene films. While the 3D films are conductive, flexible, and offer improved capacity, cycling stability, rate capability, and when utilized as sodium-ion battery anodes in comparison to traditional MXene structures, the hollow spheres are stable, readily dispersible, and appropriate for environmental and biomedical applications. The significance of electrode design in improving the functionality of MXene-based materials is highlighted by that work.

For hybrid Mg^{2+}/Li^+ batteries, Byeon *et al.* [62] investigated 2D $Ti_3C_2T_x$ as a cathode. With flexible $Ti_3C_2T_x$ /carbon nanotube nanocomposite electrodes, 80 mAh/g was maintained during 500 cycles at 1 C, with about 100 mAh/g at 0.1 C and 50 mAh/g at 10 C. Moreover, Mo_2CT_x MXene worked well as a cathode. For hybrid Mg^{2+}/Li^{2+} battery cathodes, this work indicates the possibility of many 2D MXenes with good conductivity and huge intercalation capacity.

In a related method, Lieu *et al.* [63] created a spherical templating methodology for lithium-sulfur batteries (LSBs) that involved functionalizing $Ti_3C_2T_x$ MXene nanosheets with polymorphic $CoSe_2$ nanoparticles. The multistep sulfur reduction reaction's kinetics are improved by this design, which reduces MXene aggregation and increases electrocatalytic activity. Significant performance enhancements over conventional MXene-based electrodes were demonstrated by the resultant S/MXene- $CoSe_2$ cathode, which showed an extended cycle life of 1000 cycles with a low-capacity decay rate of 0.06 % per cycle.

In order to reduce competing oxygen evolution events and overcome the hydrophobic characteristic of carbon electrodes, Botling *et al.* [64] investigated $Mo_2TiC_2T_x$ MXene-coated carbon electrodes for vanadium redox flow batteries (VRFBs). Using a drop-casting technique, three different kinds of carbon paper were either heat-treated or coated with MXene. The existence of Mo and Ti elements as well as consistent MXene coating were verified by SEM and XPS analysis. The results of electrochemical testing showed that MXene-coated electrodes held their own against heat-treated electrodes in terms of reaction rates, diffusion coefficients, and discharge capacity retention (75 %). However, the coated electrodes had a relatively greater resistance ($1.2 \Omega \text{ cm}^2$ compared to $0.8 \Omega \text{ cm}^2$) and a lower energy efficiency (71 % vs. 79 %). The MXene layer's stability was validated by post-cycling XPS analysis, underscoring its potential as a successful surface modification for VRFB electrodes.

As a high-performance cathode for lithium-ion batteries (LIBs), Zhang *et al.* [65] studied carbon-coated $LiFePO_4$ (C@LFP/MXene) decorated with hierarchically porous $Ti_3C_2T_x$ MXene. $LiFePO_4$ has weak electrical conductivity and low lithium-ion diffusivity; however, the MXene decoration improved ion and electron transport by adding a conductive network and porous architecture. MXene's partial oxidation to carbon and TiO_2 during cycling promoted the diffusion of lithium even further. The best performance was obtained by C@LFP/MX-3.0 among composites with different MXene contents, with discharge capacities of 165.9, 164.1, 161.0, 154.7, 147.7, and 140.3 mAh/g at 0.5, 1, 2, 5, 10, and 20 C, respectively. It also demonstrated outstanding long-term cycling stability, holding onto 156.6 mAh/g (94.8 %) after 500 cycles, and a low charge-transfer resistance ($R_{ct} = 17.26 \Omega$). The efficiency of C@LFP/MX-3.0 is demonstrated by the flat voltage plateaus and strong capacity retention across various rates (Fig. 5), underscoring the promise of 2D MXenes for multifunctional electrode design in high-rate LIBs.

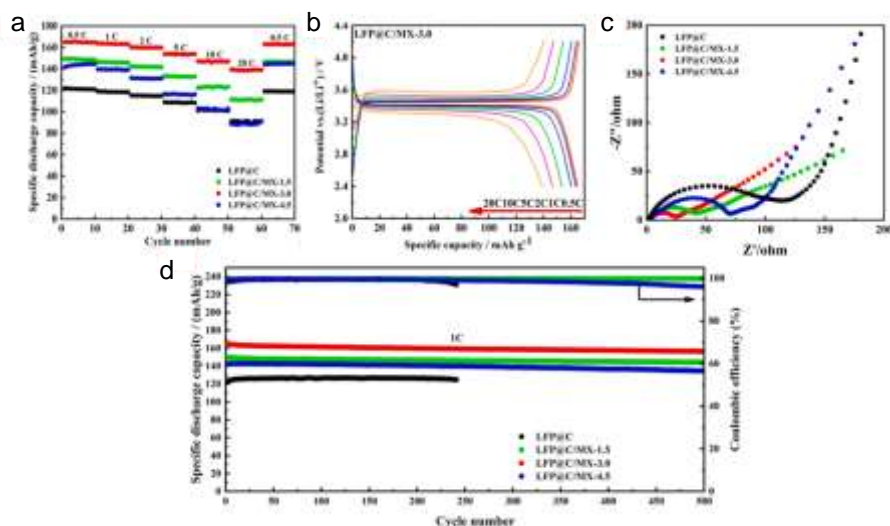


Fig. 5. (a) Carbon-coated LiFePO₄, carbon-coated LiFePO₄/Ti₃C₂T_x-1.5, carbon-coated LiFePO₄/Ti₃C₂T_x-3.0, and carbon-coated LiFePO₄/Ti₃C₂T_x-4.5 rate performance. (b) Initial charge/discharge curves of carbon-coated LiFePO₄/Ti₃C₂T_x-3.0 electrodes with various rates. (c) Nyquist curves and (d) cycle number of carbon-coated LiFePO₄, carbon-coated LiFePO₄/Ti₃C₂T_x-1.5, carbon-coated LiFePO₄/Ti₃C₂T_x-3.0, and carbon-coated LiFePO₄/Ti₃C₂T_x-4.5 electrodes. Reproduced with permission [65]. Copyright 2021, Elsevier.

A self-supporting 3D cathode made of MXene, carbon nanotubes (CNTs), cellulose, and LiFePO₄ (3D-MCC-LFP) was created by Dong *et al.* [66] to solve structural instability, transport restrictions, and Li⁺ loss in high-loading cathodes. 3D-MCC-LFP offers better electrochemical performance, increased electrical and ionic conductivity, and larger active material loading (up to 120 mg/cm²) than traditional LFP cathodes. In comparison to conventional electrodes, the 3D-MCC-LFP10 demonstrated superior performance, achieving 0.86 mAh/cm² at 5 C and maintaining 1.45 mAh/cm² after 500 cycles. The ultrahigh areal capacity of 19.2 mAh/cm² was provided by the high-loading 3D-MCC-LFP₁₂₀, whereas the entire cell of a 3D-MCC-LFP60/SnO₂ achieved 6.3 mAh/cm² at 1.6 mA/cm². The potential of 3D-MCC-LFP cathodes for high-energy density LIBs is demonstrated by these results. Beyond cathodes, MXene has also been employed as a conductive, adaptable, and electrochemically active binder in flexible supercapacitor electrodes. By embedding activated carbon particles within MXene layers, insulating polymer binders are eliminated, and a 3D conductive network with expanded interlayer spacing is formed. In this configuration, MXene simultaneously serves as active material, conductive additive, binder, and structural backbone, leading to enhanced capacitance and rate capability. Such electrodes demonstrate promising performance for high-efficiency flexible supercapacitors, achieving a specific capacitance of 126 F/g at 0.1 A/g and retaining 57.9 % of the capacitance at 100 A/g in organic electrolytes.

Asymmetric bilayered V₂O₅ supercapacitors using vanadium and niobium MXenes were investigated by Saraf *et al.* [67]. At high anodic potentials, MXenes experience irreversible oxidation while having excellent conductivity and redox capacitance. They can improve energy storage and widen the voltage window when combined with oxides. Although it has low cyclability, hydrated lithium-preintercalated V₂O₅ (δ -Li_xV₂O₅·nH₂O) offers excellent capacity at increased potentials. It was used with V₂C and Nb₄C₃ MXenes to get around this. The voltage windows of asymmetric devices with δ -Li_xV₂O₅·nH₂O/CNT as the positive electrode and Li-V₂C or TMA-Nb₄C₃ as the negative electrode in 5 m LiCl were 2 and 1.6 V, respectively. It maintained around 95 % of its capacitance after 10,000 cycles.

To print micro-supercapacitors directly, Zhang *et al.* [60] created additive-free Ti₃C₂T_x MXene inks. The resolution and scalability of conventional printed inks are limited by their low concentrations or frequent requirement for surfactants. Aqueous and organic MXene inks, on the other hand, were developed with no additives for extrusion and inkjet printing, allowing for the creation of homogeneous, high-resolution structures on untreated plastic and paper, including resistors, conductive tracks, and micro-supercapacitors. Volumetric capacitance and energy density of the printed micro-supercapacitors were significantly higher than those of previously printed materials, indicating the promise of additive-free MXene inks for integrated, scalable printed electronics.

3.4 Advances in science and technology to meet challenges

In conclusion, MXenes have demonstrated clear advantages as electrode materials for advanced energy storage, owing to their mechanical robustness, two-dimensional architecture, and high electrical conductivity. Their performance has benefited from progress in synthesis control, surface chemistry tuning, and heterostructure design with other two-dimensional materials. However, the realization of practical device applications depends increasingly on industrial feasibility. Key priorities include lowering synthesis costs, developing environmentally benign and scalable production routes, and establishing standardized processing methods that are compatible with large-area and high-throughput manufacturing. Equally important is the systematic evaluation of environmental and lifecycle impacts to ensure sustainable deployment. With coordinated advances in scalable synthesis, device integration, and

sustainability frameworks, MXenes are expected to play a central role in the development of next-generation energy storage technologies.

4. 2D covalent organic frameworks for energy conversion and storage

Lei Hao, Qitao Zhang*

4.1 Status

Two-dimensional covalent organic frameworks (2D COFs) represent a class of materials featuring 2D networks formed by organic molecules interconnected *via* covalent bonds [68,69]. They possess highly ordered pore channels, tunable chemical composition, and excellent charge transport properties. In the field of energy conversion and storage, 2D COFs demonstrate broad application potential due to their unique physicochemical characteristics, such as large specific surface area, high porosity, and designable band structures [70,71]. As illustrated in Fig. 6, 2D COFs are employed in photovoltaic solar cells, photocatalysis, electrocatalysis and photoelectrocatalysis, including water splitting (water oxidation), CO₂ reduction and H₂O₂ synthesis, serving as catalysts or supports for metal active sites. They enhance energy conversion efficiency by facilitating the efficient separation of photogenerated charge carriers [72,73]. In energy storage, covalent organic frameworks exhibit promising capacitive responses and high capacitance potential. This capacitive behavior of COFs, owing to their strong designability and tunability, has attracted significant attention. However, their further development in energy conversion and storage applications is severely constrained by high electron-hole recombination rates and limited electrical conductivity [74,75].

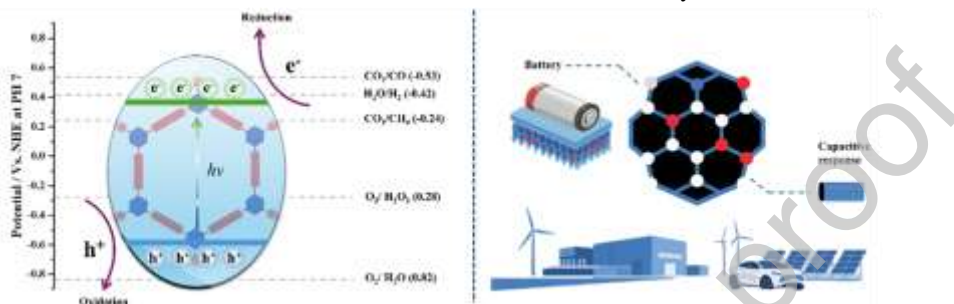


Fig. 6. Energy conversion and storage of 2D COF.

In recent years, researchers have further improved the charge carrier separation capability of 2D COFs by modulating the donor-acceptor (D-A) characteristics of their building blocks to enhance the push-pull ability towards photogenerated electrons within the framework. This approach has subsequently led to the development of structures like D- π -A and D-A-A, which suppress charge carrier recombination and thereby enhance photocatalytic performance [76-78]. Additionally, functionalizing the structural backbone represents a significant strategy for boosting the performance of 2D COF-based materials in energy conversion. Grafting functional groups with different electronegativities significantly influences charge carrier transport dynamics within the COF framework, consequently affecting its performance [79,80]. Finally, constructing heterojunctions, particularly COF/organic/inorganic heterojunction interfaces formed *via in situ* or one-pot methods, markedly improves interfacial charge carrier transport efficiency. The incorporation of materials like conductive polymers, metal chalcogenides, and metal oxides to create hybrid systems enhances both mass and charge transfer efficiency [81-83].

4.2 Current and future challenges

Despite their promising potential in energy applications, the practical deployment of 2D COFs faces multiple challenges. High electron-hole recombination rates and limited electrical conductivity remain major bottlenecks hindering their further development in energy conversion and storage [84,85]. Currently, the primary limiting factors in the energy conversion field include the uncertain structure-property relationships, ambiguous active sites, and severe charge carrier recombination [86]. Firstly, the highly challenging preparation of single-crystalline 2D COF-based materials has resulted in a lack of precise structural validation for non-single-crystalline COF materials when correlating theoretical calculations with experimental observations. This impedes the effective understanding of exact active sites and specific reaction mechanisms [87]. Secondly, severe charge carrier recombination arises from the combined effects of intrinsic structural defects in 2D COF semiconductors, dimensional confinement, and external perturbations. High exciton binding energy hinders the generation of free charge carriers, while low carrier mobility and ubiquitous structural imperfections markedly increase the probability of recombination [88]. Furthermore, the weak interlayer coupling in 2D COFs represents a major bottleneck that limits the establishment of efficient vertical charge transport pathways, thereby aggravating charge carrier recombination. Although in-plane π -conjugation and ordered frameworks provide favorable charge transport channels, interlayer connections typically rely only on weak van der Waals forces or π - π stacking interactions. This poor interlayer coupling makes vertical charge migration difficult, causing charge carriers to accumulate within individual layers. As a result, photogenerated electrons and holes cannot be effectively separated in space, which further accelerates intralayer recombination processes [89]. To address this issue, several synthetic and post-synthetic strategies have been developed to enhance interlayer electronic interactions and construct more efficient three-dimensional charge transport networks.

(1) Interlayer covalent linkage. Introducing covalent cross-linkers or dynamic covalent bonds between adjacent COF layers can transform weak van der Waals stacking into robust conjugated frameworks. For example, post-synthetic imine-to-amide conversion or boronate ester crosslinking has been demonstrated to form strong interlayer bridges, thereby promoting orbital overlap and facilitating charge delocalization across layers.

(2) π - π stacking engineering. Rational modulation of the planarity and electronic structure of organic building blocks (*e.g.*, incorporating larger π -conjugated units, electron-rich donors, or electron-deficient acceptors) can enhance face-to-face stacking. Stronger π - π interactions reduce interlayer spacing, increase wavefunction overlap, and accelerate interlayer charge hopping kinetics.

(3) Pillared and hybrid architectures. Introducing rigid molecular pillars or integrating 1D/2D inorganic units between layers enables the formation of ordered pillared COFs or hybrid COF-MOF heterostructures. These architectures provide well-defined vertical charge transport channels and improve dimensional connectivity, effectively bridging the interlayer gap.

(4) External-field and templating strategies. Applying external stimuli such as pressure-assisted synthesis, epitaxial growth, or electrochemical induction can improve crystallinity, minimize stacking disorder, and align layers more regularly. This structural alignment facilitates efficient interlayer charge transfer.

Collectively, these strategies transcend simple in-plane π -conjugation by establishing interconnected 3D charge percolation networks. Such enhanced dimensionality not only suppresses exciton recombination but also significantly improves photocatalytic and photoelectrochemical performance. This layered-to-3D transition is anticipated to be a pivotal design paradigm for next-generation high-performance COF-based energy conversion and storage systems.

In energy storage, while 2D COFs show promising potential due to their inherent material advantages, challenges remain. The inherent organic framework generally results in poor intrinsic electronic conductivity, leading to inefficient charge transport kinetics and limited ion transport rates within the pores; this constrains the improvement of charge carrier mobility in electrochemical applications [90,91]. Furthermore, the chemical and structural stability under long-term electrochemical cycling, especially under extreme potentials or in electrolyte environments, requires further validation and enhancement. Precise modulation of pore size, shape, and surface chemistry to fully optimize specific energy storage mechanisms (*e.g.*, ion size matching, solvation effects) remains difficult [92]. Finally, their synthesis typically involves complex solvothermal processes, high costs, and difficulties in large-scale production, limiting its applications.

4.3 Advances in science and technology to meet challenges

To overcome the aforementioned challenges and advance 2D COFs in energy conversion and storage, researchers have proposed a variety of practical and feasible solutions to address these issues, as summarized in Fig. 7. For instance, numerous COF-based materials by altering the combinations of diverse synthetic building blocks were designed and synthesized, significantly propelling their development. Utilizing different chemical reactions, COFs with varied covalent linkages (*e.g.*, imine, amide, C=C double bonds, azo bonds) have been prepared, partially improving the stability and catalytic performance of 2D COF-based materials [93]. Changes in building block configuration also alter the pore structure, which plays a crucial role in enhancing ion and charge transport. Furthermore, introducing heteroatoms into the framework provides an excellent platform for band structure modulation, orbital tuning, and subsequent single-atom coordination and anchoring. Particularly in electrocatalysis, precisely incorporating heteroatom-containing functional units (*e.g.*, bipyridine, imide) optimizes the coordination environment and electronic structure of active metal centers (*e.g.*, Cu, Ni single atoms), enhancing their adsorption and conformational control of key intermediates [94-96]. Simultaneously, the confinement effect of their ordered nanochannels finely regulates reactant concentration, intermediate conformation, and product diffusion. This synergistic "spatial confinement" and "electronic structure modulation" significantly improve the selectivity for high-value products. Precise functionalization of the structural backbone (*e.g.*, quinone, phenazine, bipyridinium salts, triphenylamine) enables accurate design and arrangement of redox sites, which is essential for achieving high-density, rapid-response Faradaic reactions. This design significantly enhances specific capacitance, broadens the operating voltage window, while maintaining fast charge/discharge rates and ultra-long cycle life [97].

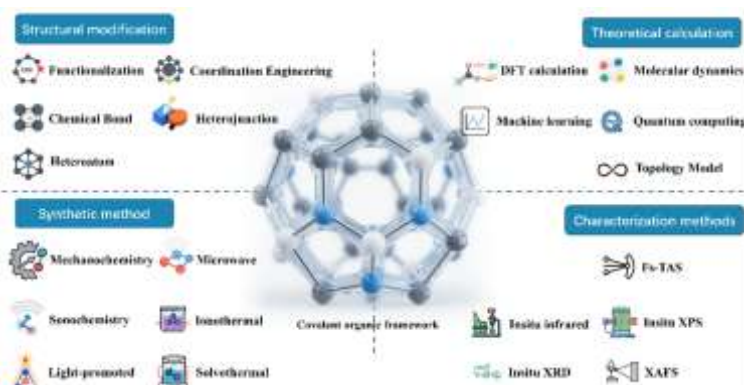


Fig. 7. The scientific and technological progress of 2D COF in meeting challenges.

In synthetic techniques, to meet the demands of diverse application scenarios, several methods beyond traditional solvothermal synthesis have been developed, including physical grinding, ultrasonication, melt synthesis, and microwave-assisted synthesis. These novel approaches broaden the application scope of 2D COFs with varied morphologies and crystallinities [85,98]. They also provide technical support for the *in situ* construction of various 2D COF/organic/inorganic heterojunctions [99]. COF-based heterojunction composites, particularly those based on Z-scheme or S-scheme architectures, optimize charge separation efficiency through band alignment, significantly increasing the utilization of active electrons [100-102]. Hydrophobic surface modifications enhance electrolyte compatibility and reduce catalytic site deactivation [103]. Furthermore, the development of single-crystalline 2D COFs remains in its early stages, while the controllable synthesis of large-area films/nanosheets represents another key area of advancement. The controlled fabrication of these devices is advancing 2D COFs from laboratory research toward practical energy devices.

The development of 2D COFs in energy conversion and storage is inseparable from computational modeling and *in situ* characterization, while their advancement simultaneously drives progress in these fields. In recent years, revolutionary advances in theoretical calculations and *in situ* characterization techniques have mutually driven and deeply integrated, forming the core driving force for revealing structure-property relationships, understanding working mechanisms, and guiding rational design. Theoretical calculations have evolved from static structure prediction to dynamic process simulation: DFT and higher-accuracy methods can precisely predict and optimize the band structure, charge carrier mobility, active site distribution, and ion diffusion pathways of 2D COFs [104-106]. High-throughput computation combined with machine learning algorithms enables efficient screening of candidate structures with target properties (*e.g.*, high specific capacity, superior catalytic activity, rapid ion conduction) from vast libraries of potential monomers [107-109]. Multiscale simulations (from quantum chemistry to molecular dynamics) provide deep insights into the kinetics of ion intercalation/deintercalation during charge/discharge cycles, charge transfer mechanisms along catalytic reaction pathways, and the microscopic origins of material structural stability changes, offering crucial theoretical guidance for experimental synthesis and device design [110]. Concurrently, *in situ* X-ray diffraction (XRD) and small-angle X-ray scattering (SAXS) track the evolution of crystal structure, phase transitions, and changes in order in real-time; *In situ* spectroscopic techniques (Raman, IR, UV-vis absorption, X-ray absorption fine structure spectroscopy (XAFS)) dynamically monitor chemical bond vibrations, electronic structure transitions, elemental valence states, coordination environments, and active site status [92]. These data directly verify and refine theoretical models, accurately revealing previously elusive key processes such as rate-limiting steps in ion storage/transport, the dynamic formation and evolution mechanisms of catalytic active centers, and structural degradation pathways during cycling. The strong coupling between theoretical calculations and *in situ* characterization not only greatly accelerates the targeted development of high-performance 2D COF materials but also advances mechanism-level understanding of complex energy conversion and storage processes.

4.4 Concluding remarks and prospects

2D COFs have emerged as highly attractive platform materials in energy conversion and storage due to their highly ordered pore structures, tunable chemical composition, and excellent charge transport potential. In recent years, significant breakthroughs have been achieved in enhancing charge carrier separation efficiency, optimizing band structures, improving electrical conductivity, and refining ion transport kinetics. These advances are realized through rational structural design (*e.g.*, D-A, D- π -A units, precise functionalization), innovations in synthetic techniques (diverse bonding motifs, novel synthetic methods), and composite strategies (heterojunction construction, single-atom anchoring). The deep integration of theoretical calculations with *in situ* characterization techniques—particularly multiscale simulations and dynamic process monitoring—has not only profoundly deepened the understanding of structure-property relationships, charge transfer mechanisms, and reaction pathways but also accelerated the targeted development of high-performance 2D COF materials.

Nevertheless, core challenges for 2D COFs in energy conversion and storage remain severe: High electron-hole recombination rates and inherent low electrical conductivity persist as performance bottlenecks. Difficulties in preparing single-crystalline materials impede precise structural validation for active site and reaction mechanism studies. Weak interlayer interactions restrict interlayer charge transport. For energy storage, long-term cycling stability, precise pore modulation, and scalable production require urgent solutions. Future research must focus on multidimensional collaborative optimization. Developing universal techniques for the controllable synthesis of single crystals/large-area films is essential to provide a foundation for precisely resolving active centers and mechanisms. Exploring high-mobility frameworks (*e.g.*, fused-ring aromatics, graphdiyne-type COFs), innovating dimensional engineering (*e.g.*, vertical orientation, intercalation modulation), and integrating multifunctional elements (*e.g.*, redox-active moieties, ion channel modification) should synergistically enhance charge separation, transport, and interfacial kinetics. Utilizing advanced *in situ*/operando characterization combined with artificial intelligence will enable real-time analysis of carrier behavior, interfacial reactions, and structural evolution to guide precise design. Developing green, efficient, and scalable synthetic processes, along with systematic evaluation of material stability and lifespan under realistic device conditions, is crucial. The advancement of 2D COFs will increasingly rely on deep interdisciplinary integration. Converging synthetic chemistry, condensed matter physics, computational science, and chemical engineering will enable the atomically precise construction of intelligent framework materials possessing high

activity, conductivity, stability, and rapid mass transport. This integrated approach will propel 2D COFs from laboratory prototypes toward practical energy devices, offering transformative solutions for efficient and clean energy conversion and storage.

5. 2D metal oxide nanosheet-based electrodes for charge storage devices

Artem Lobinsky*, Maria Kaneva, Vadim Popkov

5.1 Status

Metal oxide nanosheets in 2D have become a highly promising class of materials for energy storage technologies because of their unique physicochemical properties compared to their bulk counterparts [111]. Their ultrathin morphology offers very high specific surface area, many electroactive sites, and shorter ion diffusion pathways, while also providing significant structural stability upon cycling because of intrinsic in-plane rigidity and out-of-plane flexibility. Additionally, the layered structures of these oxides facilitate the intercalation/deintercalation of ions; they can also be functionalized differently, through doping, defects, or incorporation of small molecules or anions to improve electronic conductivity and increase redox activity. Many of these features essentially define their applicability and attractiveness as electrode materials in advanced charge storage technologies [112,113].

A wide spectrum of binary oxides such as RuO_2 , MnO_2 , NiO , TiO_2 , Co_3O_4 , V_2O_5 , and MoO_3 , together with ternary systems including FeCo_2O_4 , CuCo_2O_4 , NiCo_2O_4 , ZnCo_2O_4 , and related compounds, have been systematically investigated as electrodes for supercapacitors, Li/Na/K-ion batteries, and hybrid energy storage devices. Recent studies demonstrate that 2D oxide electrodes can simultaneously improve cyclic lifetime, power density, and energy density, while also enhancing the storage capacity of conventional materials. Over the past five years, research has increasingly shifted toward the design of heterostructured and composite electrodes, particularly hybrids of 2D nanosheets with carbonaceous matrices (graphene, MXenes, CNTs) or conductive polymers. Such configurations generate pronounced synergistic effects, enabling enhanced conductivity, mechanical integrity, and charge-storage kinetics, and ultimately delivering improved energy–power balance together with prolonged cycling stability [114].

Multiple synthetic approaches have been developed for 2D metal oxide nanosheets, which are generally classified into “top-down” and “bottom-up” methodologies. Both top-down (exfoliation or chemical etching) and bottom-up (hydrothermal growth, sol-gel processing, and chemical vapor deposition) processes facilitate unique access to nanosheets. Top-down processes provide greater scale-up to produce nanosheets which could be important for application and commercialization, while bottom-up methods could allow higher control over nanosheet thickness, phase composition, and defect density. Among these, bottom-up methods are particularly advantageous because of their capability to fine-tune composition, morphology, and crystallinity [115,116]. Within this category, techniques such as successive ionic layer adsorption and reaction (SILAR), atomic layer deposition (ALD), and CVD are especially effective for producing ultrathin nanosheets with well-defined parameters [117,118].

Recent developments support more sophisticated atomic-scale modifications (*e.g.*, oxygen vacancies, edge engineering, and strain control) to fine-tune electrochemical behavior. Although atomic-level design is relatively recent, operando and *in situ* spectroscopic or microscopic measurement techniques have provided unparalleled insights into the ion transport, phase changes, and structural dynamics of 2D oxide electrodes, providing building blocks for designer principles for next-generation charge storage devices [119].

Collectively, these advances emphasize the strong potential of 2D metal oxide nanosheets to overcome the traditional trade-off between high energy density and rapid charge–discharge performance.

5.2 Current and future challenges

Despite remarkable progress, the intrinsically low electronic conductivity of 2D metal oxide nanosheets remains a key bottleneck for their practical implementation in energy storage devices. Compared with carbon-based or metallic 2D materials, their poor charge transport severely limits rate capability. Current strategies mainly rely on hybridizing oxide nanosheets with conductive matrices such as graphene, MXenes, and carbon nanotubes to construct external transport pathways. While effective, these approaches increase system complexity, lower volumetric energy density, and may introduce interfacial resistance, restricting large-scale deployment. To address these limitations, recent studies have increasingly focused on intrinsic conductivity enhancement through electronic structure engineering, aiming to metallize or semi-metallize oxide nanosheets without external additives. Representative strategies include heteroatom doping, which tailors band structures and increases free carrier concentration [120]; Defect engineering, through the introduction of oxygen vacancies or precisely controlled point defects, creates localized electronic states near the conduction band, thereby facilitating improved electronic conduction [121]; Phase transformation, which stabilizes metastable conductive polymorphs with narrowed bandgaps and metallic behavior; and mixed-valence engineering, in which partial reduction of metal centers produces delocalized electrons and enhances carrier density [122]. These intrinsic strategies mark a paradigm shift from conventional composite approaches toward electronic structure–driven performance optimization. By inducing semi-metallic or metallic behavior within the oxide lattice, they minimize interfacial resistance, accelerate charge transport, and improve both rate capability and cycling stability. Moving forward, integrating these methods with scalable synthesis and advanced *in situ* characterization will be critical to unlocking the full potential of 2D metal oxides for next-generation energy storage technologies.

Another major potential limitation relates to mechanical degradation during repeated cycling because of advancing strain in the oxide lattice, leading to restacking of nanosheets, lattice distortion, and eventual degradation of the electrode material. Over time, this will

lead to loss of capacity retention. This is particularly critical in high-capacity oxides such as MnO_2 or V_2O_5 where lattice strain is severe and structural collapse is nearly unavoidable at fast charge–discharge rates [123-125].

A component preventing the development of 2D metal oxide nanosheets is producing nanosheets that can be scaled for practical applications. Bottom-up approaches are precise and tunable but are generally time- and energy-intensive methods that limit throughput and cost. Conversely, top-down approaches produce nanosheets that have heterogeneous sizes and irregular thicknesses, and defect density. Developing a synthesis protocol that promotes structural precision and industrial-scale synthesis, is a challenge that has not been totally resolved while maintaining the structural integrity and electrochemical performance of nanosheets.

From the application perspective, integration into flexible-, wearable- and micro-scale devices creates additional complications. These include working with devices that need to be sensitized and mechanistically functional post bending, twisting or any other repeated deformation, together with working with flexible electrolytes, and working in environments requiring safe control under dynamic activity. Managing these issues, in concert with improving conductivity, structural stability, scalability to commercial manufacturing, and scalability of synthesis, will shape the future of electrochemical devices using nanosheets of 2D metal oxide over the next ten years.

5.3 Advances in science and technology to meet challenges

In recent years, various efforts have focused on overcoming the limitations of 2D metal oxide nanosheets. An effective approach has been to fabricate composites and hybrid systems with metal oxides and other functional nanomaterials. Constructing hierarchical structures with MXenes, graphene, or conducting polymers could significantly enhance the electrical conductivity, mechanical strength, and electrochemical stability. Studies have demonstrated that defect engineering (*e.g.*, oxygen vacancies and heteroatom substitution), element doping, and coupling with conductive substrates can significantly enhance charge transport and redox activity. The interlayer spacing of nanosheets can also be increased to enable greater ion access, while also improving charge–discharge capacity.

Additionally, preventing nanosheets from restacking is another important avenue. Interlayer engineering *via* pillaring with organic molecules, polymer spacers, or other nanoscale inorganic materials will help to maintain the exposed surface area and ionic diffusion pathways. Strain engineering and modulating phases by converting between amorphous and crystalline domains have also been shown to thwart degradation by volumetric changes during long-term cycling [126,127].

Concurrently, computational modeling and machine learning are accelerating the discovery of new materials. Data-driven methods allow for the rapid screening of not only dopant chemistries and defect structures including 2D materials but also heterostructure architectures, aimed at designing an electrochemical process that achieves optimal performance. When combined with state-of-the-art "operando" instrumentation like synchrotron X-ray diffraction, cryo-TEM, or *in situ* spectroscopy, this will provide information on charge storage at the atomic scale, as well as the changes in structure while operating. Sustainability of materials will also transform the landscape of research. More attention is being devoted to oxide materials derived from Earth abundant and environmentally benign materials like Fe, Mn, and Ti. The synthesis of green oxides using biomolecule templates or low-temperature aqueous based methods, or the use of clean and energy-efficient fabrication methods, is taking hold and further aligns the field with the mission of sustainable energy technology. Together, these advances establish 2D metal oxide nanosheets as a platform for optimized charge storage in high performance electrodes, but more broadly, as flexible systems that merge foundational materials research with real world applications in devices.

5.4 Concluding remarks and prospects

The rapid advancement of 2D metal oxide nanosheets has highlighted their critical potential for the next-generation of advanced energy storage technologies. With their tunable structure, large electroactive surface area and affinity for use within different hybrid systems, nanosheets can mitigate the longstanding compromise regarding energy-density and power density.

While nanosheet-based electrodes have demonstrated good performance with respect to both energy and power delivery, further optimization of their structure is required to enhance their cycling stability. Nanocomposites and nanohybrids in particular have proven beneficial in instigating synergistic effects, thereby addressing the aforementioned requirements of contemporary charge storage devices. However, the translation of these advances from laboratory level research to industrial manufacture continues to be challenging, and more innovations are needed towards that end. These aspects are summarized in a schematic roadmap shown in Fig. 8.



Fig. 8. Schematic representation of the roadmap for 2D metal oxide nanosheet-based electrodes.

On the other hand, the incorporation of 2D nanosheet into flexible, wearable, and microscale devices will reveal one of the most compelling avenues forward. Their natural mechanical flexibility facilitates their utilization in portable electronics, biomedical implants, and self-powered sensors. In addition, simultaneous attempts to couple nanosheets to solid state and quasi-solid-state electrolytes will generate even safer and higher performance miniaturized storage systems.

In addition to classic electrochemical storage, the multifunctionality of 2D metal oxides provides opportunities for applications in electrocatalysis and sensing, as well as environmental applications like water purification. These emerging pathways also indicate that “all-in-one” devices, in which energy storage functions will be combined with catalytic or sensing functions, could become possible. We expect the convergence of nanomaterials chemistry, computational design, and innovative manufacturing pathways, such as 3D printing and roll-to-roll deposition, to play a decisive role in enabling future commercialization routes.

In conclusion, 2D metal oxide nanosheets remain a versatile and forward-thinking platform that spans the interface of fundamental science and applied technology. Continued advances in synthesis, characterization and integration routes, should bolster their potential to change the landscape of electrochemical energy storage in the next decade.

6. MOF for energy conversion and storage

Zhipeng Yu*

6.1 Status

2D metal-organic frameworks (2D MOFs) have rapidly emerged as promising materials for electrochemical energy conversion and storage [128-130]. Their ultrathin, layered morphology endows them with high surface-to-volume ratios, abundant accessible metal sites, short ion diffusion pathways, and in some cases, intrinsic conductivity through extended π -d conjugation [131]. Compared with traditional 3D MOFs, 2D MOFs avoid the problem of buried active sites and enable better charge and mass transfer, making them highly attractive for rechargeable batteries, supercapacitors, and electrocatalytic processes [128,132]. Moreover, their structural tunability allows the integration of multiple functions, storage, conduction, and catalysis, within a single framework.

6.2 Current and future challenges

Although significant progress has been made in the development of 2D MOFs, several fundamental challenges continue to hinder their practical application in electrochemical devices. First, the scalable and reproducible synthesis of high-quality nanosheets with controlled thickness, lateral size, and defect density remains difficult [131]. Exfoliation and interfacial assembly methods often suffer from low yield, poor crystallinity, or limited size control, which restricts large-scale deployment [133]. Despite considerable progress in the development of 2D MOFs, several intrinsic challenges in their bottom-up synthesis continue to hinder large-scale and reproducible production. Fundamentally, the formation of high-quality crystalline nanosheets is constrained by both thermodynamic and kinetic factors. Thermodynamically, the strong anisotropy in coordination bonding can favor uncontrolled nucleation, leading to the coexistence of multiple crystal facets and inherent defects such as vacancies or stacking disorders. Kinetically, rapid nucleation rates and limited mass transport in conventional batch reactions often result in uneven growth, polydispersity in lateral size, and non-uniform thickness. These issues are exacerbated by the sensitivity of MOF precursors to solvent polarity, temperature fluctuations, and reaction time, making the reproducibility of high-quality 2D nanosheets particularly challenging.

Second, the structural stability of 2D MOFs under repeated electrochemical cycling is insufficient; many frameworks collapse, undergo ligand leaching, or degrade in highly acidic/alkaline electrolytes, leading to rapid capacity fading [134]. Third, while conjugated 2D MOFs have demonstrated improved conductivity compared with conventional 3D frameworks, their intrinsic conductivities are still inferior to benchmark 2D materials such as graphene and MXenes, necessitating hybridization or post-synthetic modification [131]. Finally, the successful integration of 2D MOFs into full devices requires precise interfacial engineering [134]. Achieving intimate contact with substrates, ensuring efficient electron/ion transport across interfaces, and maintaining robust

mechanical adhesion during prolonged cycling remain unresolved bottlenecks [133]. Together, these issues highlight the urgent need for breakthroughs in synthesis, stabilization, and device-level assembly strategies.

6.3 Advances in science and technology to meet challenges

Recent advances in the design, synthesis, and processing of 2D MOFs are providing effective strategies to overcome current challenges in scalability, defect control, and reproducibility.

(1) Advanced synthetic strategies. Recent advances in the design and processing of 2D MOFs are providing effective strategies to address these challenges. Microfluidic-assisted synthesis has emerged as a powerful tool to precisely control nucleation and growth kinetics, enabling uniform nanosheet thickness, lateral size, and reduced defect density [135]. Continuous-flow reactors further enhance mass and heat transfer, allowing scalable production with high reproducibility while minimizing batch-to-batch variability [136]. Modulated self-assembly and ligand engineering approaches enable fine-tuning of coordination kinetics and crystal facet exposure, which suppress defect formation and improve overall crystallinity. Additionally, post-synthetic treatments such as mild thermal annealing or solvent-assisted recrystallization have been demonstrated to repair vacancies and enhance structural stability. The integration of *in situ* characterization techniques, including synchrotron X-ray scattering and real-time spectroscopy, with computational modeling provides predictive insights into growth pathways, defect formation, and crystallization dynamics, allowing rational optimization of synthetic conditions.

(2) Rational framework design. Molecular-level engineering has enabled the creation of intrinsically conductive 2D conjugated MOFs using redox-active ligands (*e.g.*, hexahydroxytriphenylene, HHTP; 1,3,5-benzenetricarboxylate, BTC) coordinated with square-planar Cu^{2+} or Ni^{2+} nodes. These materials exhibit strong in-plane π -d conjugation, yielding conductivities orders of magnitude higher than conventional 3D MOFs [131]. A representative case is the Zn-HHTP 2D MOF, which illustrated a highly reversible capacity of 150 mAh/g at 100 mA/g in sodium ion batteries (Figs. 9a and b), demonstrating how structural conjugation can deliver exceptional energy storage performance [137].

(3) Controlled thin-film fabrication. To improve electrode integration, thin and uniform 2D MOF films have been fabricated *via* interfacial growth, surfactant-assisted methods, and layer-by-layer assembly. These techniques yield large-area monolayer nanosheets with lateral sizes reaching tens of micrometers, directly deposited on conductive substrates [128]. Such architecture reduces interfacial resistance, improves accessibility, and is compatible with flexible devices. An example of interfacial assembly at liquid-liquid boundaries is shown in Fig. 9c, which highlights the potential for scalable and device-ready electrodes [133].

(4) Hybridization and derivative engineering. To address the limited conductivity and durability of pristine 2D MOFs, researchers have developed derivative materials and composites [138]. For instance, Cu-BTC MOFs have been converted into CuNP-NC catalysts *via* pyrolysis, which preserved the framework porosity while enhancing electrical conductivity, resulting in stable electrocatalytic carbon dioxide reduction performance (Fig. 9d) [139]. Similarly, hybridization of MOF with graphene oxide, has yielded composites with synergistic improvements in charge transfer and mechanical robustness, advancing their use in both supercapacitors and electrocatalysis [138].

(5) Mechanistic insights *via* advanced characterization. *In situ* and operando techniques, including synchrotron X-ray absorption spectroscopy, Raman mapping, and electrochemical impedance analysis, have provided direct evidence of redox transitions in both ligands and metal centers during cycling [140]. These studies (Fig. 9e) reveal correlations between structural evolution and performance, offering guidance for designing frameworks with optimized electronic structures, enhanced stability, and strain-tolerant architectures.

Taken together, advances in molecular design, thin-film fabrication, hybrid material engineering, and mechanistic understanding are rapidly transforming 2D MOFs from laboratory-scale studies into promising candidates for next-generation energy storage and conversion devices.

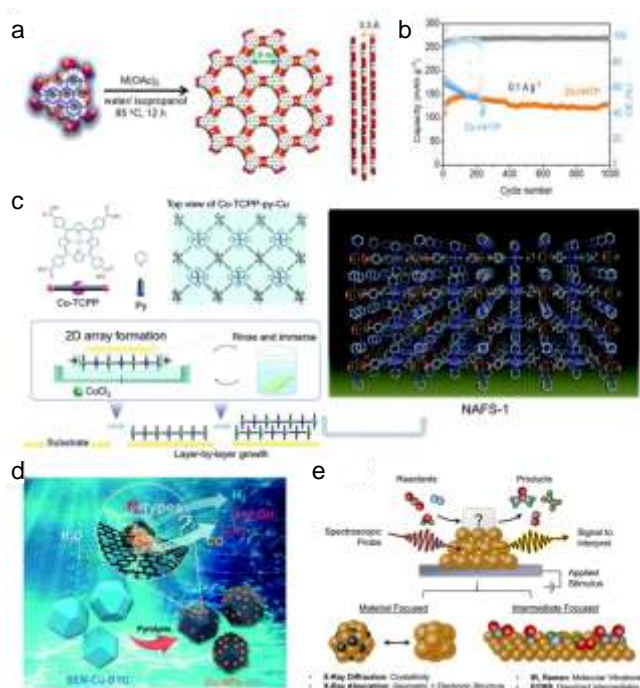


Fig. 9. (a) Synthetic diagram and molecular packing and (b) Cycling stability of Zn-HHTP electrodes at 100 mA/g. Reproduced with permission [137]. Copyright 2021, Wiley. (c) Schematic illustration of MOF-derived CuNP-NC catalysts for CO₂ electroreduction. Reproduced with permission [139]. Copyright 2019, Royal Society of Chemistry. (d) Schematic illustration of fabrication method of NAFS-1. Reproduced with permission [133]. Copyright 2010, Springer Nature. (e) Overview of analytical techniques for mechanistic studies of electrocatalytic systems. Reproduced with permission [140]. Copyright 2025, Springer Nature.

6.4 Concluding remarks and prospects

By 2030, 2D MOFs are anticipated to progress from laboratory-scale demonstrations to integration in practical energy storage and conversion devices. Their inherent structural design flexibility allows precise control over porosity, redox-active sites, and electronic pathways, making them highly attractive for multifunctional electrode architectures. Achieving this transition will require the development of scalable and reproducible synthetic methodologies that yield stable and conductive two-dimensional frameworks, together with device-level engineering strategies that ensure intimate interfacial contact, efficient charge transport, and long-term operational durability. If these challenges are successfully addressed, two-dimensional metal-organic frameworks have the potential to support high-energy-density rechargeable batteries, fast-charging supercapacitors, and efficient electrocatalytic systems. Their deployment could play a substantive role in advancing sustainable energy infrastructures and accelerating the transition toward carbon-neutral technologies.

7. 2D Metal sulfides for energy conversion and storage

Jun Li*

7.1 Status

Photocatalysis has emerged as a transformative technology for addressing global energy shortages and environmental pollution by converting solar energy into chemical energy [141,142]. Among various semiconductor photocatalysts, metal sulfides—such as CdS, MoS₂, and ZnIn₂S₄—have attracted considerable interest due to their narrow bandgaps (1.5–2.5 eV), strong visible-light absorption, and adjustable electronic structures, making them highly efficient for solar-driven applications including hydrogen evolution, CO₂ reduction, H₂O₂ synthesis, and organic pollutant degradation [143–146]. Despite their advantages, single-component metal sulfides often face critical challenges, such as rapid charge recombination, insufficient redox potential, and structural instability, limiting their practical applications [111,147]. To overcome these limitations, recent research has focused on advanced modification strategies (Fig. 10), including: heterojunction engineering (*e.g.*, Z-scheme, S-scheme, and type-II heterostructures) to enhance charge separation and redox efficiency [148–152]. Defect modulation (*e.g.*, sulfur vacancies, metal doping) to optimize electronic structure and surface reactivity [153,154]. Nanostructural design (*e.g.*, ultrathin 2D nanosheets, quantum dots, and hollow structures) to increase active sites and light utilization [155,156]. Particularly, 2D transition metal dichalcogenides (TMDs, *e.g.*, MoS₂, WS₂) have gained prominence due to their unique electronic properties, high surface-to-volume ratio, and tunable band structures [157,158]. Additionally, emerging strategies such as plasmonic enhancement, covalent organic framework (COF) hybridization, and machine learning-assisted catalyst design are opening new avenues for optimizing metal sulfide photocatalysts.

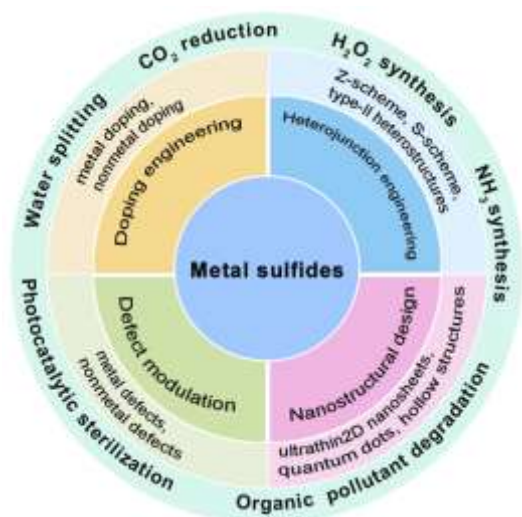


Fig. 10. Schematic illustrations of various strategies for designing metal sulfides and their applications.

7.2 Current and future challenges

Despite their exceptional visible-light absorption and tunable band structures, pristine 2D transition metal dichalcogenides (TMDs, *e.g.*, MoS₂, WS₂) exhibit limited photoactivity due to rapid interlayer charge recombination, abundant basal-plane defects, and inherent susceptibility to photocorrosion. Current research strategies to enhance their performance converge on a core principle: optimizing charge separation dynamics through atomic-scale structural modulation. Crucially, synergistic effects often concurrently address multiple limitations (*e.g.*, increased active sites, improved stability), thereby amplifying photocatalytic efficiency. Upon photoexcitation (femtosecond scale), charge recombination in TMDs typically occurs within picoseconds to nanoseconds—orders of magnitude faster than surface redox reactions. Effective suppression of recombination is thus paramount to maximizing the flux of reactive carriers available for catalysis.

The most direct approaches to engineer charge dynamics involve atomic substitution (doping) and vacancy engineering. Introducing heteroatoms (*e.g.*, N, P) or creating controlled sulfur vacancies (S_v) tailors the electronic band structures and generates charge-trapping sites. However, these modifications risk distorting lattice symmetry: while moderate S_v concentrations enhance charge separation by forming mid-gap states, excessive vacancies act as recombination centers. The atomistic mechanisms governing defect-mediated charge transport remain incompletely resolved, necessitating advanced *in situ* characterization techniques such as valence electron energy loss spectroscopy. A transformative strategy lies in constructing interfacial electric fields *via* heterojunctions. The unique 2D morphology of TMDs facilitates intimate 2D/2D interfaces (*e.g.*, g-C₃N₄/MoS₂, CdS/ZnIn₂S₄), which maximize the contact area and minimize charge-transfer barriers [159,160]. Band alignment engineering—particularly S-scheme or Z-scheme configurations—preserves high redox potentials while enabling spatial carrier separation. Yet, challenges persist: few studies systematically explore how the dimensionality (0D quantum dots, 1D nanowires) of coupled materials affects interfacial electron tunneling in TMD-based heterojunctions. Comprehensive operando studies probing the electronic evolution of both components during catalysis are also scarce.

Synthesis methodology critically dictates structural quality. Conventional hydrothermal methods yield TMDs with high defect densities and inconsistent layer stacking. In contrast, CVD enables wafer-scale growth of single-crystalline monolayer TMDs with minimized defects, uniform thickness, and tunable orientations. The resulting ordered lattices exhibit enhanced interlayer charge transport channels and exposed catalytically active edge sites. Future challenges include scaling CVD production cost-effectively and achieving atomic-level vacancy control *via* techniques like focused ion beam milling.

7.3 Advances in science and technology to meet challenges

Significant efforts have been dedicated to designing efficient catalysts for photocatalysis. This review systematically examines four established strategies for enhancing the visible-light photocatalytic efficiency of TMDs: (1) Elemental doping or defect engineering; (2) nanostructure morphology optimization; (3) coupling with visible-light-responsive materials; and (4) constructing heterojunctions with complementary semiconductors.

Elemental doping, encompassing both cationic and anionic substitutions, serves as a critical strategy for modulating the band structures of metal sulfides. Specifically, incorporating foreign atoms into sulfide lattices introduces impurity states within the bandgap or facilitates solid-solution formation, thereby regulating the oxidative potential of photogenerated holes. This mechanism offers a promising pathway to enhance the photocatalytic stability of metal sulfides. For instance, Shi *et al.* reported an interstitial P-doped CdS with rich S vacancies (CdS-P) achieving photocatalytic hydrogen evolution from pure water without sacrificial agents. P doping positions S-vacancy impurity levels near the Fermi level, creating electron traps that prolong electron lifetimes [161]. This enables long-lived electrons to reach surface sites for efficient redox reactions. Atomic Cu doping in ZnIn₂S₄ nanosheets creates adaptive S

vacancies (Vs), synergistically regulating charge flow and enabling gradient H migration for enhanced photocatalytic hydrogen evolution. Cu substitutes Zn, inducing Vs formation with associated Cu-S bond shrinkage and Zn-S bond distortion. The Vs lowers the interlayer internal electric field, concentrating electrons locally, while Cu acts as a hole trap (Figs. 11a and b). This optimized 5 mol% Cu-ZnIn₂S₄ achieves 37.11 % AQE for photocatalytic H₂ generation at 420 nm [162].

Defect engineering is a modification strategy that effectively extends light absorption and reduces the adsorption and activation energies of intermediates on metal sulfides. Generally, because of the lower formation energy of surface sulfur vacancies relative to cation vacancies, surface sulfur vacancies are employed to regulate the local coordination structure to achieve superior photocatalytic activity. Nonetheless, the introduction of surface sulfur vacancies fails to stabilize the lattice S²⁻ ions, which is attributed to the lack of efficient hole extraction behavior. In contrast, cation vacancies tend to upshift the valence band (VB) position. This shift is beneficial for reducing the oxidation ability of photogenerated holes. For instance, Zou *et al.* fabricated a Zn-deficient ZnS photocatalyst using sodium sulfide as the sulfur source. The resulting Zn vacancy defects weakened the hole oxidation capacity, thereby preventing ZnS photocorrosion. To fully leverage defect engineering for enhancing the activity and stability of metal sulfides, integrating both cation and anion vacancies is a promising strategy [163].

Interface engineering, particularly through heterojunction design, effectively mitigates the anodic dissolution of metal sulfides by redirecting photogenerated holes. Diverse configurations, including Type I/II band alignments and S-scheme charge-transfer pathways, demonstrate significant potential. For example, a chemically bonded Mn_{0.5}Cd_{0.5}S/BiOBr S-scheme heterostructure with oxygen vacancies has been developed [164]. The remarkable enhancement in photo-redox activity originates from the formation of a strong internal electric field (IEF), which provides a robust driving force and efficient charge transfer pathway through interfacial chemical bonding, thereby facilitating S-scheme charge separation. Furthermore, the IEF at the heterojunction promotes the rapid consumption of photogenerated holes in Mn_{0.5}Cd_{0.5}S by electrons from BiOBr, significantly increasing the density of active charge carriers while effectively suppressing the photocorrosion of Mn_{0.5}Cd_{0.5}S (Fig. 11c). This achievement indicates the vast potential of chemically bonded S-scheme photosystems with structural defects in the design of photo-responsive materials for efficient wastewater treatment.

Leveraging the advantages of S-scheme heterojunctions, Xu *et al.* fabricated a 0D/2D TiO₂/Ce₂S₃ (TC) S-scheme photocatalyst to enhance aniline production [165]. DFT calculations determine the work function and Fermi level of TC, confirming electron transfer from Ce₂S₃ to TiO₂ upon contact and revealing the formation of an S-scheme heterojunction between the two components. Furthermore, femtosecond transient absorption spectroscopy was employed to investigate the charge-transfer kinetics within the S-scheme heterojunction, indicating slower photocarrier recombination in TC5. This behavior is attributed to the trapping of more photoelectrons in the conduction band (CB) of TiO₂ by Ce₂S₃, while simultaneously providing new relaxation pathways for photoexcited electrons in TiO₂ via recombination with holes in Ce₂S₃, resulting in greatly enhanced photocatalytic activity.

To further address the issue of photocorrosion, rational heterojunction design offers an effective pathway to regulate charge transfer and spatially separate redox-active species. For S-scheme heterojunctions, strong interfacial electric fields and staggered band structures enable selective recombination between low-energy electrons and holes at the interface, while retaining high-energy electrons and holes in the CB and VB of the respective photocatalysts. This spatial separation minimizes direct hole accumulation in CdS, thereby effectively suppressing anodic dissolution and maintaining structural integrity [166-168]. For Z-scheme systems, photogenerated electrons from one semiconductor recombine with holes from another, leaving behind electrons and holes with stronger redox potentials in their respective components. Importantly, holes are localized on the more oxidation-stable photocatalyst, avoiding direct attack on CdS lattice [169]. This charge transfer mechanism allows Z-scheme architectures to preserve high driving force for oxidation and reduction reactions while significantly enhancing photocorrosion resistance. To quantitatively evaluate the suppression of photocorrosion and improved operational stability, several complementary techniques are recommended, including time-resolved photocatalytic activity measurements to assess long-term durability, ICP-OES to monitor Cd²⁺ leaching, XPS to track S 2p and Cd 3d states, and operando or post-reaction structural characterizations (XRD and TEM) to confirm lattice preservation. These metrics provide direct evidence of how S-scheme and Z-scheme heterojunction engineering improves the longevity of metal sulfide photocatalysts.

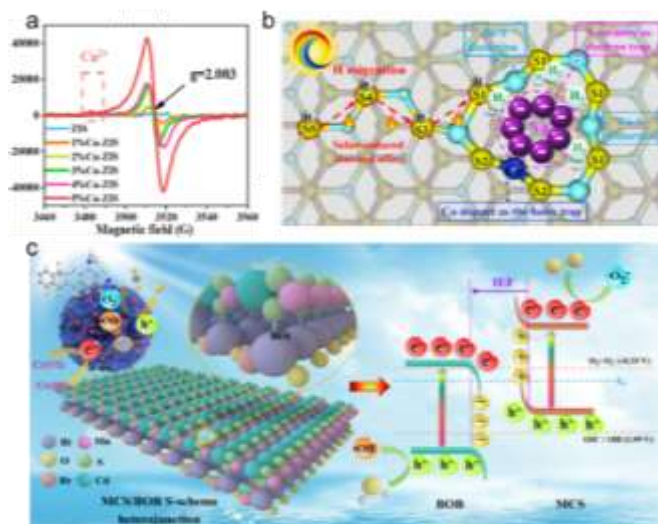


Fig. 11. (a) EPR spectra of S 2p over ZIS and xCu-ZIS ($x = 1 \text{ \%} - 5 \text{ \%}$), (b) Schematic illustration of gradient H migration for H_2 evolution on Zn facet over Cu-ZIS, Reproduced with permission [162]. Copyright 2021, American Chemical Society. (c) The photoreaction mechanism for TC and Cr(VI) eradication by MCS/BOB-2. Reproduced with permission [164]. Copyright 2024, Elsevier.

7.4 Concluding remarks and prospects

This work has systematically examined the latest advancements in 2D metal sulfides for solar energy conversion. We have discussed their unique electronic structures (*e.g.*, layer-dependent bandgaps, strong excitonic effects), synthesis methodologies, and fundamental reaction mechanisms. Particular emphasis has been placed on rational design principles—from defect engineering to heterostructure construction—for simultaneously enhancing photocatalytic activity and stability. Despite significant progress, critical challenges persist. The solar-to-fuel conversion efficiency of most 2D sulfides is still below 10 %, the industrial viability threshold. Innovations such as interlayer exciton dissociation in twisted multilayer MoS_2 and plasmonic coupling may overcome this limitation. Although 2D sulfides exhibit high C_1 -product selectivity (*e.g.*, CO, CH_4) in CO_2 reduction, the generation of C_{2+} species (*e.g.*, C_2H_4 , ethanol) remains elusive due to inefficient C-C coupling on basal planes. Edge-site functionalization or biohybrid systems could overcome this. Large-area synthesis of defect-engineered 2D sulfides requires advances in spatially selective atomic etching and CVD process control. High-throughput screening of ternary sulfides *via* descriptor-based models (*e.g.*, d-band center, vacancy formation energy) could expedite catalyst discovery. The future of 2D metal sulfides lies in multiscale design to achieve high-efficiency artificial photosynthesis.

8. 2D Perovskite materials for energy conversion and storage

Amir Sultan, Kun Zheng*

8.1 Status

Rapid urbanization and sustained population growth have substantially increased the demand for renewable energy sources, driven by the finite availability of fossil fuels. Moreover, the combustion of fossil fuels is a major contributor to climate change and global warming [170]. Although fossil fuels have dominated global energy production for centuries, the past few decades have witnessed a significant shift toward renewable energy sources such as solar, wind, and hydropower [171]. Extensive research efforts have been devoted to advancing technologies for the conversion and storage of energy derived from these sources. Given the intermittent nature of solar and wind energy, efficient energy storage systems, such as supercapacitors, batteries, and fuel cells, are essential to ensure a reliable energy supply and effective utilization [170-175]. Energy conversion and storage devices must balance cost-effectiveness with high performance. Several key challenges exist in the fabrication of such devices, particularly in optimizing cyclic stability, lifetime, size, and shape to meet desired specifications. The use of appropriate type of materials for the development of such devices has addressed most of the challenges [176-178]. Nevertheless, there are some key challenges in the complete development of sustainable energy technologies. Researchers have been pursuing modern and advanced materials to address the problems and limitations of energy conversion and storage devices. Among the functional materials, perovskites have emerged as promising materials for energy conversion and storage applications, including batteries, capacitors, solid oxide cells, solar cells [179-182].

Over the last few decades, perovskite-type oxides, with a general formula of ABO_3 , have gained wider application in materials science, catalytic processes, and energy applications. Perovskite-based oxides have been suggested as favorable materials for a supercapacitor due to the presence of oxygen vacancies and different charge storage capabilities [183-185]. For example, a $\text{LaMnO}_{3-\delta}$ -based supercapacitor perovskite-type oxide exhibits large oxygen vacancies and has demonstrated a high specific capacitance of 973.5 F/g at 1 A/g current density [186]. Owing to significant anion vacancies, which support charge storage in a supercapacitor, $\text{LaMnO}_{3\pm\delta}$ nanocrystals revealed a high energy density of 61.2 Wh/kg with a power density of 220.4 W/kg [187]. Similarly, $\text{La}_{0.85}\text{Sr}_{0.15}\text{MnO}_3$

perovskite has been investigated in a supercapacitor and revealed a specific capacitance of 198 F/g at 0.5 A/g current density [188]. In 2009, perovskite materials were first explored for use in the fabrication of solar cells [189]. Then, in 2012, the first perovskite solar cell was constructed, achieving a power conversion efficiency of 9 % [190]. Subsequently, the $\text{CH}_3\text{NH}_3\text{PbI}_{3-x}\text{Br}_x$ perovskite material demonstrated an efficiency of 12.3 % in a solar cell [191]. Furthermore, SrSnO_3 perovskite oxide has been employed as a key component in n-i-p planar heterojunction solar cell, achieving an efficiency of 19 % [191].

Additionally, perovskite materials have also shown potential applications in different components, such as the cathode, anode, and electrolyte of the batteries. Different types of perovskite anodes have been fabricated, namely 3D ($\text{CH}_3\text{NH}_3\text{PbI}_3$), 2D ($\text{C}_4\text{H}_9\text{NH}_3)_2\text{PbI}_4$), and 1D ($\text{C}_6\text{H}_9\text{I}_3\text{NOP}_b$), which showed a discharge capacity of 1580, 1650, and 476 mAh/g, respectively, and reversible capacities of 646, 508, and 202 mAh/g, respectively, at 100 mA/g [192]. Recently, Cs_4PbBr_6 perovskite was utilized as an anode in a Li-ion battery, which showed a high discharge capacity, *i.e.*, 377 mAh/g [193]. The (EDBE)[CuCl_4] 2D perovskite was synthesized and explored as a cathode material for a Li-ion battery, which displayed the average gravimetric capacities of 26 mAh/g at 22 °C and 75 mAh/g at 40 °C [194].

Moreover, perovskite materials have emerged as promising candidates for light-emitting diode (LED) technologies owing to their low-temperature solution processability, narrow emission spectra, tunable bandgap, and long carrier diffusion length [195]. The incorporation of perovskite materials has enabled significant advancements in LED performance, marking a major milestone in the field. For the first time, luminescence from perovskite materials was observed at room temperature, achieving external quantum efficiencies of 0.76 % in the near-infrared region (754 nm) and 0.1 % in the green region (517 nm). Nowadays, the external efficiency for red, near infrared, and green exceeds 20 %, with photoluminescence quantum efficiencies of about 70 % [196].

Perovskites, especially the 3D perovskite materials, have performed well and demonstrated superior performance in energy conversion and storage devices. However, their challenging operational stability limits their practical application in the complete development of future generations' energy technologies [197]. In the last decade, 2D perovskite materials have gained significant attention for energy technology applications due to their distinctive chemical and physical properties, as well as their superior thermal stability compared to 3D perovskites [198]. 2D perovskites are now being explored across various energy applications. In this study, we review phase-engineering strategies and the unique properties of 2D perovskites, highlighting their significance and potential applications in energy conversion and storage technologies.

8.2 Current and future challenges

Researchers have investigated a wide range of modern and advanced materials to address the challenges and limitations associated with energy conversion and storage devices. Among these functional materials, perovskites have garnered significant attention as promising candidates for next-generation energy technologies. Their unique physical and chemical properties, including versatile solid-state characteristics that can exhibit insulating, metallic, semiconducting, and even superconducting behavior, make them highly attractive for diverse energy applications [199,200]. The general formula for the perovskites crystal structure is ABX_3 , where A and B denote cations and X denotes anions (Fig. 12a). Modifying the structural composition within the general perovskite crystal framework has been shown to yield tunable and distinctive optoelectronic properties. These distinctive properties make perovskite materials highly promising candidates for energy conversion and storage applications, such as batteries, capacitors, solid oxide cells, solar cells, *etc.* [179-182,201]. The 3D perovskites have demonstrated exceptional performance, however, their challenging operational stability limits practical applications [197]. In addition to the operational stability, several other challenges in energy conversion and storage devices, including the performance of the electrodes and thermal mismatch in solid oxide cells, long-term cycling performance issues in batteries, energy loss in the charging-discharging process in capacitors, power conversion efficiency issue in solar cells, external quantum efficiency problem in LEDs, as well as weak kinetics in CO_2 reduction, oxygen evolution, and hydrogen evolution reactions, persist as key challenges in electrocatalysis. Thus, enhancing the overall properties of perovskite materials has a focal point for the researchers to use them in energy technology applications [202,203].

8.3 Advances in science and technology to meet challenges

Various strategies have been employed to modify perovskites and improve their properties. Among these, interfacial engineering has emerged as a particularly effective approach, enhancing the operational stability and performance of perovskite-based devices by mitigating interfacial defects or by transitioning from 3D to more stable 2D perovskite structures [196,204,205].

2D perovskite materials are derived by dimensionally reducing their counterpart 3D perovskites and have been depicted as an emerging group of layered perovskite materials that offer superior operational stability and distinctive properties for energy technology applications compared to 3D perovskites [206]. Mostly, 2D perovskite materials adopt the Ruddlesden-Popper structure, which has the general chemical formula of $\text{A}'_2\text{A}_{n-1}\text{B}_n\text{X}_{3n+1}$ (where A' and A are organic-inorganic spacer cations, B is a metal cation, and X is halide anion, n represents the number of octahedral layers), where organic spacer cations are separated by inorganic oxide or halide layers (Figs. 12b and c) [207]. This unique geometry endows 2D perovskite materials with enhanced operational stability in humid atmospheres, tunable band gaps, remarkable thermal properties, and strong quantum confinement compared to their 3D counterparts. Moreover, structural flexibility, high charge carrier mobility, and the exposure of active sites make the 2D perovskite highly promising candidates for the next generation energy devices [208].

2D perovskite materials exhibit exceptional diversity in their crystal structures and can be categorized into distinct groups based on their in-plane structural offset, which varies with spacer chemistry. Different phases, such as Ruddlesden-Popper, alternating cations

in interlayer space, and Dion-Jacobson, in the crystal structure of 2D perovskite materials, as shown in Fig. 12. However, mixed-phase formation is a common challenge during the fabrication of 2D perovskite film, often resulting in electronic disorder, charge trapping, and reduced environmental stability. Achieving phase-pure, large-area perovskite films requires precise synthetic control. Critical strategies include spacer cation engineering to regulate the dimensionality of the crystal lattice, solvent-antisolvent engineering to control nucleation and growth kinetics, temperature-gradient deposition to avoid intermediate phase formation, and optimized post-annealing to improve crystallinity and eliminate unwanted mixed phases. Moreover, tuning the precursor concentration and controlling solvent evaporation rate have been demonstrated to favor the selective crystallization of Ruddlesden-Popper or Dion-Jacobson phases over undesired intermediates.

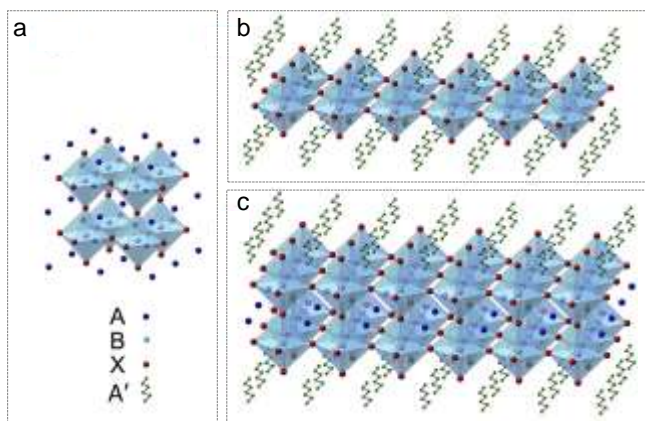


Fig. 12. Schematic illustration of the crystal structure of (a) 3D perovskites with a chemical formula ABX_3 , (b) Ruddlesden-Popper perovskites with $n = 1$, (c) Ruddlesden-Popper perovskites with $n = 2$. Reproduced with permission [207]. Copyright 2019, American Chemical Society.

Phase purity has a direct correlation with device performance. Highly phase-pure 2D perovskite films exhibit reduced non-radiative recombination, enhanced carrier mobility, and prolonged exciton lifetimes, leading to improved power conversion efficiency and operational stability. For instance, devices based on phase-pure ($n = 1-3$) Ruddlesden-Popper perovskites typically demonstrate enhanced thermal and moisture resistance compared to their mixed-phase counterparts, with operational lifetimes extending from several hundred to over 1000 h under ambient conditions. Similarly, phase-pure Dion-Jacobson structures, with robust hydrogen-bonded frameworks, show improved thermal stability above 100 °C, making them suitable for long-term energy storage and optoelectronic applications. Building on these general considerations of phase purity control and its impact on device performance, the different 2D perovskite structural phases exhibit distinct synthetic behaviors and stability characteristics, as discussed below.

8.3.1 Ruddlesden-Popper phase

Ruddlesden-Popper phase of 2D perovskites is denoted by the general formula of $A'_2A_{n-1}B_nX_{3n+1}$, and its crystal structure is defined by an octahedral unit with a $(\frac{1}{2}, \frac{1}{2})$ in-plane offset. In the Ruddlesden-Popper structure, the organic spacers (A') carry a +1 charge and are typically aromatic monovalent organic, *e.g.*, phenylethylammonium, butylammonium, benzylammonium, propylammonium, and phenylammonium, or long chain spacers are used to make the Ruddlesden-Popper phase [209,210]. A distinctive feature, such as narrow van der Waals gaps, are present between the spacer cations in the Ruddlesden-Popper phase (Fig. 13a), which facilitate the exfoliation of the Ruddlesden-Popper phase layers. The van der Waals gaps enable mechanical exfoliation using Scotch tape between the layers of the Ruddlesden-Popper phase, analogous to the exfoliation of graphene from graphite [211]. The phase purity of Ruddlesden-Popper structures can be finely tuned through cation-solvent interactions and careful control of crystallization front propagation during film formation, which plays a decisive role in minimizing structural defects and enhancing electronic coupling between layers [205].

8.3.2 Alternating cations in interlayer space phase

The general chemical formula for alternating cations in the interlayer space is $A'A_nB_nX_{3n+1}$, and its crystal structure features an octahedral unit with $(\frac{1}{2}, 0)$ in-plane offset. In the crystal structure, the bulky organic spacer cations A' and inorganic cations A are alternately located with each other between the layers (Fig. 13b). According to the literature, the guanidinium (GA^+) cation has proven to be an effective and distinctive spacer material for alternating cations in interlayer space phase [212,213]. The 2D alternating cations in interlayer space phase perovskite materials exhibit both van der Waals gaps and hydrogen bonds within their crystal structure [213]. The remarkable structural configuration, *i.e.*, in-plane offset with octahedral rotation, and the coexistence of both hydrogen bonds and van der Waals gaps, make the alternating cations in interlayer space phase of 2D perovskite materials a critical design and a promising roadmap for tailoring materials toward sustainable energy storage and conversion technologies in the near future.

8.3.3 Dion-Jacobson phase

The Dion-Jacobson phase is represented by the general chemical formula of $A'A_{n-1}B_nX_{3n+1}$, and possesses a unique set of properties. For instance, the spacer cations carry a +2 charge and exhibit a $(0, 0)$ in-plane offset rotation in their crystal structure. In

contrast to the Ruddlesden-Popper and alternating cations in interlayer space phases, the van der Waals gaps are absent in the Dion-Jacobson Phase and contain only hydrogen bonds, which is pivotal for its enhanced thermal stability (Fig. 13c) [214]. Bulky divalent organic spacers, such as 4-(ammonium methyl) piperidinium, 1,4-butanediamine, 1,3-propanediamine, and 3-(ammonium methyl) piperidinium are used to form the Dion-Jacobson phase [215,216]. Phase-pure Dion-Jacobson structures are typically achieved *via* temperature-controlled solution processing and slow crystallization, which prevent unwanted RP-phase formation and ensure uniform layer orientation. Such high phase purity contributes directly to enhanced device durability, particularly under thermal and moisture stress conditions. These exceptional properties of the Dion-Jacobson Phase of 2D perovskites make it the best candidate for the application of energy technology, where devices requiring high thermal stability, such as batteries, capacitors, light-emitting diodes (LEDs) and solar cells.

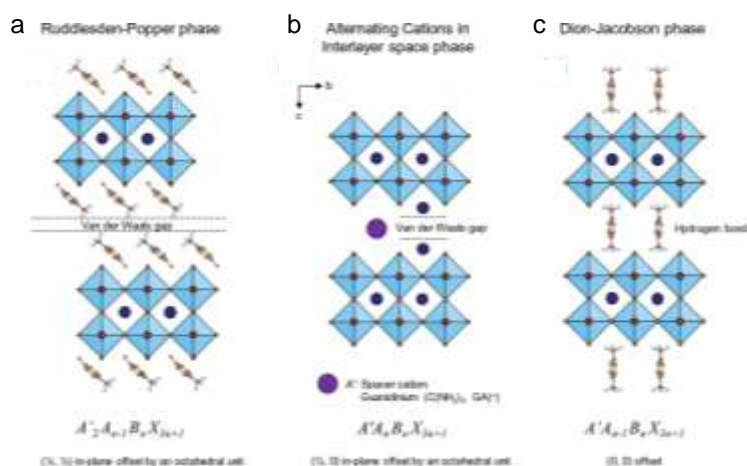


Fig.13. Schematic illustration of different phases in 2D perovskite materials: (a) Ruddlesden-Popper phase, (b) Alternating cations in interlayer space phase, and (c) Dion-Jacobson Phase. Reproduced with permission [196]. Copyright 2024, Springer Nature Link.

8.3.4 Exceptional properties of 2D perovskite materials

As discussed, 2D perovskite materials have a unique geometry that offers enhanced operational stability and remarkable chemical and physical properties compared to their 3D counterparts. These properties make the 2D perovskites highly promising candidates for next-generation energy conversion and storage devices, such as batteries, capacitors, LEDs, and solar cells. 2D perovskite materials demonstrated a promising application in future generation batteries due to their structural flexibility, exceptional thermal stability, and high charge carrier mobility. For example, the $C_4H_9NH_3)_2PbI_4$ 2D perovskite studied was studied as an anode for batteries and showed a discharge and reversible capacity of 1650 and 508 mAh/g, respectively, at 100 mA/g [192]. Similarly, the $(CH_3(CH_2)_2NH_3)_2(CH_3NH_3)_2Pb_3Br_{10}$ perovskite has been investigated as an electrode material for batteries, improving the performance by achieving a high reversible capacity (>242 mAh/g) for 30 cycles at 0.13 mA/cm² [217]. Furthermore, the (EDBE)[CuCl₄] perovskite was prepared as a cathode for a Li-ion battery and displayed the average gravimetric capacities of 26 mAh/g at 22 °C and 75 mAh/g at 40 °C [194].

In the past years, 2D perovskites have made rapid progress in enhancing the efficiency of solar cells due to their excellent light absorption, exceptional chemical and thermal stability, tunable band gaps, increased moisture resistance, and high charge-carrier mobilities compared to 3D perovskites. With the application of 2D perovskite materials has led to a remarkable increase in solar cell power efficiency, which has soared from 3.8 % to 26.1 % in a very short period of approximately 15 years [196,218]. For example, the $BA_2MA_3Pb_4I_{13}$ 2D perovskite has been fabricated for a solar cell that exhibits a power efficiency of 12.52 % with no degradation over 2250 h under 64 % humid air [210]. Similarly, $AVA_2PbI_4/MAPbI_3$ has shown a power efficiency of 14.6 % for more than 10,000 h without any degradation under operation [219]. In addition, several other 2D perovskites, such as $FA_{0.83}Cs_{0.17}Pb(IyBr_{1-y})_3$ revealed a power efficiency of 17.5 % with 20 % degradation after 1000 h in air [220], $PEA_2MA_4Pb_5I_{16}/MAPbI_3$ showed a power efficiency of 14.94 % with 24 % degradation after 19 days in 75 % humid air [220], and $BA_2(MA_{0.95}Cs_{0.05})_3Pb_4I_{13}$ acquired a 13.7 % power efficiency with 10 % degradation after 1400 h under 30 % humid air [221]. Moreover, the use of $MAPbBr_3$ (methylammonium lead bromide) and $MAPbI_3$ (methylammonium lead iodide) perovskites in solar cells attained limited stability with a power efficiency of 3.8 % [189]. When $FAPbI_3$ (formamidinium lead iodide) replaced the $MAPbI_3$, the cell achieved a power efficiency of 20 % with enhanced performance [222]. Overall, the 2D perovskites offer improved stability against heat, chemical degradation, and humidity due to their hydrophobic organic cations nature in solar cells compared to 3D perovskites. The enhanced stability makes the 2D perovskites a favorable alternative for the fabrication of reliable and durable solar cell applications [223].

While 3D perovskite-based LEDs have low external quantum efficiency and photoluminescence quantum yields due to high trap densities and low exciton binding energies ($E_b \approx 50$ meV), which restrain bimolecular radiative recombination [224]. On the other hand, 2D perovskites have higher exciton binding energies ($E_b \approx 300$ meV) due to efficient radiative recombination [225]. The 2D

perovskite (PEA)₂PbBr₄ nanoplates have been utilized in an LED, which revealed an external quantum efficiency of 0.04 % with strong light emissions. This efficiency was impressively high at that time for blue LED [226]. The (C₆H₅CH₂NH₃)₂PbI₄ perovskite-based LED device gave an external quantum efficiency of 0.005 % which was quite low, and it might be because of the strong exciton–phonon coupling in the 2D perovskite’s single layer [227]. Reported studies found that mixed phases of 2D perovskite-based LEDs reveal enhanced performance and high external quantum efficiency compared to the LEDs that were made with a single component. For instance, a mixed phase (PEA₂MA_{n-1}Pb_nI_{3n+1}) 2D perovskite-based LEDs achieved an external quantum efficiency of 8.8 % [228]. Similarly, mixed-phases NMA₂FA_{n-1}Pb_nI_{3n+1} (NMA = C₁₀H₇CH₂NH₃⁺) 2D perovskite showed an external quantum efficiency of 11.7 %, exceptional performance, and good stability [229]. And BA₂MA_{n-1}Pb_nX_{3n+1} (X = Br, I) nano-crystal (n ~ 19) revealed excellent performance and gave an external quantum efficiency of 9.3 % for X = Br and 10.4 % for X = I [230].

Recent studies showed that 2D perovskite materials are promising and more robust in improving the electrochemical performance, efficiency, and stability of supercapacitors due to their confined and layered structure. The layered structure of 2D perovskite materials enhances the redox reaction, promoting fast ion diffusion and charge transfer [231]. For example, the LaNiO₃ perovskite nanosheet revealed a high capacitance of 139.2 mAh/g at a current density of 1.0 A/g with excellent cycle stability and good rate capability [232]. A lead-free Cs₃Bi₂Cl₉ achieved a capacitance of 64 mF/cm², an energy density of 6.6 μWh/cm², and it revealed improved stability. The capacitance is 8–10 times higher, and the energy density is 3–4 times higher than that of the lead-based devices [233]. A 2D high-κ perovskite (Ca₂Na_{m-3}Nb_mO_{3m+1}; m = 3–6) nanosheet demonstrated a high efficiency (>90 %), ultrahigh energy density of 174–272 J/cm³, and excellent reliability (>10⁷) cycles [234].

8.3.5 Operational stability and thermal properties of 2D perovskites

The 2D perovskites, especially the halide perovskites, have largely been incorporated by hydrophobic aromatic organic or aliphatic spacer cations; these characteristics grant exceptional stability in humid atmospheres compared to their 3D counterpart [235]. These aromatic organic or aliphatic spacer cations generate a hydrophobic surface, as denoted by the large water droplets' contact angle measured on the surface of the perovskite layers. Hence, these organic spacer cations help the creation of densely packed films, which efficiently stabilize grain boundaries. The densely packed films serve as protective sheets that prevent direct contact with moisture, inhibit chemical degradation, and restrict water infiltration, thereby suppressing hydration and significantly boosting the overall operational stability of the materials [236].

The thermal properties of 2D perovskites are unique and distinct from their 3D counterparts. The exceptional feature of 2D perovskites is their ultralow thermal conductivity, which typically lies between 0.10–0.19 W m⁻¹ K⁻¹, compared to the thermal conductivity of 3D perovskite, which is between 0.34–0.73 W m⁻¹ K⁻¹ [237,238]. The remarkably low thermal conductivity in 2D perovskites arises predominantly from the weak van der Waals forces that are present within their layers. Moreover, the anisotropic crystalline structure of the 2D perovskites also plays a key role in influencing their thermal behavior. The low thermal conductivity prevents material degradation, decreases thermal stress, and helps maintain heat, thereby improving the stability of 2D perovskites [239].

8.4 Concluding remarks

The exceptional stability, versatile phase engineering, low thermal conductivity, tunable layered structures, and customizable interlayer cation design make 2D perovskite materials highly promising candidates for next-generation energy conversion and storage devices, including batteries, capacitors, electrocatalysts, solar cells, and LEDs. They’re thermally insulating, and anisotropic nature can enhance device durability and safety by mitigating thermal degradation and mechanical stress. Moreover, the abundance of surface-active sites and tunable electronic structure can accelerate reaction kinetics and facilitate efficient charge transfer. The high dielectric constant and layered architecture of 2D perovskites can optimize charge-discharge processes in capacitors, thereby improving energy storage capacity. Similarly, their low thermal conductivity and excellent stability can extend the long-term cycling performance of batteries by minimizing thermal stress. These unique attributes also hold great potential for improving the power conversion efficiency of solar cells and the external quantum efficiency of LEDs. Despite the advantages, several challenges still remain, including scalable synthesis with stringent phase purity control, long term stability under ambient and operating conditions, interfacial/ionic migration management, eco toxicity, and end of life considerations (especially for Pb based systems), and seamless integration into existing device architectures. Addressing these limitations through innovative materials design, mechanistic insights, and scalable manufacturing will be crucial for translating 2D perovskites into practical technologies. With continued research and technological progress, 2D perovskites are poised to play a transformative role in sustainable energy.

9. Vertically aligned nanosheets as electrode materials for high-performance rechargeable batteries

Gan Qu*

9.1 Status

In the past decades, the popularity of portable electronics and electric vehicles promote the development of the advanced storage technologies such as the lithium ion batteries (LIBs), sodium ion batteries (SIBs), and zinc ion batteries (ZIBs). In order to meet the growing demand for high energy density devices, tremendous efforts have been devoted to fabricating the novel electrode materials. It has been widely demonstrated that the structure design of an electrode plays a key role in determining its reaction kinetics, the capability of mass transportation with electrolyte, and consequently the performance of an electrochemical energy storage or conversion system. Nowadays, a variety of nanostructured materials have been engineered to shorten the ion diffusion paths and

mitigate the polarization effect. Unfortunately, the actual requirements still cannot be satisfied due to the limited volumetric and areal energy densities for the reported nanomaterial electrodes. Therefore, rational design of composite architectures is urgently desired to further enhance the energy storage performance [240].

The 3D nanoscale-structured electrode, for example the vertically aligned nanosheets, enables enhanced ion and electron transport, improves mechanical stability, and increases active material loading, which display a significant potential in energy storage fields [241]. In addition, the electrode materials with 2D features and tunable interlayer chemistry have been demonstrated to facilitate the high-power energy storage applications. The vertically aligned nanosheets offer abundant and ordered channels for ion transportation, thus avoiding the local ion depletion at fast charge/discharge operation. Furthermore, the channels provide sufficient interspace to accommodate the electrode expansion under working conditions, thereby maintaining the structural integrity of electrode. The electrode architectures contribute to the large active surface and extensive accessible sites, facilitating the uniform current distribution on the whole electrode. More importantly, the energy density and areal capacity of the electrodes can be enhanced through increasing the area of nanosheets. Based on its excellent combined properties, the vertically aligned nanosheets have presented great promises as a building material for the development of new electrodes. More specially, the vertically aligned nanosheets can also simultaneously act as the structural backbone and current collector in a free-standing/binder-free electrode, which allows the construction of lightweight and flexible devices. In line with this strategy, various electrodes with vertically aligned nanosheets have been studied and applied for high-performance rechargeable batteries.

9.2 Current and future challenges

To promote the application of vertically aligned nanosheets electrodes in rechargeable batteries, some challenges and restrictions still need to be addressed. Although many experimental methods have been put forward to synthesize the vertically aligned nanosheets, most of the reported approaches are tedious or equipment-intensive [242]. In addition, it is still a huge challenge to control the thickness and area of the nanosheets and to load the active materials uniformly over the surface of the electrode. The understanding for the growth of the vertically aligned nanosheets is still lacking. The present methods are still based on several trial and error approaches. Nowadays, the preparation of vertically aligned nanosheets is mainly by the hydrothermal and CVD methods, leading to the low yields. The current synthetic methods and raw materials are relatively expensive. Consequently, although the laboratory-scale production has been achieved, it is challenging for the large-scale manufacturing. Therefore, a facile, cost-effective, and scalable production approach is urgently required. The performance of the rechargeable batteries is closely related with the vertically aligned structures. The conductivity anisotropy (parallel versus perpendicular to the plane of nanosheets) in the 3D electrode leads to low utilization of the active material even under slow charge-discharge rates [243]. Furthermore, the compression can exacerbate the conductivity anisotropy and block the ion transport in the highly stacked active materials. During the charge and discharge process, restacking is one of the main challenges for the 3D architectures of electrodes, which will block the electrolyte migration and restrict its power performance. In the battery applications, the irreversible capacity of the initial cycle should be minimized from the practical point of view. However, there is limited strategies to enhance the first Coulomb efficiency and improve its cycling performance. Another concern is that there is still a lack of an available synthetic approach to precisely construct and tune the electronic structure of the vertically aligned materials.

9.3 Advances in science and technology to meet challenges

Recent advances in synthetic strategies and mechanistic understanding have significantly promoted the development of vertically aligned nanosheets for next-generation rechargeable batteries. Beyond improving synthesis efficiency, a growing research focus is on deciphering the underlying thermodynamic and kinetic principles governing vertical alignment, aiming to establish a universal model applicable across various material systems. Controlled vertical growth is primarily determined by the competition between in-plane and out-of-plane growth rates, interfacial energy regulation, and solvent-mediated crystallization dynamics. Rational design of precursor chemistry, surface functionalization, and directional freezing or templating can modulate these parameters to achieve deterministic orientation control. By integrating *in situ* characterization with multiscale simulations, it is expected that generalized thermodynamic/kinetic descriptors (*e.g.*, interfacial free energy, supersaturation gradients, and surface diffusion coefficients) can be identified, providing predictive guidance for scalable synthesis of vertically aligned architectures.

Based on the inherent advantages, vertically aligned nanosheets have been widely applied in the next-generation rechargeable batteries. In lithium-ion batteries (LIBs), Chen *et al.* [244] adopt a facile ice template assisted blade coating method to prepare vertically aligned $\text{Ti}_3\text{C}_2\text{T}_x$ nanosheet arrays (v- $\text{Ti}_3\text{C}_2\text{T}_x$) as host electrodes (Fig. 14a). The low tortuosity of vertical structure cannot only effectively homogenize the Li ion flux and the electric field, but also enrich the active surface area for Li deposition. The vertical $\text{Ti}_3\text{C}_2\text{T}_x$ electrode with a uniform SEI layer can realize dendrite-free lithium deposition and maintain the structure stable during the Li plating/stripping cycles. Dai *et al.* [245] further design a self-supported electrode composed of vertically aligned 2D $\text{Ti}_3\text{C}_2\text{T}_x$ MXene/ V_2O_5 heterostructures *via* a facile ice-crystallization-induced strategy followed by mechanical pressing. The pliable 2D V_2O_5 nanosheets are particularly selected to assemble with rigid MXene nanosheets in a “face-to-face” manner, ensuring the efficient electrical contacts throughout the electrode. The vertically aligned configuration with low tortuosity endows thick electrode fast ion diffusion channels, while MXene scaffold further accommodates the volume change of V_2O_5 during lithiation/delithiation.

In sodium-ion batteries (SIBs), Zhang *et al.* [246] report 3D cross-linked MoS_2 nanosheets with expanding interplanar spacing by the role of CTAB aligned vertically on highly conductive $\text{Ti}_3\text{C}_2\text{T}_x$ MXene nanosheets with partially oxidized rutile and anatase dual-phased TiO_2 ($\text{MoS}_2@\text{MXene}@D\text{-TiO}_2$) through a one-step hydrothermal method as anode materials without further annealing for

SIBs. This unique structure with expanded MoS_2 layer spacing is suitable to the transmission of Na^+ , while the heterogeneous nanoarchitecture prevents aggregation between MoS_2 nanoflowers, buffers volume expansion of the bulk, and reduces structural crumble caused by Na^+ intercalation. Wang *et al.* [247] fabricate a vertical $\text{MoS}_2/\text{ZnS}/\text{G}$ structure through a facile and scalable hydrothermal method (Fig. 14b). The resultant $\text{MoS}_2/\text{ZnS}/\text{G}$ structure provides open channels for fast ion transport and improves its electronic conductivity, facilitating the efficient sodium-ion storage.

In zinc-ion batteries (ZIBs), Zhu *et al.* [248] report the vertically aligned Zn-Al layered double hydroxide nanosheets, *in situ* formed on the zinc foil (LDH@Zn). The LDH@Zn anode accelerated and homogenized zinc ion transport, while its vertical layered structure provided rapid and direct diffusion paths for zinc ions to the anode/electrolyte interface. As a result, the LDH@Zn anode enabled dendrite-free zinc deposition and much-enhanced electrochemical performances (Fig. 14c). Wang *et al.* [249] report self-supporting $\text{Ti}_3\text{C}_2\text{T}_x/\text{V}_2\text{O}_5 \cdot 1.6\text{H}_2\text{O}$ heterostructured electrodes with vertically aligned architecture through the utilization of a directional freezing technique. The vertical alignment, which minimizes tortuosity, can offers the advantage of facilitated ionic transport within the structure. Consequently, the heterostructured electrode exhibits remarkable resilience to mechanical deformations and low-temperature environment.

In dual-ion batteries (DIBs), Shang *et al.* [250] first propose the vertical graphite nanosheets (VGNs) as cathode materials to guide mass and charge transport directionally by reducing electrode tortuosity (Fig. 14d). The perpendicular open structures of VGNs not only provide directional and shortened ion channels for uniform ion gradient and electric fields, promoting fast anion diffusion, but also accommodate intercalation volume expansion through the ordered interspaces. As a result, DIBs featuring the VGNs as cathode materials demonstrate an ultrahigh specific capacity of ~ 220 mAh/g at 300 mA/g, along with superior rate capability of up to 2000 mA/g, benefiting from the perpendicular open architectures.

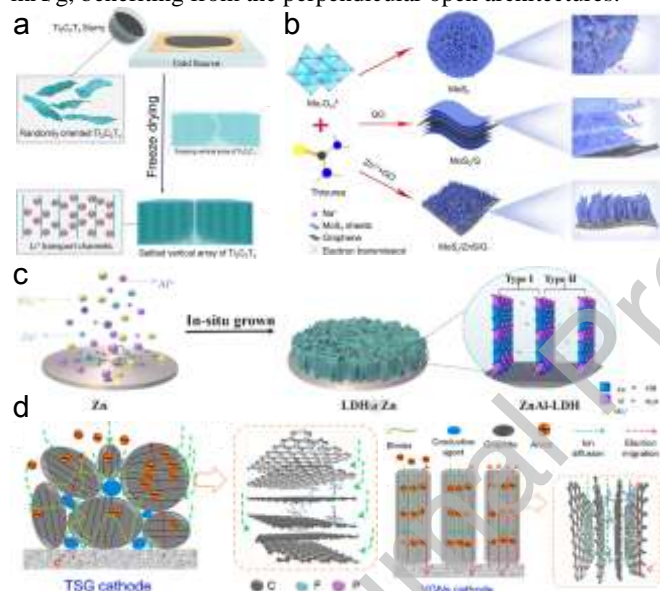


Fig. 14. (a) The synthesis schematic diagram of v- $\text{Ti}_3\text{C}_2\text{T}_x$ electrodes. Reproduced with permission [244]. Copyright 2022, Wiley. (b) Schematic illustration for synthesis and structural illustration of MoS_2 , MoS_2/G , and $\text{MoS}_2/\text{ZnS}/\text{G}$. Reproduced with permission [247]. Copyright 2024, Springer Nature Link. (c) Schematic diagram of the fabrication of LDN@ZN and the crystal structure of LDH. Reproduced with permission [248]. Copyright 2025, Elsevier. (d) The VGNs cathode. Reproduced with permission [250]. Copyright 2024, Elsevier.

9.4 Concluding remarks and prospects

The cost-effectiveness and simultaneously environmentally friendly synthetic methods is expected to be developed in the large scale production of the vertically aligned nanosheets electrodes. In addition, smarter synthesis methods is required to enhance the quality and the structural integrity of the vertically aligned structures. Constructing dense and thick nanomaterial electrodes is urgently desired to achieve both high volumetric and areal energy densities in electrochemical energy conversion and storage devices. The precise tailoring and optimized tuning of materials properties not only make them attractive for fundamental studies but also lead them in different areas. In order to maintain the high rate and power capability of electrode, the doping, defect, and phase engineering can be employed to modify the nanosheets electrodes and tune its properties such as electronic, optical, magnetic, thermal, mechanical, and wettability. The optimization on electronic and structural functionalities provides a great opportunity to enrich their application in diverse scenarios. According to the minimum energy configuration, the vertically aligned nanosheets tend to aggregate during the electrochemical process. One possible means to prevent the restacking phenomenon is to coat the nanosheets with various polymers. Through the physical barrier, the structural and chemical stability of the electrodes can be improved. There is still room for modifying the vertically aligned nanosheets through multidisciplinary and interdisciplinary intersection research from the perspectives of

experiments and theories. In addition, some basic scientific obstacles must be focused on to correlate the scientific hypothesis with the intrinsic electrochemical performance in high-energy batteries. The intrinsic mechanism should be revealed among the electrode modification process, while the electrochemical reactions should be monitored under working conditions. Understanding their electronic structures and reaction mechanism facilitates the following enhancement on the battery performance of vertically aligned materials for various applications. The combining between theoretical study and realistic device can create more opportunities for the materials.

10. 2D Carbide materials for energy conversion and storage

Dandan Ma, Jian-Wen Shi*

10.1 Status

$g-C_3N_4$ (CN) is a 2D organic polymer semiconductor composed of carbon and nitrogen atoms linked by covalent bonds, it can be readily synthesized through the thermal polymerization of cost-effective, nitrogen-rich precursors [86,251,252]. The sp^2 -hybridized structure confers considerable stability to CN under various environmental conditions such as acids and alkalis [253]. Furthermore, CN possesses a layered structure with an interlayer spacing of approximately 0.32 nm, this unique architecture endows CN with high specific surface area, substantial porosity, and abundant active sites [254]. In addition, the high modifiability of the unsaturated N atom enables versatile tuning of its bandgap, conductivity, and surface electronegativity, which also facilitates the facile loading of active functional groups or small molecules, allowing for customized physicochemical properties (Fig. 15). All of these merits make CN a highly promising candidate in energy conversion and storage, particularly in photocatalysis, electrocatalysis, and rechargeable batteries [255].

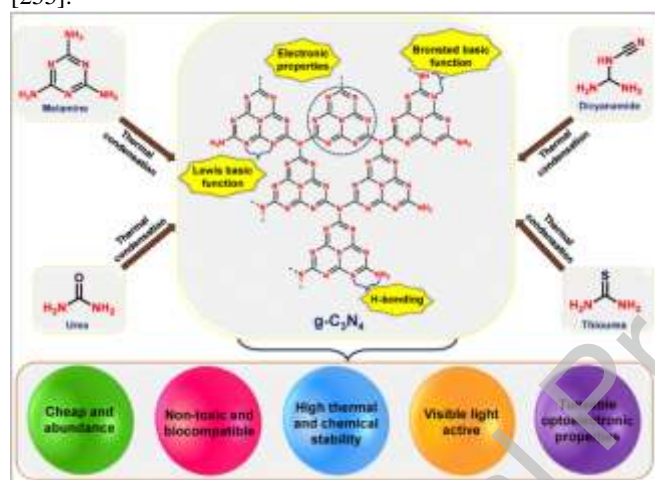


Fig. 15 Schematic diagram the fabrication of CN from various precursors and the various modification active sites. Reproduced with permission [254]. Copyright 2025, Royal Society of Chemistry.

10.2 Current and future challenges

Solar energy conversion: $g-C_3N_4$ is a wide band gap semiconductor with an energy band gap of around 2.7 eV, the conductive band of $g-C_3N_4$ is about -1.12 eV, which is thermodynamically favorable for many reduction reactions, many researches have demonstrated the potential of $g-C_3N_4$ in photocatalytic H_2 evolution, nitrogen fixation and CO_2 reduction [251,253,256-258]. The application of $g-C_3N_4$ is limited by some inherent insufficiency in terms of visible light absorption, carrier separation, and active sites. The efforts in improving the photocatalytic performance of $g-C_3N_4$ mainly focus on two perspectives: the modification of $g-C_3N_4$ itself and the combination of $g-C_3N_4$ with other materials [256,257]. However, many explanations to the modification strategies still stay at a surface level, there is lack of discussion about mechanism and essential meaning of these methods. The missed in-depth insight to the structure-performance relationship limited the studies on the development of reasonably designed catalysts to meet the demands of practical application. Recent studies increasingly highlight that atomic-level structural motifs such as tri-s-triazine units, terminal amine groups ($-NH_2$), nitrogen vacancies, and interlayer hydrogen bonding critically determine light absorption, carrier transport, and catalytic active site distribution. For example, nitrogen vacancies can promote charge delocalization and act as active centers for redox reactions, while terminal amine groups modulate band positions and surface hydrophilicity, influencing the adsorption-activation process of reactants [259]. However, controlling these structural features precisely during synthesis remains a major challenge due to the complexity of the polycondensation process and its sensitivity to temperature, precursor composition, and reaction atmosphere. This lack of controllability fundamentally restricts the establishment of clear structure-performance correlations for targeted photocatalytic applications.

Electrocatalysis: Although the electrical conductivity of $g-C_3N_4$ is lower than many traditional electrocatalysts, the merits of high specific area, excellent stability in acidic and alkaline conditions, and easily modifiable electronic structure still make this material highly valued in the field of electrocatalysis [260-262]. By combining CN with high-conductive materials, the stability of the catalyst

can be significantly enhanced while maintaining its catalytic activity, but it still unsolved in controlling the layer amount of CN and interface interaction between CN and electrolyte.

Rechargeable battery: The chemical durability and the soft 2D structure make CN a favor candidate in rechargeable batteries to lessen the sensitivity of device for lithium dendrites and increase the durability of the durability of the system, especially Li-metal batteries. In addition, CN can also be used as a modifier for cathode materials of Li-S batteries to improve the cycle stability and rate performance of Li-S batteries, and thus improve the electrochemical performance [255,263,264]. According to the reports, the energy storage capacity of CN participated batteries is influenced by variety of parameters, including conductance, surface area, nitrogen concentration, crystalline nature, and other elements. Unfortunately, as there were insufficient studies on this response process, precise implications could not be formed.

10.3 Advances in science and technology to meet challenges

As a 2D material, the properties of CN is directly affected by the morphology and structure of itself, adequately fabrication of well-shaped CN with adjustable layers amounts, size, and surface characteristics remained unexplored despite the fact that it enables us to evaluate their individual structures and attain optimum performance in many disciplines [253,262]. The current research based on CN is still very limited, this is due to the complex structure characteristic and the uncontrollable microscopic reaction processes. The lack of a clear understanding of the growth process hinders the accurate regulation of its domain morphology, and further, this uncontrollability also becomes a reason for hindering the understanding to the role of CN in the energy conversion process. Therefore, the precise control over the size and layer numbers of CN through preparation processes remains important but highly challenging.

To date, research efforts have predominantly focused on enhancing the conductivity, specific surface area, and light absorption of CN. However, insufficient attention has been given to the compatibility between the structure and its specific applications. To overcome this, several advanced synthetic strategies, such as precursor engineering, templated growth, and atmosphere-regulated thermal polymerization, have been explored to introduce or control atomic-level features like nitrogen vacancies, terminal amine groups, and defect density in a predictable manner. Xiao *et al.* [265] employed the rapid heating and cooling capability of flash Joule heating (Fig. 16a) to introduce and precisely regulate defects while preserving the structural integrity of the synthesized g-C₃N₄. By tuning the processing parameters, the band structure of g-C₃N₄ was optimized, effectively suppressing electron-hole recombination and substantially enhancing its photocatalytic hydrogen evolution efficiency from water splitting (Fig. 16b). This approach reduced the production cost to one-twelfth of the conventional value, decreased energy consumption to one-twenty-third, and lowered CO₂ emissions to less than one-eighth of those associated with the traditional thermal polymerization method under comparable conditions.

By coupling *in situ* characterization techniques (e.g., synchrotron X-ray, solid-state NMR, EPR) with theoretical simulations, the formation and evolution of key structural units (e.g., tri-s-triazine motifs) can be monitored and correlated with catalytic performance. Chen *et al.* [266] designed g-C₃N₄ nanosheets with controllable doping and nitrogen vacancies (Fig. 16c) for the efficient and selective conversion of CO₂ into C₂H₆. *In situ* infrared spectroscopy (Fig. 16d) and theoretical calculations (Fig. 16e) further confirmed that the bridged carbon sites and nitrogen vacancies play crucial roles in activating CO₂ molecules and facilitating the formation of C-C coupled intermediates (OCCO), which are highly favorable for C₂H₆ production. This integrated approach provides a pathway toward the rational design of g-C₃N₄ materials with application-oriented functionalities. By systematically correlating the physicochemical properties of CN with its intended functions, and conducting precise structural design and targeted modifications, it is expected to significantly enhance its performance in photocatalytic hydrogen evolution, CO₂ reduction, and N₂ fixation.

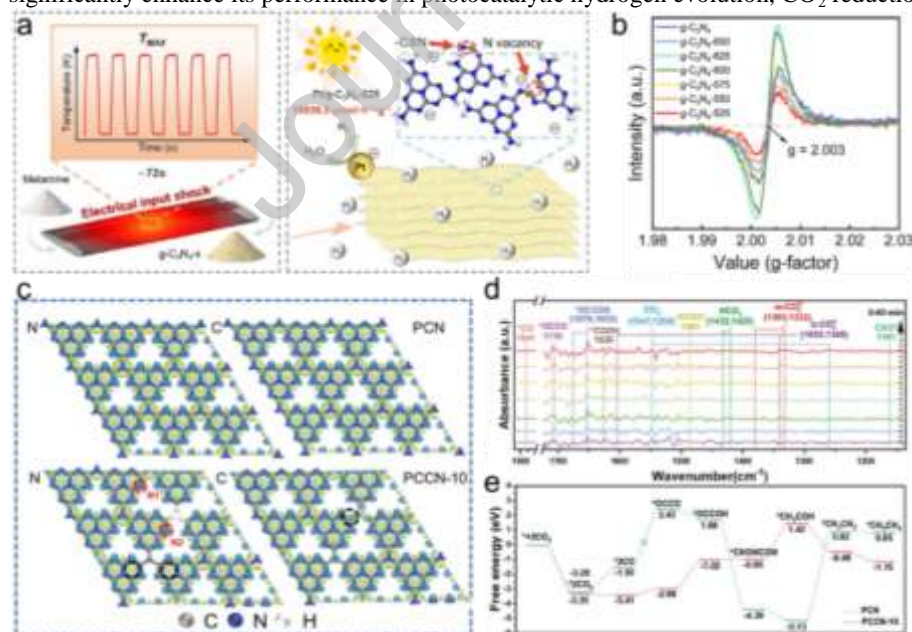


Fig. 16. (a) The preparation of layered mesoporous nitrogen-defective carbon nitride, (b) EPR spectra of g-C₃N_{4-x} (x = 525, 550, 575, 600, 625, 650) and g-C₃N₄. Reproduced with permission [265]. Copyright 2025, Wiley. (c) Difference in electron density of elemental C and elemental N for PCN and PCCN-10. (d) *In situ* DRIFTS detections on the PCCN-10 photocatalyst in CO₂ atmosphere under irradiation. (e) Proposed mechanism for the photocatalytic reactions in PCCN-10. Reproduced with permission [266]. Copyright 2025, Wiley.

10.4 Concluding remarks and prospects

CN has shown great potential in energy conversion and storage. The exploration on the application of CN has just begun, there is still large space for further improvements in applications and synthetic strategies. With the continuous advancement of theoretical research and experiments, it is expected that the application scope of CN in energy conversion will continue to expand and the development of related fields will be promoted.

CN has demonstrated considerable potential in the field of energy conversion and storage. Although its application is still in the early stages, there remains substantial room for advancing both synthetic strategies and device engineering. Continued progress in theoretical understanding, coupled with the development of precise structural modulation and surface chemistry control, is expected to further enhance its catalytic activity, electrical conductivity, and stability. With sustained innovation in material design and integration into practical device architectures, the application scope of CN in energy conversion systems will continue to broaden. These advancements are anticipated to accelerate the development of high-efficiency, low-cost, and sustainable energy technologies, thereby promoting progress across related research fields.

11. Hydrotalcite for energy conversion and storage

Ahmed Ismail*

11.1 Status

Hydrotalcite, also known as a layered double hydroxide (LDH), is a naturally occurring mineral belonging to the family of anionic clays. It has a brucite-like 269 layered structure in which divalent cations are partially substituted by trivalent metal cations [267,268]. Due to its layered structure, it exhibits unique properties such as tunable composition and anion exchange capacity. These properties make hydrotalcite and hydrotalcite-based composite highly active in different energy conversion and storage systems (Fig. 17), such as Li/Na-ion batteries, Li/S batteries, supercapacitors and electrocatalysis [269].

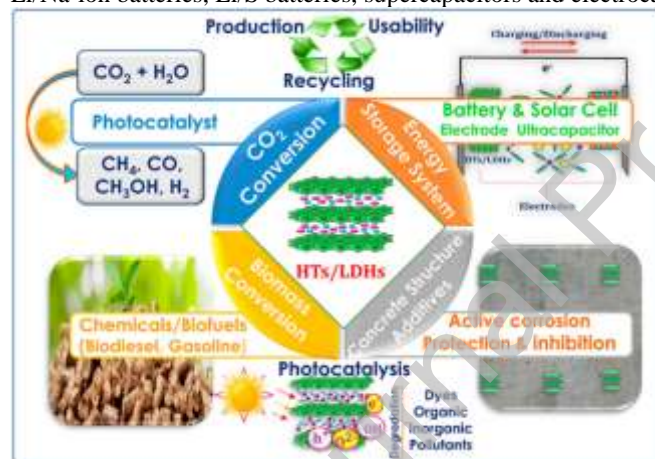


Fig. 17. Hydrotalcite for energy conversion and storage. Reproduced with permission [269]. Copyright 2023, Elsevier.

11.2 Current and future challenges

As layered material anions (e.g., CO₃²⁻ and NO₃⁻) are located in the interlayer voids of hydrotalcite, so it has attracted significant interest in aqueous alkaline batteries due to the possibility of adjusting the metal cations and the intercalating anions [270]. The layered structure with large interlayer spacing offers unique diffusion pathways for fast Li⁺ storage. For example, layered cobalt hydrotalcite (LCH) as advanced anode material with large interlayer spacing provides sufficient spacing for Li-ion insertion and as a result displayed a 743.9 and 643.4 mAh/g high reversible capacity at 500 and 2000 mA/h/g over 600 and 2000 cycles. They also showed an outstanding 490.0 mA h/g rate capability at 5000 mA/g in Li ion half cells [271]. Despite of these promising results, hydrotalcite face challenges in Li ion batteries such as voltage instability, structural complexity, volume changes on cycling, limitations related to Li ion diffusion and safety.

Supercapacitors represent a highly promising class of energy storage devices, primarily due to their elevated power density and prolonged operational lifespan. These devices can be broadly categorized into two types based on their distinct energy storage mechanisms: electric double layer capacitors (EDLCs) and pseudocapacitors. Despite hydrotalcite several advantages such as large electrochemically active surface area and metal ions embedded in the layers, it fails to achieve their theoretical specific capacitance. This is due to low ionic conductivity, restacking of layers and a lack of active functional groups. Therefore, hydrotalcite structure

modulation by morphological as well as composition engineering, heteroatom doping and composite formation can effectively address these shortcomings and can improve the electrochemical performances of hydrotalcite in energy storage systems [272].

Fuel cell and metal-air batteries are a typical energy conversion device, which rely on the efficiency of oxygen evolution (OER) and reduction (ORR) reactions, meanwhile electrolysis totally relies on hydrogen evolution (HER) and OER reactions. Hydrotalcite with layer-to-layer assists exfoliation, yielding large surface area with ultrathin nanosheets, cations and anions flexibility and memory effect permits the usage of hydrotalcite in sea water electrolysis to produce H_2 . Hydrotalcite with surface/interface engineering, An-site regulation by interlayer intercalation and tuning of layered metal divalent and trivalent cations are effective approaches to gain supreme catalytic performance. As layered material with adjustable surface chemistry and high conductivity, it also affords a strong backbone to earth-abundant metal-based nanoparticles. Hydrotalcite as electrocatalysts and current collector integrated air-electrodes are promising for energy conversion devices [273]. The layered structure, surface area, and the number of active sites in the hydrotalcite have crucial impact on the electrochemical performance of these devices. For example, hydrotalcite like $Ni(OH)_2/NF$ electrode showed excellent electrocatalytic activity and stability for the HER as well as OER and the overall water splitting. The electrode reaches a current density of 20 mA/cm^2 at an overpotential of 172 mV for the HER, 50 mA/cm^2 at 330 mV for the OER, and 10 mA/cm^2 at a cell voltage of 1.68 V during overall water splitting in 1.0 mol/L KOH [274].

Li-S batteries are considered a promising option for future energy storage solutions due to the high theoretical capacities of lithium, at 3861 mAh/g, and sulfur, at 1675 mAh/g [275]. Hydrotalcite incorporation into the separator or cathode can suppress the polysulfide shuttle effect, that is the primary cause of sulfur loss and battery degradation in Li-S batteries. Besides intercalation, hydrotalcite has been applied as a sulfur host to control conversion and dissolution of lithium polysulfides [276].

11.3 Advances in science and technology to meet challenges

Hydrotalcite-based materials have recently seen significant progress toward solving key obstacles in their use for energy conversion and storage. Through co-doping strategy, researchers have prepared materials with good OER and HER rates for many redox cycles and stable structure. Ma *et al.* co-doped Ru and Mn in NiCo-LDH and NiCoP by electrodeposition and simple phosphorization method (Fig. 18a). The Ru and Mn co-doped NiCo-LDH showed excellent OER activity (342 mV at 500 mA/cm^2) in alkaline solution, while Ru and Mn co-doped NiCoP demonstrated high HER activity (200 mV at 500 mA/cm^2) (Figs. 18b-d) [277].

Introducing oxygen vacancies in Cobalt aluminum hydrotalcite is an effective way to improve the sluggish charge transfer and ion diffusion in hydrotalcite materials. Wang *et al.* introduced oxygen vacancies in CoAl LDHs through $NaBH_4$ treatment, that improved the electrochemical energy storage performance of pure CoAl LDHs. The CoAl LDHs-0.5 showed 799.2 F/g specific capacity at 1 A/g current density and retained 81.1% capacity even at 20 A/g density [278].

Hydrotalcite still lacks practical performance in high energy storage systems due to self-stacking, slow reaction kinetics, poor conductivity and poor ion diffusion. The construction of synergistic and complementary composite electrode materials using 2D dimensional conductive materials are considered as promising candidates for improving the conductivity, ion diffusion and mechanical properties of hydrotalcite. Luo *et al.* synergistically coupled ternary hydrotalcite (NiCoMn-LDH) and $Ti_3C_2T_x$ -MXene nanosheets for boosting electron transportation, structural stability and electrolyte accessibility in energy storage [279]. As a result, the intriguing “lace-like” structure fully utilizes the high activity of NiCoMn-LDH and the excellent conductivity of $Ti_3C_2T_x$, allowing LDH/ $Ti_3C_2T_x$ to exhibit an impressive output capacitance of 1102.9 F/g at 1 A/g , coupled with notable rate capability (66.87% at 20 A/g). The constructed LDH/ $Ti_3C_2T_x$ //AC hybrid supercapacitor (HSC) achieves a remarkable energy density of 47.3 Wh/kg (Figs. 18e-g).

Beyond these advances, recent studies have revealed that the electrochemical behavior of hydrotalcite-based composites is critically governed by the atomic or molecular structure of the interface between hydrotalcite and conductive substrates (MXenes). An ideal interface typically involves the formation of strong interfacial coupling through hydrogen bonding, electrostatic interactions, or covalent M–O–M linkages (where M represents transition metals such as Ni, Co, or Ti). This intimate contact minimizes interfacial resistance and enables rapid bidirectional electron transfer pathways. Meanwhile, the presence of ordered interfacial channels or defect-rich regions promotes efficient ion diffusion perpendicular to the plane, synergistically enhancing reaction kinetics. In particular, $Ti_3C_2T_x$ MXene substrates with surface –OH, –F, and –O terminations can provide abundant anchoring sites for LDH nucleation, thereby forming well-aligned heterointerfaces with strong electronic coupling. Such rationally engineered interfaces not only facilitate ultrafast charge migration across the heterostructure but also maintain structural stability during long-term cycling. This interfacial design concept represents a fundamental scientific basis for achieving high energy density and long lifespan in hydrotalcite-based energy storage systems.

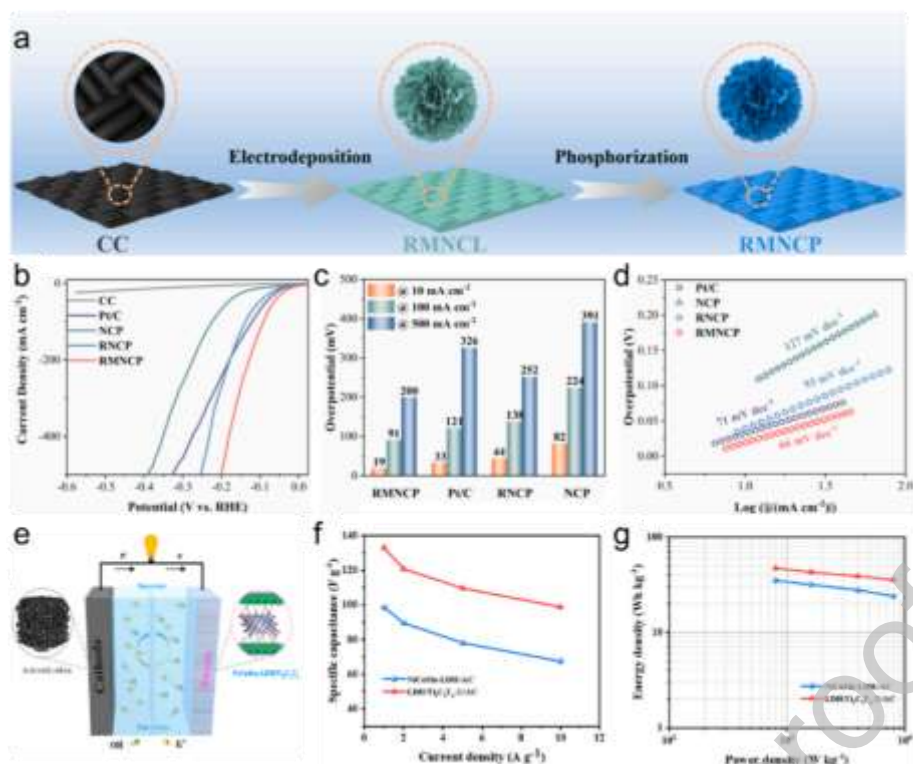


Fig. 18. (a) Schematic diagram of synthesizing RMNCL and RMNCP, (b) HER polarization curves, (c) overpotentials at 10, 100 and 500 mA/cm², (d) Tafel plots of different catalysts. Reproduced with permission [277]. Copyright 2024, Elsevier. (e) Schematic diagram of LDH/Ti₃C₂T_x//AC HSC, (f, g) The specific capacity and Ragone plots of NiCoMn-LDH//AC and LDH/Ti₃C₂T_x//AC HSCs. Reproduced with permission [279]. Copyright 2024, Elsevier.

The charge transfer kinetics in hydrotalcite depends on the interlayer spacing, the larger the interlayer spacing, more improvement in electrochemical performance was observed. Anion intercalation has been proven to promote the interlayer spacing in hydrotalcite, which in turn enhances the amount of available active sites, diffusion phenomena and specific capacity. Cui *et al.* intercalated PO₄³⁻ in NiCo-LDH which showed 287.5 mAh/g specific capacity. In addition, the asymmetric supercapacitor assembled with this material as the cathode achieved a notable energy density of 49.2 Wh/kg.

11.4 Concluding remarks and prospects

Due to its inherent characteristics, hydrotalcite is regarded as a promising candidate for energy storage applications. The interaction at the interface between hydrotalcite and other materials is vital for boosting the electrochemical performance of batteries and supercapacitors. However, there are still several obstacles to overcome. Impurities and structural flaws that arise during the synthesis of hydrotalcite can adversely affect its electrochemical properties. Additionally, the performance of layered hydrotalcite is significantly influenced by the number of layers, making it crucial to fabricate materials with precisely controlled layer thickness. Furthermore, the current synthesis methods are often intricate and expensive, limiting large-scale production and wider application. Thus, it is necessary to develop more efficient and cost-effective processing techniques to enhance quality, reduce expenses, and speed up the practical application of hydrotalcite in energy storage systems. So far, much research has focused on material preparation and characterization, with limited emphasis on understanding the fundamental mechanisms that dictate hydrotalcite's electrochemical properties. Gaining a deeper understanding of these mechanisms and fully harnessing hydrotalcite's potential are essential for advancing its role in energy storage. Hydrotalcite is a promising material for energy-related uses, but it faces several obstacles. Many theoretical analyses and experimental studies have been performed, with hopes of achieving more substantial advancements in the future.

12. 2D Materials: Heterostructures, roadmap, and device-level integration for energy technologies

Lan Ding, Kezhen Qi*

12.1 Status

In recent years, 2D-2D heterostructures have emerged as one of the most promising strategies to overcome the intrinsic limitations of individual 2D materials and to unlock new functionalities in energy storage and conversion applications. Unlike 0D/2D or 1D/2D combinations, 2D-2D architectures provide atomically intimate interfacial contact, maximized active surface exposure, and efficient charge/ion transport pathways, which are highly advantageous for batteries, supercapacitors, photocatalysis, and electrocatalysis.

Representative 2D-2D systems include MXene/COF, TMD/graphene, MOF/perovskite, and LDH/MXene heterostructures [280-282]. For instance, a covalent self-assembly strategy has been employed to construct COFs/MXene heterojunctions, which are further

utilized as efficient electrocatalysts for modified separators in lithium-sulfur batteries. Benefiting from interfacial coupling, the curvature engineering of COFs induces interfacial charge redistribution within the COFs/MXene heterojunction, thereby markedly enhancing both ion and electron transport kinetics across the interface and lowering the nucleation/decomposition energy barriers of Li_2S . As a result, highly efficient relay-type bidirectional catalysis is achieved [283]. Similarly, the selective preferential dissolution of alternating layers in spinel structures can lead to a progressive topotactic transformation from spinel to LDH. During this gradual conversion, a chemically bonded 2D/2D in-plane spinel/LDH heterojunction is formed. The presence of covalently bridged 2D/2D in-plane interfaces induces pronounced charge transfer and redistribution. Such charge rearrangement at the oxide/hydroxide 2D/2D interface significantly accelerates both HER and OER reaction kinetics [284]. Moreover, 2D-2D heterojunctions can be rationally designed to tailor band alignment and built-in electric fields, which accelerate charge carrier separation in photocatalytic and electrocatalytic systems. For example, BP/CoNiSe₂ and CoWO₄/g-C₃N₄ 2D heterointerfaces display boosted HER and OER activity, with overpotentials significantly lower than their single-component counterparts. These advances position 2D-2D heterostructures as a powerful platform for developing next-generation sustainable energy technologies [285,286].

12.2 Current and future challenges

Despite these advances, several critical scientific and technological challenges still impede the large-scale application of 2D-2D heterostructures. A major concern lies in the intrinsic interfacial stability under electrochemical operating conditions. Many heterostructures exhibit weak interfacial bonding, leading to delamination or phase transformation during extended cycling, particularly in Zn^{2+} or Mg^{2+} aqueous systems where strong ion-solvent interactions accelerate structural degradation. Another bottleneck is the lack of precise and scalable assembly techniques. Current fabrication methods, such as vacuum filtration, solvothermal growth, or electrostatic self-assembly, often result in random orientation, poor interfacial control, and defects that impede optimal charge and ion transport. Achieving atomically defined, controllable stacking remains a formidable challenge.

Furthermore, interfacial charge and ion transport behavior is still not fully understood, especially for large-radius hydrated ions like Na^+ , K^+ , Zn^{2+} , and Mg^{2+} . The heterointerface can simultaneously accelerate and hinder transport depending on its structure, chemistry, and interlayer spacing. Recent studies have suggested that universal descriptors such as interlayer spacing, ion solvation energy, and surface functional groups govern ion intercalation kinetics across diverse 2D systems. These parameters collectively determine ion diffusion barriers and interfacial charge transfer efficiency, yet their quantitative correlation with electrochemical performance remains unclear. For instance, small ions (Li^+ , Na^+) typically show faster diffusion and lower desolvation barriers, whereas multivalent ions (Zn^{2+} , Mg^{2+}) experience stronger solvation and stronger electrostatic interactions, leading to sluggish kinetics and higher overpotentials. Correlating these parameters with electrochemical performance requires deeper mechanistic insight. From a practical perspective, most 2D-2D heterostructures remain at the laboratory scale, and there is still a long way to go toward realizing scalable manufacturing compatible with commercial electrodes and devices. In addition, real-time tracking of interfacial processes remains limited. Although *in situ* and operando characterization tools have made progress, direct observation of interfacial electron redistribution, intermediate states, and structural evolution under realistic working conditions is still challenging. A systematic understanding of these descriptors will thus be critical for rational interface design and predictive modeling of ion transport behavior. These factors collectively restrict the rational design and optimization of high-performance 2D-2D heterostructures.

12.3 Advances in science and technology to meet challenges

To address the aforementioned challenges, recent research efforts have focused on interfacial engineering, structural modulation, and the development of advanced characterization techniques. One of the most effective approaches is to strengthen interfacial bonding and electronic coupling between two 2D components. Covalent or ionic bridging strategies have been widely adopted to achieve this goal. For example, functional group engineering using $-\text{OH}$ or $-\text{COOH}$ linkers between $\text{Ti}_3\text{C}_2\text{T}_x$ MXene and COF nanosheets can generate robust interfacial bonding, significantly enhancing electrochemical stability during Li^+ and Na^+ intercalation. Similarly, heteroatom doping at the interface, such as nitrogen, sulfur, or phosphorus, can modulate electronic structures, lower energy barriers, and boost electrocatalytic activity for HER and OER reactions.

A representative example highlighting the effectiveness of 2D-2D interface engineering was reported by Liu *et al.* [287]. They designed a lithium-ion-activated 2D-2D tin sulfide/graphene nanocomposite membrane (A-SnS-G) as an artificial SEI layer to stabilize ultrathin (100 μm) sodium metal foils. This A-SnS-G membrane, initially placed on a polypropylene separator, can be *in situ* transferred onto the Na surface during cycling to form a robust and ion-conductive interface. The protected Na anode exhibited outstanding cycling stability at 4 mA/cm^2 for 500 cycles, achieving a cumulative areal capacity of 1000 mAh/cm^2 and an A/F ratio of 90.9. Post-mortem and operando analyses revealed that A-SnS-G effectively suppressed dendrite growth and dead sodium formation, while XPS confirmed the formation of a stable SEI containing Sn-Na alloys, Li_2CO_3 , ROCO_2Li , and LiF even after 300 cycles. Furthermore, a sodium metal full cell using a high-mass-loading NVP cathode (6 mg/cm^2) retained a capacity of 74 mAh/g at 0.4 C after 400 cycles. This study exemplifies how rational design of 2D-2D heterointerfaces can dramatically enhance interfacial stability and enable practical high-energy-density metal batteries.

Beyond chemical bonding, structural modulation plays a crucial role in optimizing charge and ion transport across 2D-2D heterostructures. Interlayer spacing engineering, for example, is particularly important for accommodating large hydrated ions such as Zn^{2+} or Mg^{2+} . The introduction of organic spacers or soft templates can effectively enlarge interlayer distances and reduce ion diffusion resistance. Layer-by-layer assembled MoS_2 /graphene heterostructures with well-controlled interlayer spacing have demonstrated ion

diffusion coefficients an order of magnitude higher than those of pristine MoS₂, illustrating the power of nanoscale structural regulation. Moreover, tailoring solvation environments and surface terminations has recently emerged as an additional design handle to modulate ion transport descriptors. By introducing functional moieties (*e.g.*, –OH, –F, –O) or ionic liquids at interfaces, researchers can fine-tune solvation dynamics and weaken hydration shells, accelerating interfacial diffusion particularly for multivalent ions. Meanwhile, band alignment engineering, including S-scheme and Z-scheme designs, has emerged as an efficient strategy to manipulate interfacial built-in electric fields and facilitate charge carrier separation [288-290]. Notable examples include Bi₂O₃/MXene and g-C₃N₄/MoS₂ heterojunctions, which exhibit enhanced photocatalytic hydrogen evolution and CO₂ reduction efficiency under simulated solar irradiation.

To further deepen the mechanistic understanding of 2D-2D heterostructures, advanced operando characterization techniques are being increasingly employed. Synchrotron-based XRD and XAS, in combination with cryo-TEM, have enabled direct observation of interfacial structural evolution, electron redistribution, and intermediate species formation during ion intercalation or catalytic reactions. Such real-time insights are critical for guiding rational interface design. Combining these techniques with computational modeling now allows quantitative mapping of universal descriptors, including interlayer spacing, solvation energy, and surface chemistry, with experimentally measured ion diffusion coefficients. This integrated approach bridges the gap between theory and experiment, providing a mechanistic framework to guide the rational optimization of charge/ion transport in complex 2D heterostructures. Encouragingly, several 2D-2D heterostructures have already been successfully integrated into practical energy storage and conversion devices, including Zn-ion hybrid capacitors, solid-state Li-ion batteries, and alkaline water electrolyzers. These devices exhibit high areal capacity, rapid charge-discharge capability, and long-term cycling stability, showcasing the transformative potential of 2D-2D heterostructures in next-generation sustainable energy technologies.

12.4 Concluding remarks and prospects

Overall, 2D-2D heterostructures represent a new paradigm in the design of functional materials for energy conversion and storage. By integrating complementary characteristics, for example the high electronic conductivity of MXenes with the tunable porosity of covalent organic frameworks, or the superior catalytic activity of transition metal dichalcogenides with the rapid charge transport of graphene, these systems create synergistic interfacial domains that cannot be achieved in single-phase materials. Looking toward 2030, several promising research directions are expected to shape the development of this field. A key emerging priority is the establishment of universal descriptors that can quantitatively link structural and chemical parameters to ion transport behavior. Interlayer spacing, solvation energy, and surface functional groups have been identified as the most relevant descriptors governing ion intercalation kinetics. For small ions like Li⁺ and Na⁺, optimal spacing and low solvation barriers promote fast diffusion, while for multivalent ions such as Zn²⁺ and Mg²⁺, strong solvation and electrostatic coupling dominate transport dynamics. Understanding these correlations will provide predictive rules for designing next-generation heterostructures. Such descriptors will guide rational selection of material pairs and interfacial configurations.

At the same time, scalable and controllable fabrication strategies, including bottom-up growth, roll-to-roll assembly, and solution-phase synthesis, will be critical for translating 2D-2D heterostructures from laboratory research to industrial applications. Future research should also emphasize multifunctional interface design to simultaneously optimize electronic, ionic, and catalytic properties, enabling hybrid devices that integrate energy storage and conversion functions, such as rechargeable Zn-air batteries or integrated HER/OER electrodes for overall water splitting. Furthermore, incorporating descriptor-based design principles into machine learning and high-throughput screening workflows will accelerate the discovery of optimal material combinations and interfacial architectures. Meanwhile, the combination of machine learning with high-throughput simulations and experimental databases is expected to accelerate the discovery of optimal heterostructure combinations and architectures. With continued progress in interface science, characterization, and manufacturing technologies, 2D-2D heterostructures are poised to play a central role in next-generation high-performance and sustainable energy systems.

12.5 Competitive landscape and 2030 roadmap of 2D materials

Toward 2030, the competitive landscape of 2D materials is expected to be strongly application-dependent. For high-power devices such as supercapacitors, graphene and MXenes are poised to dominate due to their exceptional conductivity, high surface area, and rapid ion transport, with composite and heteroatom strategies further enhancing performance. For high-energy batteries, black phosphorus, 2D metal sulfides, and 2D perovskites offer high theoretical capacities and layered architectures conducive to efficient ion intercalation, with recent advances in defect engineering and interlayer modulation addressing structural stability challenges. In energy conversion, COFs, MOFs, hydrothermalites, and 2D carbides provide tunable electronic structures, abundant active sites, and favorable charge transport, enabling efficient photocatalysis and electrocatalysis. 2D-2D heterostructures are expected to become increasingly central, exploiting synergistic effects to simultaneously optimize energy and power densities. Overall, future progress will hinge on interface design, defect and strain modulation, and hybridization strategies to fully realize the potential of 2D materials for sustainable energy technologies.

To provide a coherent and quantitative perspective across these diverse materials, we introduce an integrated analytical framework in combination with a 2030 development roadmap. A comprehensive performance comparison table (Table 1) systematically summarizes key electrochemical and structural parameters, including conductivity, capacity or catalytic activity, stability, and other functional characteristics relevant to energy storage and conversion, thereby enabling direct cross-comparison among representative

classes of two-dimensional materials. This unified comparison highlights the correlations between performance and structure and clarifies the relative advantages, limitations, and complementarities of different material systems.

Table 1 Performance comparison of representative 2D materials for energy storage and conversion.

| 2D Materials | Representative material | Conductivity | Capacity/Activity | Stability | Key features & applications |
|-------------------------------|--|--------------|-------------------|-----------|---|
| Graphene & Composites | Graphene, rGO, N-doped graphene | High | Medium | Excellent | High conductivity, fast ion transport; Li-/Na-ion batteries, supercapacitors |
| Black Phosphorus | BP nanosheets | Medium | Very high | Good | Ultra-high capacity, tunable bandgap; Li-ion batteries, photocatalysis |
| MXenes | Ti ₃ C ₂ T _x , Nb ₂ CT _x , V ₂ CT _x | High | Medium-high | Excellent | Metallic conductivity, surface tunability; batteries, HER/OER, supercapacitors |
| 2D Porous Frameworks | COFs, MOFs | Low-Medium | Medium | Variable | Tunable pore structure, abundant active sites; electrocatalysis, photocatalysis |
| 2D Metal Oxides | TiO ₂ , MnO ₂ nanosheets | Low | Medium | Good | Chemically stable, layered structure; batteries, photocatalysis, electrocatalysis |
| 2D Metal Sulfides | MoS ₂ , WS ₂ , VS ₂ | Medium | High | Good | Layered structure, abundant sites; Li-/Na-ion batteries, HER |
| 2D Perovskites | ABX ₃ -type nanosheets | Medium | High | Good | Tunable bandgap, layered structure; batteries, photocatalysis |
| Vertically Aligned Nanosheets | VA-MoS ₂ , VA-TiO ₂ | Medium | High | Good | Short ion diffusion path; high-power rechargeable batteries |
| 2D Carbides | g-C ₃ N ₄ | High | Medium | Excellent | High conductivity, robust; supercapacitors, batteries, HER/OER |
| Hydroxalicates | MgAl-LDH, NiFe-LDH | Low-Medium | Medium | Good | Layered structure, tunable composition; electrocatalysis, OER/HER |

Building on this framework, a 2030 development roadmap (Fig. 19) integrates material innovation (e.g., defect and interface engineering), process engineering (e.g., scalable synthesis and structural stabilization), and system integration (e.g., device-level performance and industrialization), delineating the technological trajectory of 2D materials toward high-performance, sustainable energy technologies. Collectively, this unified perspective highlights both the competitive advantages of each material class and the strategic pathways required to realize their full potential in next-generation energy storage and conversion systems.

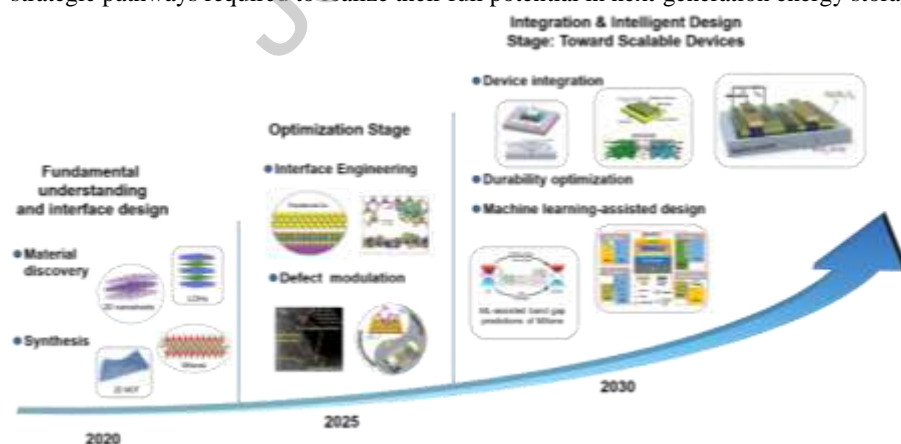


Fig. 19. 2030 roadmap for 2D materials in energy storage and conversion.

12.6 Device-level integration challenges and interdisciplinary strategies

Beyond material-level properties, practical deployment of 2D materials in energy devices faces critical device-level integration challenges. Electrode fabrication and slurry processing must address nanosheet dispersibility, restacking, and mass loading while maintaining efficient ion/electron transport through optimized binders, solvents, and coating methods. Electrolyte compatibility and interfacial stability are essential, as surface terminations may react with electrolytes, forming passivation layers or causing degradation; protective coatings, artificial solid–electrolyte interphases, and compatible electrolytes are key strategies. Mechanical and structural integrity must be ensured in multilayer, large-area, or flexible electrodes to prevent delamination and restacking, while thermal and electrochemical management mitigates local heating and uneven ion distribution under high-rate operation. Addressing these challenges requires interdisciplinary approaches integrating materials science, chemical engineering, electrochemistry, and mechanical design, supported by computational modeling and machine learning to optimize electrode architecture, mass loading, and ion transport. Incorporating these device-level considerations alongside material-level insights provides a comprehensive roadmap for realizing high-performance, practical energy devices based on 2D materials.

In addition to their role in material discovery, AI and ML tools offer transformative potential for addressing core challenges in 2D materials development. Predicting synthesis pathways using AI/ML models trained on experimental and computational datasets enables rational design of defect-free, scalable 2D nanosheets, enhancing reproducibility and synthesis efficiency. For multi-objective performance optimization, ML approaches can simultaneously consider trade-offs among capacity, rate capability, and cycle life, guiding the design of electrode compositions, layer architectures, and heterostructures tailored to specific applications. Moreover, AI-driven analytics can forecast long-term degradation mechanisms by correlating structural evolution, electrochemical cycling data, and environmental factors, informing strategies for interfacial engineering, electrolyte selection, and device-level optimization. Integrating these AI/ML-driven strategies across synthesis, performance optimization, and durability assessment provides a comprehensive framework to accelerate the translation of 2D materials from fundamental discovery to high-performance, practical energy storage and conversion devices.

Acknowledgments

This work was supported by the National Natural Science Foundation of China (Nos. 52272287, 22268003, 22102095, 52204320, U20A20246 and 12275199, U22A20418, 22075196, 21972110, 52202208, 52504346), National Key Research and Development Program of China (Nos. 2023YFA1507903, 2022YFB3803600, 2022YFB4002501), Yunnan Provincial Science and Technology Plan Project (Nos. 202305AF150116, 202405AF140007), SINOPEC (Beijing) Research Institute of Chemical Industry Co., Ltd. (No. 223239), the Fundamental Research Funds for the Central Universities (No. CCNU22JC017), the Postdoctoral Science Foundation of China (No. 2021M692535), the Natural Science Foundation of Shaanxi Province (No. 2022JQ-095), Guangdong Basic and Applied Basic Research Foundation (No. 2024A1515010976), Shenzhen Natural Science Foundation in Basic Research Fund (No. 20250530111628004), the Basic Research Project Foundation of Xi'an Jiaotong University (No. xzy012024012), the Youth Foundation of State Key Laboratory of Electrical Insulation and Power Equipment (No. EIPE2131), the Russian Science Foundation (No. 22-13-00035), the Ministry of Science and Higher Education within the framework of a State Assignment of the Ioffe Institute, Russian Academy of Sciences (No. FFUG-2024-0036), the Russian Science Foundation (No. 24-19-20060) and St. Petersburg Science Foundation (No. 24-19-20060), and the Research Project Supported by Shanxi Scholarship Council of China (No. 2022-050), Hunan Province Furong Plan Young Talents in Science and Technology Innovation (No. 2025RC3013), National Science Centre, Poland (NCN), based on the decision number UMO-2021/43/D/ST5/00824, and the research project within the program, Excellence Initiative – Research University* for the AGH University of Krakow.

CRedit authorship contribution statement

Lan Ding: Writing – review & editing. **Kezhen Qi:** Writing – original draft. **Zimo Huang:** Writing – original draft. **Ying Yu:** Writing – original draft. **Ze Yang:** Writing – original draft. **Sepehr Tabibi:** Writing – original draft. **Alireza Khataee:** Writing – original draft. **Lei Hao:** Writing – original draft. **Qitao Zhang:** Writing – original draft. **Vadim Popkov:** Writing – original draft. **Maria Kaneva:** Writing – original draft. **Artem Lobinsky:** Writing – original draft. **Zhipeng Yu:** Writing – original draft. **Jun Li:** Writing – original draft. **Amir Sultan:** Writing – original draft. **Kun Zheng:** Writing – original draft. **Gan Qu:** Writing – original draft. **Dandan Ma:** Writing – original draft. **Jian-Wen Shi:** Writing – original draft. **Ahmed Ismail:** Writing – original draft.

References

- [1] J. Qin, Z. Yang, J. Ma, et al., *Chin. Chem. Lett.* 35 (2024) 108845.
- [2] S. Wang, D. Yan, W. Zhang, L. Wang, *Chin. Chem. Lett.* 36 (2025) 110611.
- [3] Q. Zhou, L. Wang, W. Ju, et al., *Electrochim. Acta* 461 (2023) 142655.
- [4] T. Liu, L. Zhang, B. Cheng, X. Hu, J. Yu, *Cell. Rep. Phys. Sci.* 1 (2020) 100215.
- [5] S. Wu, G. Chen, N.Y. Kim, et al., *Small*. 12 (2016) 2376-2384.
- [6] D. Malavekar, D. Pawar, A. Bagde, et al., *Chem. Eng. J.* 501 (2024) 157533.
- [7] Q. Chen, J. Kim, M. Choi, S. Jeon, *Nano. Converg.* 12 (2025) 1-24.
- [8] L.M. Shaker, A.A. Abdulamier, A.A. Al-Amieri, *J. Alloys Compd.* 1036 (2025) 182079.

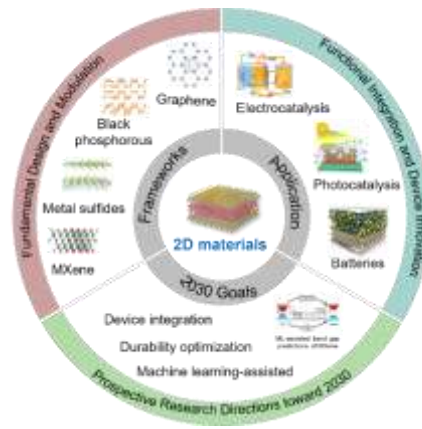
- [9] S. Hemmati, M.M. Heravi, B. Karmakar, H. Veisi, *Sci. Rep.* 11 (2021) 12362.
- [10] Y. Mu, M. Han, B. Wu, et al., *Adv. Sci.* 9 (2022) 2104685.
- [11] E.S. Agudos, E.C. Abdullah, A. Numan, et al., *Sci. Rep.* 10 (2020) 11214.
- [12] Y. Li, J. Xie, R. Wang, et al., *Nano-Micro Lett.* 16 (2024) 79.
- [13] Y. Chen, Y. Liu, L. Li, et al., *Adv. Funct. Mater.* 34 (2024) 2401452.
- [14] S. Das, Monika, S. Ali, et al., *Adv. Energy Mater.* 15 (2025) 2500138.
- [15] X.T. Yin, E.M. You, R.Y. Zhou, et al., *Nat. Commun.* 15 (2024) 5624.
- [16] X.H. Lu, J. Liu, C. Shu, et al., *Adv. Funct. Mater.* 35 (2025) 2417324.
- [17] M. Liu, Y. Xie, F. Liu, et al., *Adv. Funct. Mater.* 35 (2025) 2509429.
- [18] Y. Zhao, H. Hao, T. Song, et al., *J. Alloys Compd.* 914 (2022) 165343.
- [19] Y. Zhao, S. Chen, B. Sun, et al., *Sci. Rep.* 5 (2015) 7629.
- [20] Y. Xia, H. Qin, W. Tong, et al., *Adv. Mater.* 37 (2025) 2417462.
- [21] H. Heo, J. Lee, Y.R. Jo, G.H. An, *Adv. Energy Mater.* 15 (2025) 2570095.
- [22] H.J. Shin, J.T. Kim, Y.M. Kim, D. Han, et al., *Adv. Energy Mater.* 15 (2025) 2403247.
- [23] W. Liu, P. Li, W. Wang, et al., *ACS Nano* 12 (2018) 12255-12268.
- [24] Y. Xu, S. Li, Y. He, et al., *J. Energy Chem.* 103 (2025) 344-352.
- [25] X. Wu, H. Zeng, S. He, et al., *Adv. Funct. Mater.* (2025), <https://doi.org/10.1002/adfm.202519001>.
- [26] M. Lemaalem, S.C. Selvaraj, I. Papailias, et al., *Appl. Energy* 401 (2025) 126693.
- [27] J. Zhou, C. Zhang, C. Hu, et al., *Chin. Chem. Lett.* 35 (2024) 109561.
- [28] Y. Ma, Y. Zhou, M. Yu, et al., *Chin. Chem. Lett.* 35 (2024) 109453.
- [29] H. Tian, J. Wang, G. Lai, et al., *Chem. Soc. Rev.* 52 (2023) 5388-5484.
- [30] X. Han, H. Gong, H. Li, J. Sun, *Chem. Rev.* 124 (2024) 6903-6951.
- [31] Q. Tang, Y. Zhang, X. Zhu, et al., *Adv. Funct. Mater.* 34 (2024) 2410005.
- [32] B. Sun, S. Wang, C. Mao, et al., *Angew. Chem. Int. Ed.* 64 (2025) e202412867.
- [33] C. Peng, B. Wang, L. Wu, et al., *Angew. Chem. Int. Ed.* 64 (2025) e202508454.
- [34] Z. Wu, Y. Lyu, Y. Zhang, et al., *Nat. Mater.* 20 (2021) 1203-1209.
- [35] Y. Ma, K. Wang, Y. Xu, et al., *Adv. Energy Mater.* 14 (2024) 2304408.
- [36] J. Sun, H.W. Lee, M. Pasta, et al., *Nat. Nanotechnol.* 10 (2015) 980-985.
- [37] R. Sun, Y. Bai, Z. Bai, et al., *Adv. Energy Mater.* 12 (2022) 2102739.
- [38] Y. Gogotsi, B. Anasori, *ACS Nano*. 2019, 13, 8491-8494.
- [39] L. Hou, X. Peng, S. Lyu, et al., *Chin. Chem. Lett.* 36 (2025) 110392.
- [40] M. Wu, X. Fan, W. Zhang, *Chin. Chem. Lett.* 35 (2024) 109258.
- [41] B. Anasori, Y. Gogotsi, *Graphene 2D Mater. Technol.* 8 (2023) 39-41.
- [42] M. Naguib, J. Come, B. Dyatkin, et al., *Electrochem. Commun.* 16 (2012) 61-64.
- [43] B. Anasori, Y. Xie, M. Beidaghi, et al., *ACS Nano* 9 (2015) 9507-9516.
- [44] A. VahidMohammadi, J. Rosen, Y. Gogotsi, *Science* 372 (2021) eabf1581.
- [45] N. Goossens, T. Lapauw, K. Lambrinou, J. Vleugels, *J. Eur. Ceram. Soc.* 42 (2022) 7389-7402.
- [46] K.R.G. Lim, M. Shekhirev, B.C. Wyatt, et al., *Nat. Synth.* 1 (2022) 601-614.
- [47] N. Lv, S. Lin, L. Ding, et al., *Chem. Eng. J.* 522 (2025) 167143.
- [48] J. Yoon, K.H. Park, S. Lee, et al., *Small* 21 (2025) 2411319.
- [49] W. Wang, Z. Ma, L. He, et al., *Mater. Today* 89 (2025) 402-439.
- [50] J. Gao, X. Xuan, Y. Tang, et al., *Small* 21 (2025) e05881.
- [51] M. Naguib, M. Kurtoglu, V. Presser, et al., *Adv. Mater.* 23 (2011) 4248-4253.
- [52] L.T. Alameda, P. Moradifar, Z.P. Metzger, N. Alem, R.E. Schaak, *J. Am. Chem. Soc.* 140 (2018) 8833-8840.
- [53] M. Ghidui, M.R. Lukatskaya, M.Q. Zhao, Y. Gogotsi, M.W. Barsoum, *Nature* 516 (2014) 78-81.
- [54] Z. Ansarian, A. Khataee, Y. Orooji, et al., *Mater. Today Chem.* 33 (2023) 101714.
- [55] M.R. Lukatskaya, O. Mashtalir, C.E. Ren, et al., *Science* 341 (2013) 1502-1505.
- [56] Y. Wu, Y. Sun, J. Zheng, et al., *Chem. Eng. J.* 404 (2021) 126565.
- [57] W. Zhang, S. Liu, J. Chen, et al., *ACS Appl. Mater. Interfaces* 13 (2021) 22341-22350.
- [58] X. Liang, Y. Rangom, C.Y. Kwok, Q. Pang, L.F. Nazar, *Adv. Mater.* 29 (2016) 1603040.
- [59] J. Song, D. Su, X. Xie, et al., *ACS Appl. Mater. Interfaces.* 8 (2016) 29427-29433.
- [60] C.F. Zhang, L. McKeon, M.P. Kremer, et al., *Nat. Commun.* 10 (2019) 1795.
- [61] M.Q. Zhao, X. Xie, C.E. Ren, et al., *Adv. Mater.* 29 (2017) 1702410.
- [62] A. Byeon, M.Q. Zhao, C.E. Ren, et al., *ACS Appl. Mater. Interfaces* 9 (2017) 4296-4300.
- [63] W. Y. Lieu, D. Fang, Y. Li, et al., *Nano Lett.* 22 (2022) 8679-8687.
- [64] E. Botling, R. Gond, A. Thakur, B. Anasori, A. Khataee, *RSC Adv.* 15 (2025) 13744-13752.
- [65] H. Zhang, J. Li, L. Luo, et al., *J. Alloys Compd.* 876 (2021) 160210.
- [66] G.-H. Dong, Y.Q. Mao, Y.Q. Li, P. Huang, S.Y. Fu, *Electrochim. Acta* 420 (2022) 140464.
- [67] M. Saraf, T. Zhang, T. Averianov, et al., *Small Methods* 7 (2023) 2201551.
- [68] P. Shang, X. Yan, Y. Li, et al. *Chin. Chem. Lett.* 34 (2023) 107584.
- [69] M. Li, B. Han, L. Gong, et al., *Chin. Chem. Lett.* 37 (2026) 110590.
- [70] Y. Liang, Y. Qi, N. Zhong, Y. Jin, B. Shao, *Coord. Chem. Rev.* 533 (2025) 216507.
- [71] Y. Yan, L. Hao, Z. Ren, et al., *J. Mater. Sci. Technol.* 249 (2026) 305-332.
- [72] L. Chen, L. Wang, Y. Wan, et al., *Adv. Mater.* 32 (2020) 1904433.
- [73] Z. Yong, T. Ma, *Angew. Chem. Int. Ed.* 135 (2023) e202308980.
- [74] H. Zheng, W. Yan, J. Zhang, *Electrochem. Energy Rev.* 8 (2025) 3.
- [75] X. Yan, M. Li, L. Zhang, et al., *J. Mater. Chem. A* 13 (2025) 25174-25194.
- [76] C. Yang, S. Wan, B. Zhu, J. Yu, S. Cao, *Angew. Chem. Int. Ed.* 61 (2022) e202208438.
- [77] C. Shu, X. Yang, L. Liu, et al., *Angew. Chem. Int. Ed.* 63 (2024) e202403926.
- [78] C. Shu, C. Han, X. Yang, et al., *Adv. Mater.* 33 (2021) 2008498.
- [79] L. Cao, I.C. Chen, Z. Li, et al., *Nat. Commun.* 13 (2022) 7894.
- [80] C. Wang, Z. Zhang, Y. Zhu, et al., *Adv. Mater.* 34 (2022) 2102290.
- [81] J. Zhang, J. Ma, R. Cui, et al., *Chem. Eng. J.* 503 (2024) 158427.

- [82] R. Gao, R. Shen, C. Huang, et al., *Angew. Chem. Int. Ed.* 64 (2024) e202414229.
- [83] X. Ma, S. Li, Y. Gao, et al., *Adv. Funct. Mater.* 24 (2024) 2409913.
- [84] T. He, Y. Zhao, *Angew. Chem. Int. Ed.* 62 (2023) e202303086.
- [85] H.H. Hegazy, S.S. Sana, T. Ramachandran, et al., *J. Energy Storage* 74 (2023) 109405.
- [86] X. Zhao, Q. Liu, X. Li, H. Ji, Z. Shen, *Chin. Chem. Lett.* 34 (2023) 108306.
- [87] B. Yu, R.-B. Lin, G. Xu, et al., *Nat. Chem.* 16 (2023) 114-121.
- [88] R. Shen, X. Li, C. Qin, P. Zhang, X. Li, *Adv. Energy Mater.* 13 (2023) 2203695.
- [89] L. Qin, D. Sun, D. Ma, et al., *Adv. Mater.* 37 (2025) 2504205.
- [90] Y. Zheng, N.A. Khan, X. Ni, et al., *Chem. Commun.* 59 (2023) 6314-6334.
- [91] S. Liu, M. Xu, X. Chen, *ChemElectroChem* 12 (2025) e202500163.
- [92] X. Rui, Z. Rui, L.Y. Sheng, G.J. Xi, *Coord. Chem. Rev.* 544 (2025) 216987.
- [93] H. Wang, H. Wang, Z. Wang, et al., *Chem. Soc. Rev.* 49 (2020) 4135-4165.
- [94] L. Liang, R. Yang, J. Wu, et al., *Anal. Chem.* 96 (2024) 18545-18554.
- [95] Y. Zhang, Y. Liu, H. Li, G. Bai, X. Lan, *Chem. Eng. J.* 489 (2024) 151479.
- [96] L. Wang, R. Fu, C. Li, et al., *Angew. Chem. Int. Ed.* 64 (2025) e202513165.
- [97] J. Wu, F. Huo, Z. Sun, et al., *Adv. Funct. Mater.* (2025), <https://doi.org/10.1002/adfm.202517053>.
- [98] W. Zhao, P. Yan, B. Li, et al., *J. Am. Chem. Soc.* 144 (2022) 9902-9909.
- [99] Y. Zhu, Y. Liu, Q. Ai, et al., *ACS Mater. Lett.* 4 (2022) 464-471.
- [100] Y.P. Zhang, H.L. Tang, H. Dong, et al., *J. Mater. Chem. A* 8 (2020) 4334-4340.
- [101] C. Huang, Y. Zhang, R. Shen, et al., *Adv. Mater.* (2025), <https://doi.org/10.1002/adma.202511092>
- [102] L. Hao, R. Shen, C. Qin, et al., *Sci. China Mater.* 67 (2024) 504-513.
- [103] J. Chen, D. Yuan, Y. Wang, *Adv. Funct. Mater.* 33 (2023) 2304071.
- [104] C. Jain, R. Kushwaha, D. Rase, et al., *J. Am. Chem. Soc.* 146 (2023) 487-499.
- [105] Z. Li, T. Deng, S. Ma, et al., *J. Am. Chem. Soc.* 145 (2023) 8364-8374.
- [106] X. Liu, F. Gao, T. Jin, et al., *Nat. Commun.* 14 (2023) 5097.
- [107] J. Wang, J. Zhang, P. Jin, et al., *Nat. Commun.* 16 (2025) 7346.
- [108] Z. Gao, H. Wang, Z. Qu, Z. Tang, *Appl. Therm. Eng.* 271 (2025) 126333.
- [109] T. Ju, X. Shi, Z. Si, et al., *J. Am. Chem. Soc.* 147 (2025) 23809-23818.
- [110] Z. Peng, N. Li, Y. He, et al., *J. Energy Storage.* 131 (2025) 117484.
- [111] T. Long, H. Wang, *Chin. Chem. Lett.* (2024) <https://doi.org/10.1016/j.ccl.2024.110623>.
- [112] M.A. Timmerman, R. Xia, P.T. Le, Y. Wang, J.E. Ten Elshof, *Chem. Eur. J.* 26 (2020) 9084-9098.
- [113] A. Das, S.D. Peu, M.S. Hossain, et al., *Nanomaterials.* 13 (2023) 1066.
- [114] M. Kandasamy, S. Sahoo, S.K. Nayak, B. Chakraborty, C.S. Rout, *J. Mater. Chem. A* 9 (2021) 17643-17700.
- [115] A.A. Lobinsky, V.I. Popkov, *Electrochem. Mater. Technol.* 1 (2022) 20221008.
- [116] V.P. Tolstoy, L.B. Gulina, A.A. Meleshko, *Russ. Chem. Rev.* 92 (2023) 5071.
- [117] A.A. Lobinsky, M.V. Kaneva, M.I. Tenevich, V.I. Popkov, *Micromachines* 14 (2023) 1083.
- [118] A. Lobinsky, D. Dmitriev, V. Popkov, et al. *Int. J. Hydrogen Energy* 48 (2023) 22495-22501.
- [119] Q. Zhao, K. Tao, L. Han, et al. *Dalton Trans.* 51 (2022) 17957-17961.
- [120] Y. Li, S.H. Talib, D. Liu, et al. *Appl. Catal. B: Environ.* 320 (2023) 122023.
- [121] Y. Gu, Y. Zhang, X. Wang, et al. *Nano Res.* 17 (2024) 5233-5242.
- [122] C. Wu, H. Sun, P. Dong, Y.Z. Wu, P. Li, *Adv. Funct. Mater.* 35 (2025) 2501506.
- [123] M.S. Islam, M. Mubarak, H.J. Lee, et al. *Inorganics.* 11 (2023) 183.
- [124] Y.D. Zhang, H. Xu, M.S. Ebaid, et al. *Chem. Sci.* 16 (2025) 9092-9108.
- [125] A. Shaheen, N. Raza, I. Ijaz, et al. *RSC Adv.* 15 (2025) 20469-20494.
- [126] P. Pazhamalai, V. Krishnan, M.S. Mohamed Saleem, S.J. Kim, H.W. Seo, *Nano Converg.* 11 (2024) 30.
- [127] N. Farooq, Z.U. Rehman, M.I. Khan, et al. *New J. Chem.* 48 (2024) 8933-8962.
- [128] L. Xiao, Z. Wang, J. Guan, et al. *Coord. Chem. Rev.* 472 (2022) 214777.
- [129] X. Pan, X. Hou, Y. Du, et al. *Chin. Chem. Lett.* 36 (2025) 110536.
- [130] X. Liu, C. Jia, G. Jiang, et al. *Chin. Chem. Lett.* 35 (2024) 109455.
- [131] X. Li, X. Su, T. Su, L. Chen, Z. Su, *Chem. Sci.* 16 (2025) 5353-5368.
- [132] Z. Yu, C. Si, A.P. LaGrow, et al., *ACS Catal.* 12 (2022) 9397-9409.
- [133] R. Makiura, S. Motoyama, Y. Umemura, et al., *Nat. Mater.* 9 (2010) 565-571.
- [134] B. He, Q. Zhang, Z. Pan, et al., *Chem. Rev.* 122 (2022) 10087-10125.
- [135] C. Hu, J. Su, *Coord. Chem. Rev.* 543 (2025) 216920.
- [136] S.E. Raby-Buck, J. Devlin, P. Gupta, et al., *Nat Rev Methods Prime* 5 (2025) 44.
- [137] Y. Chen, Q. Zhu, K. Fan, et al., *Angew. Chem. Int. Ed.* 60 (2021) 18769-18776.
- [138] L. Yan, Y. Xu, P. Chen, et al., *Adv. Mater.* 32 (2020) 2003313.
- [139] Y.S. Cheng, X.P. Chu, M. Ling, et al., *Catal. Sci. Technol.* 9 (2019) 5668-5675.
- [140] A. Prajapati, C. Hahn, I.M. Weidinger, et al., *Nat. Commun.* 16 (2025) 2593.
- [141] P. Jin, P. Guo, N. Luo, et al., *Science* 389 (2025) 1037-1042.
- [142] Y. Li, X. Zhang, W. Hou, et al., *Appl. Catal. B: Environ.* 380 (2025) 125758.
- [143] X. Liang, X. Wang, X. Zhang, et al., *ACS Catal.* 14 (2024) 4648-4655.
- [144] W. Liu, J. Jiang, Z. Li, et al., *Angew. Chem. Int. Ed.* 64 (2025) e202507312.
- [145] J.-P. Tang, Y. Chen, Z.Y. Wang, et al., *ACS Catal.* 15 (2024) 265-274.
- [146] Z. Huang, C. Guo, Q. Zheng, et al., *Chin. Chem. Lett.* 35 (2024) 109580.
- [147] Y. Li, Y. Li, J. Shang, X. Cheng, *Chin. Chem. Lett.* 34 (2023) 107928.
- [148] T. Bao, C. Tang, S. Li, et al., *J. Colloid Interface Sci.* 659 (2024) 788-798.
- [149] G.Z.S. Ling, S.H.W. Kok, P. Zhang, et al., *Adv. Funct. Mater.* 35 (2024) 2409320.
- [150] H. Zhang, M. Cui, Y. Lv, Y. Rao, Y. Huang, *Chin. Chem. Lett.* 36 (2024) 110108.
- [151] W. Zhao, J.H. Cao, J.J. Liao, et al., *Rare Metals* 43 (2024) 3118-3133
- [152] L. Feng, L. Ai, L. Wang, et al., *Langmuir* 40 (2024) 18896-18905.
- [153] Y. Tang, F. Ye, B. Li, et al., *Small* 20 (2024) 2400376.
- [154] X. Leng, X. Zhou, L. Ma, et al., *ACS Catal.* 14 (2024) 11554-11563.

- [155] Q. Hu, H. Yin, Y. Liu, et al., *J. Mater. Sci. Technol.* 204 (2024) 47-59.
- [156] Y. Li, M. Ma, D. Yi, et al., *Adv. Funct. Mater.* 34 (2024) 2407271.
- [157] T. Fatima, S. Husain, M. Khanuja, *Nano Mater Sci.* 7 (2024) 259-275.
- [158] S. Chauhan, R. Bhar, K. Ray, et al., *Environ. Res.* 271 (2025) 121100.
- [159] K. Liu, J. Chen, F. Sun, et al., *Int. J. Hydrogen Energy.* 48 (2023) 22319-22333.
- [160] E. Zhang, Q. Zhu, J. Huang, et al. *Appl. Catal. B: Environ.* 293 (2021) 120213.
- [161] R. Shi, H.F. Ye, F. Liang, et al., *Adv. Mater.* 30 (2017) 1705941.
- [162] S. Zhang, Z. Zhang, Y. Si, et al., *ACS Nano.* 15 (2021) 15238-15248.
- [163] X. Hao, Y. Wang, J. Zhou, et al., *Appl. Catal. B: Environ.* 221 (2017) 302-311.
- [164] S. Li, C. You, K. Rong, et al., *Adv. Powder. Mater.* 3 (2024) 100183.
- [165] F. Xu, K. Meng, S. Cao, et al., *ACS Catal.* 12 (2021) 164-172.
- [166] Y.H. Wu, Y.Q. Yan, Y.X. Deng, et al., *Chin. J. Catal.* 70 (2025) 333-340.
- [167] J. Qiu, K. Meng, Y. Zhang, et al., *Adv. Mater.* 36 (2024) 2400288.
- [168] Y. Bian, Z. Wang, M. Du, et al., *Adv. Funct. Mater.* (2025) e19493.
- [169] K. Lin, P. Qiao, Q. Liu, et al., *Adv. Funct. Mater.* (2025) e15276.
- [170] A.M. Abdalla, S. Hossain, A.T. Azad, et al. *Renew. Sust. Energ. Rev.* 82 (2018) 353-368.
- [171] P. Goel, S. Sundriyal, V. Shrivastav, et al., *Nano Energy* 80 (2020) 105552.
- [172] S. Lin, K. Qi, *Chin. Chem. Lett.* 35 (2024) 109431.
- [173] J. Zhang, L. Ding, V. Popkov, K. Qi, *Chin. Chem. Lett.* 36 (2025) 110407.
- [174] X. Li, Y. Bai, T. Ren, et al., *Adv. Energy Mater.* (2025) e03420.
- [175] L. Liu, Y. Li, T. Su, et al., *Adv. Mater.* 37 (2025) 2508595.
- [176] A.H. Khan, S. Ghosh, B. Pradhan, et al., *Bull. Chem. Soc. Jpn.* 90 (2017) 627-648.
- [177] Q. Wei, F. Xiong, S. Tan, et al., *Adv. Mater.* 29 (2017) 1602300.
- [178] B. Luo, S. Liu, L. Zhi, *Small* 8 (2011) 630-646.
- [179] P. Maji, A. Ray, P. Sadhukhan, A. Roy, S. Das, *Mater. Lett.* 227 (2018) 268-271.
- [180] J. Huang, S. Xiang, J. Yu, C.Z. Li, *Energy Environ. Sci.* 12 (2018) 929-937.
- [181] R. Chiba, *Solid. State. Ion.* 124 (1999) 281-288.
- [182] Y. Wei, Z. Cheng, J. Lin, *Chem. Soc. Rev.* 48 (2018) 310-350.
- [183] H.S. Nan, X.Y. Hu, H.W. Tian, *Mater. Sci. Semicond. Process.* 94 (2019) 35-50.
- [184] X.M. Zhao, L.W. Tang, Y. Liu, et al., *Chin. Chem. Lett.* 36 (2025) 110092.
- [185] M.S. Lassoued, F. Ahmad, Y. Zheng, *Chin. Chem. Lett.* 36 (2025) 110477.
- [186] Y.L. Song, Z.C. Wang, Y.D. Yan, et al., *J. Energy Chem.* 43 (2019) 173-181.
- [187] J.T. Mefford, W.G. Hardin, S. Dai, K.P. Johnston, K.J. Stevenson, *Nat. Mater.* 13 (2014) 726-732.
- [188] X.W. Wang, Q.Q. Zhu, X.E. Wang, et al., *J. Alloys Compd.* 675 (2016) 195-200.
- [189] A. Kojima, K. Teshima, Y. Shirai, T. Miyasaka, *J. Am. Chem. Soc.* 131 (2009) 6050-6051.
- [190] H.S. Kim, C.R. Lee, J.H. Im, et al., *Sci. Rep.* 2 (2012) 591.
- [191] H. Guo, H. Chen, H. Zhang, et al., *Nano Energy* 59 (2019) 1-9.
- [192] M. Tathavadekar, S. Krishnamurthy, A. Banerjee, et al., *J. Mater. Chem. A* 5 (2017) 18634-18642.
- [193] A. Kostopoulou, D. Vernardou, K. Savva, E. Stratakis, *Nanoscale* 11 (2018) 882-889.
- [194] A. Jaffe, H.I. Karunadasa, *Inorg. Chem.* 53 (2014) 6494-6496.
- [195] Y. He, J. Yan, L. Xu, et al., *Adv. Mater.* 33 (2021) 2006302.
- [196] S.H. Cho, Y. Jung, Y.W. Jang, et al. *Int. J. Precis. Eng. Manuf. Green Tech.* 12 (2024) 349-380.
- [197] S.H. Cho, J. Byeon, K. Jeong, et al., *Adv. Energy Mater.* 11 (2021) 2100555.
- [198] K. Hong, Q.V. Le, S.Y. Kim, H.W. Jang, *J. Mater. Chem. C* 6 (2018) 2189-2209.
- [199] K.K. Hansen, E.M. Skou, H. Christensen, T. Turek, *J. Catal.* 199 (2001) 132-140.
- [200] M.S. Lassoued, F. Ahmad, Y. Zheng, *Chin. Chem. Lett.* 36 (2025) 110477.
- [201] S.A. Kulkarni, S.G. Mhaisalkar, N. Mathews, P.P. Boix, *Small Methods.* 3 (2018) 1800231.
- [202] K. Keraman, A. Luntz, V. Viswanathan, Y.M. Chiang, Z. Chen, *J. Electrochem. Soc.* 164 (2017) A1731.
- [203] F. Su, Z.S. Wu, *J. Energy. Chem.* 53 (2020) 354-357.
- [204] X. Zhang, G. Wu, W. Fu, et al., *Adv. Energy Mater.* 8 (2018) 1702498.
- [205] C. Lan, Z. Zhou, R. Wei, J.C. Ho, *Mater. Today Energy* 11 (2018) 61-82.
- [206] H. Tao, Q. Fan, T. Ma, et al., *Prog. Mater. Sci.* 111 (2020) 100637.
- [207] M.D. Smith, B.A. Connor, H.I. Karunadasa, *Chem. Rev.* 119 (2019) 3104-3139.
- [208] B. Traore, L. Pedesseau, L. Assam, et al., *ACS Nano* 12 (2018) 3321-3332.
- [209] L. Etgar, *Energy Environ. Sci.* 11 (2017) 234-242.
- [210] H. Tsai, W. Nie, J.C. Blancon, et al., *Nature* 536 (2016) 312-316
- [211] W. Niu, A. Eiden, G. Vijaya Prakash, J.J. Baumberg, *Appl. Phys. Lett.* 104 (2014) 171111.
- [212] O. Nazarenko, M.R. Kotyrba, S. Yakunin, et al., *J. Am. Chem. Soc.* 140 (2018) 3850-3853.
- [213] C.M.M. Soe, C.C. Stoumpos, M. Kepenekian, et al., *J. Am. Chem. Soc.* 139 (2017) 16297-16309.
- [214] Y. Liu, H. Zhou, Y. Ni, et al., *Joule* 7 (2023) 1016-1032.
- [215] X. Wang, Y. Zhao, B. Li, et al., *ACS Appl. Mater. Interfaces* 14 (2021) 22879-22888.
- [216] L. Mao, W. Ke, L. Pedesseau, et al., *J. Am. Chem. Soc.* 140 (2018) 3775-3783.
- [217] Y. Fujii, D. Ramirez, N.C. Rosero-Navarro, et al., *ACS Appl. Energy Mater.* 2 (2019) 6569-6576.
- [218] M.A. Green, A. Ho-Baillie, H.J. Snaith, *Nat. Photonics* 8 (2014) 506-514.
- [219] G. Grancini, C. Roldán-Carmona, I. Zimmermann, et al., *Nat. Commun.* 8 (2017) 15684.
- [220] Z. Wang, Q. Lin, F.P. Chmiel, et al., *Nat. Energy.* 2 (2017) 17135
- [221] X. Zhang, X. Ren, B. Liu, et al., *Energy Environ. Sci.* 10 (2017) 2095-2102.
- [222] N.J. Jeon, J.H. Noh, W.S. Yang, et al., *Nature.* 517 (2015) 476-480.
- [223] B.P. Kore, W. Zhang, B.W. Hoogendoorn, M. Safdari, J.M. Gardner, *Commun. Mater.* 2 (2021) 100.
- [224] F. Zhang, B. Cai, J. Song, et al., *Adv. Funct. Mater.* 30 (2020) 2001732.
- [225] W. Deng, X. Jin, Y. Lv, et al., *Adv. Funct. Mater.* 29 (2019) 1903861.
- [226] D. Liang, Y. Peng, Y. Fu, et al., *ACS Nano.* 10 (2016) 6897-6904.
- [227] L. Ni, U. Huynh, A. Cheminal, et al., *ACS Nano* 11 (2017) 10834-10843.

- [228] M. Yuan, L.N. Quan, R. Comin, et al., *Nat. Nanotechnol.* 11 (2016) 872-877.
- [229] N. Wang, L. Cheng, R. Ge, et al., *Nat. Photonics.* 10 (2016) 699-704.
- [230] Z. Xiao, R.A. Kerner, L. Zhao, et al., *Nat. Photonics* 11 (2017) 108-115.
- [231] M. Neelakandan, P. Dhandapani, S. Ramasamy, et al., *RSC Adv.* 15 (2025) 16766-16791.
- [232] Z. Li, W. Zhang, H. Wang, B. Yang, *Electrochim. Acta* 258 (2017) 561-570.
- [233] A. Yadav, A. Saini, P. Kumar, M. Bag, *J. Mater. Chem. C* 12 (2023) 197-206.
- [234] H.-J. Kim, S. Morita, K.N. Byun, et al., *Nano Lett.* 23 (2023) 3788-3795.
- [235] J. Cho, J.T. DuBose, A.N.T. Le, P.V. Kamat, *ACS Mater. Lett.* 2 (2020) 565-570.
- [236] S. Ghimire, C. Klinke, *Nanoscale.* 13 (2021) 12394-12422.
- [237] A. Giri, A.Z. Chen, A. Mattoni, et al., *Nano Lett.* 20 (2020) 3331-3337.
- [238] G.A. Elbaz, W.-L. Ong, E.A. Doud, et al., *Nano Lett.* 17 (2017) 5734-5739.
- [239] T. Haeger, R. Heiderhoff, T. Riedl, *J. Mater. Chem. C* 8 (2020) 14289-14311.
- [240] Z. Song, J. Zhao, U. Ghani, et al., *ChemElectroChem* 11 (2024) e202300731.
- [241] K.M. Liao, Y.K. Dai, H.Y. Wang, S. Deng, G.P. Dai, *ACS Appl. Energy Mater.* 8 (2025) 3892-3903.
- [242] N. Raveendran, S. Subash, K.M. Ponnusamy, et al., *ACS Omega.* 9 (2024) 49867-49877.
- [243] Z. Ju, S.T. King, X. Xu, et al., *Proc. Natl. Acad. Sci.* 119 (2022) e2212777119.
- [244] Q. Chen, Y. Wei, X. Zhang, et al., *Adv. Energy Mater.* 12 (2022) 2200072.
- [245] H. Dai, X. Zhao, H. Xu, et al., *ACS Nano.* 16 (2022) 5556-5565.
- [246] H. Zhang, J. Song, J. Li, et al., *ACS Appl. Mater. Interfaces* 14 (2022) 16300-16309.
- [247] Y. Wang, J.P. He, H.-Q. Pan, et al. *Rare Met.* 43 (2024) 1062-1071.
- [248] M. Zhu, X. Li, W. Ni, et al., *Chem. Eng. J.* 516 (2025) 164029.
- [249] Q. Wang, H. Zhao, M. Chen, et al., *Chem. Eng. J.* 484 (2024) 149674.
- [250] L. Shang, B.Y. Shi, X. Liu, et al., *Chem. Eng. J.* 482 (2024) 149037.
- [251] Z. Pan, W. Ding, H. Chen, H. Ji, *Chin. Chem. Lett.* 35 (2024) 108567.
- [252] X. Wang, S. Dong, K. Qi, et al. *Acta Phys. Chim. Sin.* 40 (2024) 2408005.
- [253] T. Bao, X. Li, S. Li, et al., *Nano Mater Sci.* 7 (2025) 145-168.
- [254] P. Dash, A.K. Kar, R. Srivastava, K. Parida, *Mater. Horiz.* 12 (2025) 6485-6557.
- [255] A. Hayat, M. Sohail, A. El Jery, et al., *Chem. Rec.* 23 (2023) e202200171.
- [256] J. Rao, Z. Cheng, H. Lv, et al., *Diamond Relat. Mater.* 157 (2025) 112478.
- [257] Y. Li, *Langmuir* 41 (2025) 23253-23272.
- [258] Y. Yang, W. Niu, L. Dang, et al., *Front. Chem.* 10 (2022) 955065.
- [259] L. Li, H. Liu, C. Cheng, et al., *ACS Catal.* 14 (2024) 10204-10213.
- [260] M.I. Nabeel, T. Gulzar, S. Kiran, et al., *Int. J. Energy Res.* 2025 (2025) 5599894.
- [261] W. Niu, Y. Yang, *ACS Energy Lett.* 3 (2018) 2796-2815.
- [262] O. Iqbal, H. Ali, N. Li, et al., *Mater. Today Phys.* 34 (2023) 101080.
- [263] G.-M. Weng, Y. Xie, H. Wang, et al., *Angew. Chem. Int. Ed.* 58 (2019) 13727-13733.
- [264] H. Yin, J. He, B. Xiao, et al., *Nano Res. Energy* 3 (2024) e9120138.
- [265] J. Xiao, Y. Chen, C. Cai, et al., *Small* 21 (2025) 2503335.
- [266] Z. Chen, G. Ding, Z. Wang, et al., *Adv. Funct. Mater.* 35 (2025) 2423213.
- [267] S. Wang, S. Jin, X. Yang, et al., *Chin. Chem. Lett.* 35 (2024) 109890.
- [268] Z. Song, N. Zhang, J. Yu, et al., *Chin. Chem. Lett.* 37 (2026) 111804.
- [269] A. Sharma, S. Kumari, S. Sharma, et al., *Mater. Today Sustain.* 22 (2023) 100399.
- [270] S. Nishimura, A. Takagaki, K. Ebitani, *Green Chem.* 15 (2013) 2026-2042.
- [271] L. Pan, H. Huang, M. Niederberger, *J. Mater. Chem. A* 7 (2019) 21264-21269.
- [272] M. Aman, P. Konduparty, S. Sharma, et al., *J. Energy Storage.* 116 (2025) 116093.
- [273] Q. Xie, Z. Cai, P. Li, et al., *Nano Res.* 11 (2018) 4524-4534.
- [274] Y. Rao, Y. Wang, H. Ning, P. Li, M. Wu, *ACS Appl. Mater. Interfaces* 8 (2016) 33601-33607.
- [275] J. Zhu, J. Zou, H. Cheng, Y. Gu, Z. Lu, *Green Energy Environ.* 4 (2019) 345-359.
- [276] W. Yu, N. Deng, K. Cheng, et al., *J. Energy Chem.* 58 (2021) 472-499.
- [277] W. Ma, Y. Zhang, B. Wang, et al., *Chem. Eng. J.* 494 (2024) 153212.
- [278] G. Wang, Z. Jin, *J. Mater. Chem. C* 9 (2021) 620-632.
- [279] L. Luo, Q. Kong, Q. Zhang, et al., *J. Power Sources* 613 (2024) 234940.
- [280] Y. Kuai, Y. Wang, *Carbon Neutrality* 3 (2024) 36.
- [281] H. Yu, M. Dai, J. Zhang, et al., *Small* 19 (2023) 2205767.
- [282] G. Zhang, H. Yang, H. Zhou, et al., *Angew. Chem. Int. Ed.* 63 (2024) e202401903.
- [283] Y. Zhuang, H. Yang, Y. Li, et al., *ACS Nano* 19 (2025) 11058-11074.
- [284] J. Chen, Z. Li, Z. Li, Y. Zhou, Y. Lai, *Appl. Catal. B: Environ.* 355 (2024) 124204.
- [285] T. Wen, Y. Zheng, H. Wang, J. Zou, *Appl. Catal. B: Environ.* 378 (2025) 125588.
- [286] H. Wang, R. Niu, J. Liu, et al., *Nano Res.* 15 (2022) 6987-6998.
- [287] W. Liu, Z. Chen, Z. Zhang, et al., *Energy Environ. Sci.* 14 (2021) 382-395.
- [288] Y. Li, S. Wan, W. Liang, et al., *Small* 20 (2024) 2312104.
- [289] S. Wan, W. Wang, B. Cheng, et al., *Nat. Commun.* 15 (2024) 9612.
- [290] G. Tang, J. Zhang, C. Bie, et al., *Adv. Mater.* 37 (2025) e14576.

Graphical Abstract



This roadmap unifies recent progress and remaining challenges across eleven classes of 2D materials, distilling the key structure–function insights and research priorities required to advance their transition from fundamental understanding to impactful energy-conversion and storage technologies.

Journal Pre-proof